# A TECHNO-ECONOMICAL ANALYSIS OF A $CO_2$ HEAT PUMP

**Mr. W. GROENEWALD**

**M.Ing (Mechanical)**

Dissertation submitted in partial fulfilment of the requirements for the degree Master of Engineering at the Potchefstroom Campus of the North-West University

**Supervisor: Dr. M. van Eldik**

**November 2009**

Innovation through diversity

NORTH-WEST UNIVERSITY
YUNIBESITI YA BOKONE-BOPHIRIMA
NOORDWES-UNIVERSITEIT
POTCHEFSTROOM CAMPUS

**TITLE:** A TECHNO-ECONOMICAL ANALYSIS OF A $CO_2$ HEAT PUMP
**AUTHOR:** MR. W. GROENEWALD
**SUPERVISOR:** DR. M. VAN ELDIK
**QUALIFICATION:** MASTER OF ENGINEERING

***ABSTRACT***

There is a global concern for the environment and the impact we as humans have on it. The latest movement in the refrigeration sector is to phase out refrigerants such as Freons that contribute to global warming. This resulted in the industry being forced to start implementing natural refrigerants again.

One solution identified is to use carbon dioxide ($CO_2$). $CO_2$ is a natural gas found in the atmosphere, it has no ozone depleting potential and has a global warming potential of one. It is regarded as a safe gas seeing that it is non-flammable and non-toxic. The biggest challenge when using $CO_2$ as a refrigerant in water heating heat pumps is the fact that it will work in a high pressure transcritical state. The advantage on the other hand is that the use of a gas cooler makes it possible to heat water to much higher temperatures than with conventional refrigerants.

A techno-economical comparison was conducted between a water heating heat pump using $CO_2$ as refrigerant and another using R-22 as refrigerant. The comparison was based on simulated models of the mentioned heat pump systems. On comparison it was found that the $CO_2$ heat pump has on average a 15% better COP than for R-22. This results in a 9.4% improvement in energy use for a complete hot water system using a $CO_2$ heat pump rather than a conventional R-22 heat pump.

From the results found it can be concluded that a $CO_2$ heat pump system is a feasible possibility to replace HFC and HCFC refrigerants. It offers an environmentally friendly and energy efficient system for water heating in the domestic and commercial market. The outcome of this study forms the basis for future research and development on $CO_2$ water heating heat pump technology at the North-West University.

**TITEL:** 'N TEGNO-EKONOMIESE ANALISE VAN 'N $CO_2$ HITTEPOMP

**OUTEUR:** MNR. W. GROENEWALD

**STUDIELEIER:** DR. M. VAN ELDIK

**KWALIFIKASIE:** MAGISTER IN INGENIEURSWESE

*OPSOMMING*

Daar is 'n globale bekommernis oor die omgewing en die impak wat ons as mense op dit het. Daar word tans druk toegepas deur die verkoelingsbedryf om koelmiddels soos Freons uit te faseer aangesien dit lei tot aardverwarming. Dit het op sy beurt daartoe gelei dat industrieë geforseer word om natuurlike gasse te begin implimenteer.

Een oplossing wat oorweeg word is die gebruik van koolstofdioksied ($CO_2$). $CO_2$ is 'n natuurlike gas wat vry voorkom in die atmosfeer, met 'n aardverwarmingspotensiaal van een en nie skadelik is vir die osoonlaag nie. Die gas is nie-flambaar en nie-giftig nie en word daarom as 'n veilige gas beskou. Die grootste uitdaging wanneer $CO_2$ as 'n koelmiddel gebruik word is dat dit by baie hoë drukke in 'n transkritiese toestand verkeer. Die voordeel hiervan is dat daar van 'n gasverkoeler gebruik gemaak word om die gas aan die hoë druk kant af te koel en dit moontlik maak om die water tot baie hoër temperature te verhit as met konvesionele koelmiddels.

'n Tegno-ekonomiese vergelyking word getref tussen 'n $CO_2$ waterverhittings-hittepomp en 'n R-22 hittepomp. Die vergelyking word getref deur gebruik te maak van gesimuleerde modelle van die twee sisteme. Met die vergelyking van die twee sisteme is gevind dat die $CO_2$ hittepomp gemiddeld 'n 15% beter werkverrigtingskoëffisient het as vir R-22. Dit lei tot 'n 9.4% verbetering in energieverbruik van 'n volledige warmwater-stelsel bestaande uit 'n $CO_2$ hittepomp eerder as 'n R-22 hittepomp.

Uit die resultate word afgelei dat 'n $CO_2$ waterverhittings hittepomp 'n goeie alternatief is om HFC en HCFC gasse te vervang. Dit bied 'n omgewingsvriendelike en energie-effektiewe sisteem vir waterverhitting deur middel van 'n hittepompsisteem. Die uitkoms van die studie vorm die basis vir toekomstige navorsing m.b.t. $CO_2$ waterverhittings-hittepomp tegnologie by die Noord-Wes Universiteit.

# TABLE OF CONTENTS

## NOMENCLATURE

| | | |
|---|---|---|
| $c_p$ | Specific heat at constant pressure | $J/(kg \cdot K)$ |
| $h$ | Enthalpy | $J/kg$ |
| $q, Q$ | Heat transfer | $W$ |
| $T$ | Temperature | $°C$ |
| $K$ | Kelvin | $K$ |
| $KW$ | Kilowatt | - |
| $KWh$ | Kilowatt hour | - |
| $W$ | Work | $W$ |
| $kg$ | Kilogram | $kg$ |
| $p$ | Pressure | $Pa$ |
| $P$ | Power input | $W$ |
| $\dot{m}$ | Mass flow rate | $kg/s$ |
| $eta$ | Efficiency | - |

## GREEK SYMBOLS

| | | |
|---|---|---|
| $\Delta$ | Delta or difference | - |
| $\eta$ | Efficiency | - |

## ABBREVIATIONS

| | |
|---|---|
| $CO_2$ | Carbon Dioxide |
| CFC | Chlorofluoro Carbon |
| COP | Coefficient of Performance |
| Delta T | Temperature Difference |
| ESKOM | South African Electrical Supply Utility |
| EES | Engineering Equation Solver |
| GWP | Global Warming Potential |
| HFC | Hydrofluoro Carbon |
| HCFC | Hydrochlorofluoro Carbon |
| $H_2CO_3$ | Carbonic Acid |
| $H_2O$ | Water |
| HVAC | Heating Ventilation and Air Conditioning |
| HP | Heat pump |

| | |
|---|---|
| ILH | In-line heater |
| MPa | Mega Pascal |
| NTNU | Norwegian University of Science and Technology |
| $NH_3$ | Ammonia |
| ODP | Ozone Depleting Potential |
| P-h | Pressure-enthalpy |
| Pa | Pascal |
| R-744 | Refrigerant Carbon Dioxide |
| R-22 | Refrigerant number 22 |
| R-134a | Refrigerant number 134a |
| $SO_3$ | Sulphur Dioxide |
| TEWI | Total Equivalent Warming Impact |
| T-s | Temperature-entropy |
| UNEP | United Nations Environmental Program |
| U.K. | United Kingdom |
| U.S. | United States |
| VAT | Value added tax |
| VRT | Virgin rock temperature |
| WMO | World Meteorological Organization |

# LIST OF FIGURES

PAGE

## CHAPTER 2

## *CHAPTER 3*

## CHAPTER 4



## CHAPTER 5

# LIST OF TABLES

PAGE

## CHAPTER 2



## CHAPTER 3



## CHAPTER 4



## CHAPTER 5

# CHAPTER 1

# INTRODUCTION

## 1.1 Problem statement

Energy efficient means of water heating, space cooling, space heating and refrigeration received a lot of attention over the past few years. This is mainly due to the increasing dilemma of the availability of electricity especially in South Africa and the tariff increases experienced. This resulted in more emphasis being put on the implementation of energy efficient products and projects. Heat pump technology has proved itself to be a very effective solution for water heating.

Increased concerns about the environmental impact of the refrigerants used in conventional systems are pointing research towards design solutions aimed at improving the energy efficiency of the related applications (Pearson, 2005). Using eco-friendly refrigerants that have very low or no impact at all on global warming has set the trend for implementation. Conventional heat pump cycles make use of hydrofluorocarbons (HFCs) and hydrochlorofluorocarbons (HCFCs) as refrigerants. These refrigerants typically have a very high global warming potential (GWP) combined with a high ozone depleting potential (ODP). Phasing out these refrigerants have already started in Europe and other countries and is to be implemented in South Africa from the year 2012.

The emphasis on the use of natural refrigerants in heat pump cycles has globally become substantial. Five substances are recognized as natural refrigerants in modern refrigeration, being air, water-vapour, ammonia, hydrocarbons and carbon dioxide ($CO_2$). Restrictions on the first four substances mentioned above have focused global research towards the implementation of carbon dioxide ($CO_2$) as natural working refrigerant in refrigeration applications. Being a natural refrigerant, $CO_2$ has no ODP and a GWP of 1 (Flemming *et al.*).

$CO_2$ has been used in refrigeration applications in the early 1900's but with the implementation of CFCs and HCFCs it gradually became a forgotten technology. It has only been revised as a probable refrigerant since 1994, has only been implemented again from 1998 and is therefore considered to be a new technology. The implication of this is that cycle components are not yet freely available and more expensive than conventional system components (Kim *et al.*).

Though the concept of a water heating $CO_2$ heat pump cycle is still similar to that of conventional systems, there is a big difference in the conditions under which a $CO_2$

cycle operates. This resulted in the need for a thorough understanding of $CO_2$ and its properties.

It is also important to understand the techno-economical advantages/disadvantages of $CO_2$ systems compared to conventional refrigerant systems, for an energy efficient solution. A $CO_2$ system has the potential to benefit Eskom in its drive towards more energy efficient use of the electricity it generates.

## *1.2 Purpose of this study*

A thorough study is to be done on $CO_2$ to start the research and development at the North-West University, i.e. regarding this refrigerant to be used in a water heating heat pump system.

The purpose of this study is to conduct a techno-economic analysis of a water heating heat pump using $CO_2$ as refrigerant compared to a conventional R-22 heat pump with similar capacities. Comparisons made are based on simulated models for each system.

To be able to do such an analysis, a thorough literature study is required to attain a greater understanding of the properties of $CO_2$ and to investigate the feasibility of the implementation of such a system.

## *1.3 Method of investigation*

To satisfy the purpose described in section 1.2, the study will consist of the following:

- A detailed literature study on the properties of $CO_2$ as refrigerant and the cycle implementation issues will be done.
- A system simulation model of a $CO_2$ heat pump cycle will be developed.
- The results from the model will be compared against performance data on hand for a commercially available R-22 heat pump cycle, to identify the energy efficiency potential of using $CO_2$ as refrigerant.
- Both the simulated models will be compared to each other using the WHSIM Statistical program (Rousseau, 2006).

- As far as the economical aspects are concerned, a cost comparison, both capital and operational, between the $CO_2$ heat pump and the R-22 heat pump will be done.

# CHAPTER 2

# LITERATURE STUDY

# CHAPTER 2

## 2. LITERATURE STUDY

The aim of this chapter is to gain in-depth knowledge of carbon dioxide ($CO_2$), also known as R-744, and its properties. The literature study will aim to cover all relevant aspects of $CO_2$ including applications as a refrigerant. The literature study will be divided into the following categories:

- Background.
- History of $CO_2$.
- Phasing out of CFCs, HCFCs and HFCs.
- Properties of $CO_2$.
- Applications of $CO_2$:
    - Cascade systems.
    - Mobile air conditioning and heating.
    - Space heating.
    - Heat pumps for Domestic Hot Water Heating:
        - Conventional systems.
        - Transcritical systems.

## 2.1 Background

More than 20 years ago the increasing concentration of carbon dioxide ($CO_2$) in the atmosphere was not generally admitted nor did it draw any concerns. The cost of energy was relatively low and electricity was cheap to use, resulting in purchasers mainly considering the installation cost of equipment and not the energy savings potential (Pearson, 2005).

$CO_2$ forms a vital part of our eco-system and is produced as a raw material through plant photosynthesis and is also a product of human and animal respiration. Only approximately 1-2% of $CO_2$ available on earth is found in the atmosphere, the rest is absorbed by the oceans and trees, (ANON (c), s.a.). A natural greenhouse effect is created by the $CO_2$ and water vapour that protects the earth from excessive heat loss. It is documented as a fact that the earth is getting warmer. According to Butler (2007) the average global temperature is predicted to increase between $1.5K$ and $4.5K$ in the next 100 years. The warmest recorded years all occurred since 1981. There is scientific evidence that human behaviour affects the natural temperature of the earth. This is mainly due to unnecessary $CO_2$ emissions and the use of aerosols that all contribute to increasing the earth's greenhouse effect (ANON (c), s.a.).

During the last few years, more restrictions have been put on the refrigeration, air conditioning and heat pump industries. Phasing out of chlorofluorocarbon (CFC) substances has already been widely implemented, but the change-over to ozone-friendly substances has not yet been completed, as hydrochlorofluorocarbons (HCFCs) are still widely used in industry. Hydrofluorocarbons (HFCs) also made their appearance and were long thought to be a permanent replacement. Though HFCs have no ozone depleting potential (ODP) they still have a big effect on global warming. The global warming potential (GWP) is an index of a substance's ability to be a greenhouse gas. Table 2.1 gives an indication of the GWP, ODP and some properties of refrigerants known and used in refrigeration cycles. Large amounts of $CO_2$ can be recovered from waste gas and is therefore not necessary to be produced, thus eliminating the net global warming contribution of this fluid when used as a refrigerant (Fartaj *et al.*, 2004).

According to studies done by Taira (2008), water heating contributes to more than 20% of residential $CO_2$ emissions in Japan. This is due to the fact that more than

90% of water heaters in Japan are combustion systems. It is found that $CO_2$ water heaters have the potential of equivalent or better performance than HFC systems.

Table 2.1: Characteristics of some refrigerants. (Kim et al, 2003).

| | R-12 | R-22 | R-134a | R-407C[a] | R-410A[b] | R-717 | R-290 | R-744 |
|---|---|---|---|---|---|---|---|---|
| ODP/GWP[c] | 1/8500 | 0.05/1700 | 0/1300 | 0/1600 | 0/1900 | 0/0 | 0/3 | 0/1 |
| Flammability/toxicity | N/N | N/N | N/N | N/N | N/N | Y/Y | Y/N | N/N |
| Molecular mass (kg/kmol) | 120.9 | 86.5 | 102.0 | 86.2 | 72.6 | 17.0 | 44.1 | 44.0 |
| Normal boiling point[d] (°C) | −29.8 | −40.8 | −26.2 | −43.8 | −52.6 | −33.3 | −42.1 | −78.4 |
| Critical pressure (MPa) | 4.11 | 4.97 | 4.07 | 4.64 | 4.79 | 11.42 | 4.25 | 7.38 |
| Critical temperature (°C) | 112.0 | 96.0 | 101.1 | 86.1 | 70.2 | 133.0 | 96.7 | 31.1 |
| Reduced pressure[e] | 0.07 | 0.10 | 0.07 | 0.11 | 0.16 | 0.04 | 0.11 | 0.47 |
| Reduced temperature[f] | 0.71 | 0.74 | 0.73 | 0.76 | 0.79 | 0.67 | 0.74 | 0.90 |
| Refrigeration capacity[g] (kJ/m$^3$) | 2734 | 4356 | 2868 | 4029 | 6763 | 4382 | 3907 | 22545 |
| First commercial use as a refrigerant [14] | 1931 | 1936 | 1990 | 1998 | 1998 | 1859 | ? | 1869 |

[a] Ternary mixture of R-32/125/134a (23/25/52, %).
[b] Binary mixture of R-32/125 (50/50, %).
[c] Global warming potential in relation to 100 years integration time, from the Intergovernmental Panel on Climate Change (IPCC).
[d] ASRAE handbook 2001 fundamentals.
[e] Ratio of saturation pressure at 0 °C to critical pressure.
[f] Ratio of 273.15 K (0 °C) to critical temperature in Kelvin.
[g] Volumetric refrigeration capacity at 0 °C.

Hydrofluorocarbons (HFCs) are included along with hydrochlorofluorocarbons (HCFCs) and chlorofluorocarbons (CFCs) in the greenhouse gas emissions covered by the Kyoto protocol (Hasse *et al.*, 2008). Contributing to global warming and also used as a measure of release of carbon dioxide is the so-called total equivalent warming impact (TEWI). TEWI is calculated from two plant effects, namely the refrigerant escape (direct effect) and the escape of greenhouse gases which result from the plant energy consumption (indirect effect). It is given that an average of 0.65kg carbon dioxide is released for every kWh of energy used by a conventional refrigeration plant, resulting in a plant's lack of efficiency greatly contributing to global warming (Fleming *et al.*, 1992). The restrictions placed on chlorine-based substances are forcing the industry to look for completely different and long-term solutions. As a result, interest has grown in technologies based on ecologically safe and natural refrigerants. Some of these natural refrigerants include water, air, noble gasses, hydrocarbons, ammonia and carbon dioxide. Of these, the efficiency of air is low, ammonia is toxic and flammable, and hydrocarbons are also flammable, just to mention a few drawbacks. This resulted in the attention being shifted to the development of $CO_2$ technologies. Since research on $CO_2$ has once again flared up, there has been a considerable increase in the interest and development activity internationally. Over the past 5 years an increasing number of applications with $CO_2$ as refrigerant were implemented internationally (Fleming *et al.*, 1992).

Modern refrigeration only recognises five natural refrigerants. Air has been used in gas cycles and is able to achieve reasonably low temperatures, but its low efficiency has limited its use. Water vapour has been used in large applications, including centrifugal and axial turbines in open systems, but its low pressures and the fact that it cannot operate at evaporation temperatures lower than 0°C restricted its use as a refrigerant completely. Hydrocarbons, $CO_2$ and ammonia can be used in a wider range of applications, which include more of the conventional systems. Currently, phasing out hydrocarbon use is being investigated, as will be discussed later in this chapter. Ammonia is ideal in large industrial systems, but its use in the domestic and commercial sectors are limited due to its toxicity (Pearson, 2006). $CO_2$ is especially suitable for use in heat pump systems due to its high heat rejection temperature because of its low critical temperature (Kuwabara *et al.*, 2006).

There is still an argument that designing and using $CO_2$ systems are less cost-effective than using conventional systems. According to R744.com (b) two factors are influencing this argument considerably: firstly the costs of chemical fluids are becoming more expensive due to supply shortages, and fuel costs are rising. It is assumed that prices of chemical refrigerants could go up as much as 50% in the next 5 years. Not only is this playing a big role but secondly the fact that training and support of using HFCs to comply with the regulations placed on users has lowered the cost competitiveness of current systems.

## 2.2 History of $CO_2$

Because $CO_2$ is a relatively old technology, a brief look at its history and also the recent reinvention of $CO_2$ is deemed necessary for the purpose of this study, because it will give a better view of the recent activities taking place regarding this situation.

Carbon dioxide has been used for over 130 years in vapour compression cycles as a refrigerant (Pearson, 2005). The first era of refrigerants occurred roughly around the 1820's and lasted up to about 1930, where any substance that could produce refrigeration was used. According to Bensafi and Thonon (2007) and Calm (2008) this era was known as the "whatever worked" era. Up until the 1930's the most common refrigerants used were the natural refrigerants ammonia, carbon dioxide and sulphur dioxide as well as hydrocarbons such as ethane and propane. Some other refrigerants used were methyl chloride and ethyl chloride but these were flammable chemical refrigerants. 80% of $CO_2$ applications were in marine systems but it was also used in air conditioning and stationary refrigeration applications. It seems that Alexander Twining was the first to propose $CO_2$ as a refrigerant in 1850. But it was not until the late 1860's that the first $CO_2$ system was built by Thaddeus S.C. Lowe. Despite this achievement he did not continue his research in this field. In 1881 the first $CO_2$ system was built in Europe by Carl Linde. $CO_2$ technology was then taken considerably further by the German Franz Windhausen. Manufacturing of these systems was commenced by the company J. & E. Hall in Britain in 1887 and they also improved the technology. The applications of these systems were primarily in marine refrigeration which was dominated by $CO_2$ up until the 1960's (Kim *et al.*, 2003).

Because of the restrictions placed on the use of flammable and toxic refrigerants such as ammonia ($NH_3$) and sulphur dioxide ($SO_2$) in Europe at the end of the 1900's, $CO_2$ was the only choice as refrigerant. $CO_2$ was widely used in refrigeration systems throughout the United States and since the 1900's in comfort cooling. Because of the safety of $CO_2$ over $NH_3$ and $SO_2$ it enjoyed preference in the use in public systems and on board of ships. Common disadvantages of $CO_2$ were low coefficient of performance (COP) and loss in capacity at high heat rejection temperature. The high pressure at which $CO_2$ was operated was also of concern, mostly because technology in sealing was lacking at that time and containment of the refrigerant was difficult. The loss of capacity and efficiency could be reduced by

operating the system at supercritical high side pressure and various two-stage operations (Kim *et al.*, 2003).

From the 1930's the so-called safety refrigerants were introduced. These refrigerants were primarily chlorofluorocarbons (CFCs) such as R-11, R-12 and R-13, and hydro-chlorofluorocarbons (HCFCs) such as R-22 and R-502. The introduction of these refrigerants brought about the replacement of all the old working fluids in most applications. The major argument for implementing these refrigerants was because of their improved safety. $CO_2$ was also replaced by the transition to CFC refrigerants (Freund, s.a.).

It was not until the 1970's that the disastrous effects of these refrigerants on the ozone layer were discovered. The CFC problem was becoming a pressing issue in the 1980's which lead to the phasing out of these refrigerants. Chemical alternatives first introduced by the chemical industry are the various hydrofluorocarbons (HFCs) such as R-134a, R-507 and R-407c. While the HFCs have no ODP they are still synthetic greenhouse gases, contributing greatly to global warming even more than the refrigerants they replaced. With all of these problems building up, the refrigeration industry was searching for viable alternatives (Kim *et al.*, 2003).

Figure 2.1 shows the progression of refrigerants over the years according to Calm (2008).

Figure 2.1: Refrigeration Progression (Calm, 2008).

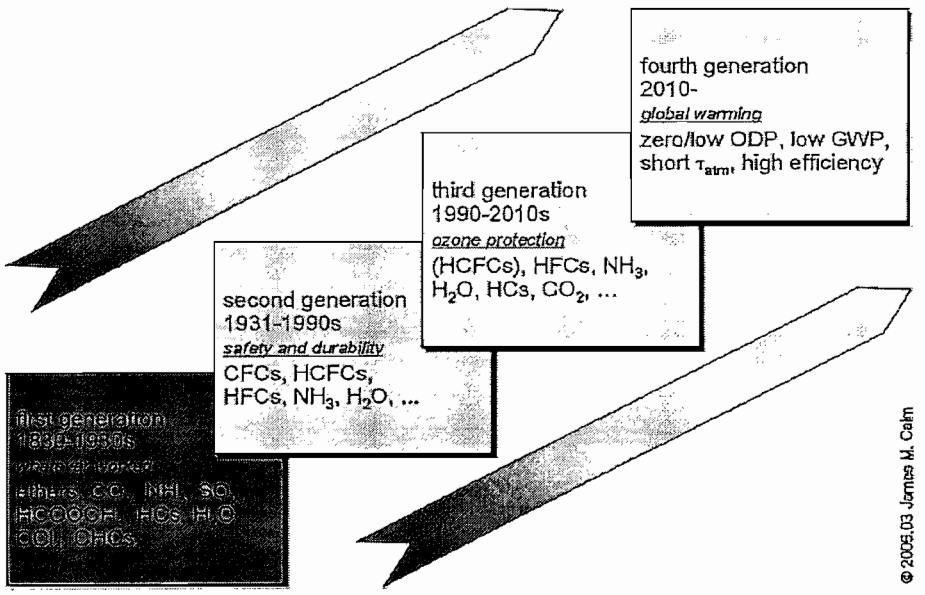

The $CO_2$ renaissance started with Professor Gustav Lorentzen in Norway. In 1989 he devised a 'trans-critical' $CO_2$ cycle, where he controlled the high side pressure with a throttling valve. This was intended for automobile air conditioning which was identified as a main contributor to CFC emissions. There was also a need for a refrigerant that was non-flammable or non-toxic. The experimental results for the first prototype $CO_2$ system for automobile air conditioning were published in 1992 by Lorentzen and Peterson. A comparison was made between a conventional R-12 system and a $CO_2$ system with the same capacities. Simple cycle calculations made beforehand showed that the $CO_2$ system will have inferior efficiency against the conventional R-12 system but a number of practical factors resulted in the two ending up having the same efficiency.

From results found in the early development of $CO_2$, interest in $CO_2$ as refrigerant started to increase throughout the 1990's, despite resistance from the fluorocarbon and automotive industries. Over the years a number of development and co-operation projects were initiated in various sectors of the refrigeration industry (Kim *et al.*, 2003).

From the brief look at the history of the refrigerants used, it is clear that, as refrigerants evolved, no global approach has been implemented to simultaneously address the various issues surrounding global warming and the effect on the ozone layer. This is mainly because of the lack of knowledge and also because scientific evidence of the effects of refrigerants was not acknowledged (Bensafi & Thonon, 2007; Calm, 2008). Until recently man-made substances were used as refrigerants mainly because their environmental effect could only be identified on a long term basis. With HFCs introduced, the problem surrounding global warming is not resolved and with the worldwide climate change becoming an ever greater concern, the use of HFCs will be regulated (Bensafi & Thonon, 2007).

## 2.3 *Phasing out of CFCs, HCFCs and HFCs.*

This section will discuss the progress around the world towards the phasing out of CFCs, HCFCs and HFCs. The Montreal and Kyoto Protocols leading to the phasing out of the above-mentioned refrigerants will also be looked at. The phasing out of conventional refrigerants has a greater impact on industries around the world than can be imagined.

Evidence that the ozone layer was getting thinner because of man-made chemicals was overwhelming in the 1980's. In 1985 the United Nations Environmental Program (UNEP) and the World Meteorological Organization (WMO) coordinated the Vienna convention which provided the framework for the Montreal Protocol (UNEP, 2007). In 1987, the Montreal Protocol on substances that deplete the ozone layer (UNEP 1987) was brought about (McQuay, 2002). In the United States the production of CFCs was stopped at the end of 1995 due to the requirements of the Montreal Protocol enforced on developed countries. According to the Montreal Protocol, HCFCs are to be phased out by up to 65% by 2010, up to 90% by 2015 and fully by 2030 in developed countries (McQuay, 2002). According to Thonon (2006), the phasing out of R-22 is scheduled for 2011.

A framework on climate change was formed by the United Nations in the 1990's. Since 1992 over 172 countries including the U.S. ratified this agreement. In 1997 the international agreement was signed in Kyoto, Japan, hence the name Kyoto Protocol. The Kyoto Protocol strives to reduce carbon dioxide emissions by 5.2% from 2008 to 2012. Each country is left with the responsibility to reduce carbon dioxide emissions on their own. So far only the United Kingdom and Germany are on track to meet their goals (McQuay, 2002).

So far all CFCs are banned and out of production. HCFCs are still used but are already being replaced by HFCs, and HCFCs are to be phased out entirely by 2015. Restrictions on phasing out HFCs are already being put into place.

The public only took notice of the potential problems when the European Parliament voted for the phasing out of refrigerants universally to be used in automotive air conditioning on March 2004 (Bullard, 2004-5).

High restrictions are being put on Denmark for phasing out HFCs. HFCs were to be phased out since 1 January 2007 with the following exceptions (Danfoss, 2002a):

- Systems with up to 10 kg charge are allowed.
- Hermetically sealed air conditioners of up to 50kg are allowed.
- Cooling in mobile transport is allowed.
- Medical and lab equipment.
- Equipment on ships and used in the military are still allowed.

Non-compliance with these laws could incur hefty fines.

Switzerland was to start phasing out HFCs since 1 January 2003. Uses of HFCs are granted only where there is no replacement technology available. A license is needed to operate systems with more than 3kg charge HFC, and only if no substitutes are available. Norway will need to pay duty and a deposit if it is looking to use an HFC system. Germany is phasing out HFCs as well (Danfoss, 2002a).

From the article, NRTB (2005) it is quoted: "the Conservatives are committed to phasing out the use of hydro fluorocarbons, or HFCs, between 2008 and 2014". He continued, saying that "HFCs have solved one problem - they do not damage the ozone layer. But they have caused another - they contribute significantly to global warming. Their impact is some thousands of times greater than $CO_2$. HFCs currently account for two percent of the UK's greenhouse gas emissions and that will have doubled by the end of the first decade of the twenty first century".

The phasing out of all refrigerants including HFCs, which was thought to be the solution, is happening all around. Soon these refrigerants will not be produced any more and components for the use in these systems will not be produced either. From this we can make the assumption that if Europe, the U.S. and other developed countries continue with the phasing out of these refrigerants, the rest of the world will have to follow, whether they are required to or not.

All off the above created doubt about the long-term availability of HFCs. No profitable business who wants to remain successful can afford to be caught unprepared because of legislation banning the substances which play a key role in their products. Therefore the need for a replacement refrigerant is of great significance (Fleming *et al.*, 1992).

## 2.4 Properties of $CO_2$

It is important to understand the properties and characteristics of carbon dioxide (R-744) for the design of refrigeration systems.

At ambient temperatures and pressures, $CO_2$ is in its vapour phase. In solid state $CO_2$ will directly sublime into its vapour condition if the pressure is below 5.1 bar. $CO_2$ is present in the atmosphere at concentration levels of about 380ppm, where one ppm is equivalent to one cubic centimetre per cubic meter. Air that is exhaled by humans contains about 4% carbon dioxide. $CO_2$ is widely available since it occurs naturally and is also a by-product of fossil fuel combustion and also industrial applications. $CO_2$ will not support combustion or burn on its own therefore air with a carbon dioxide content of more than 10% will extinguish an open flame. Liquid or gaseous carbon dioxide that is stored under pressure will form dry ice through an auto refrigeration process if rapidly depressurized (Bensafi & Thonon, 2007). Figure 2.2 shows a comparison of evaporating pressures for conventional refrigerants including blends, HFCs and carbon dioxide.

Figure 2.2: Comparison of evaporating pressures (Bensafi & Thonon, 2007).

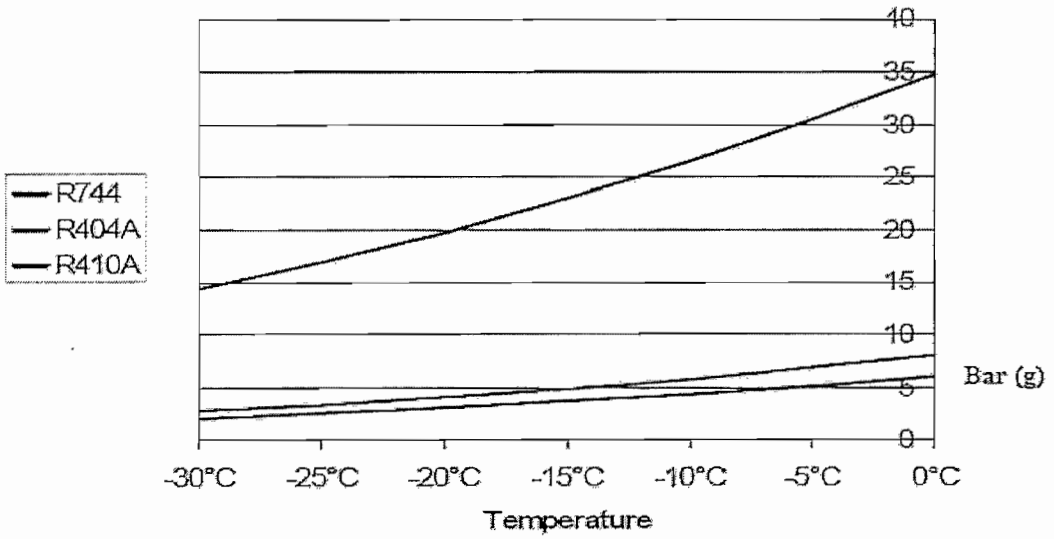


$CO_2$ has a much higher evaporating temperature than conventional refrigerants. It is noted that below a pressure of 5.2bar solid and gaseous carbon dioxide phases may occur at low temperatures. This behaviour is different from what could be observed from conventional refrigerants (Bensafi & Thonon, 2007).

Most refrigerants reject heat to the air through condensation at typical ambient temperatures; carbon dioxide operates at transcritical conditions. $CO_2$ evaporates in the subcritical region and rejects its heat at temperatures above its critical point in a gas cooler and not a condenser as conventional fluids (Bullard, 2004-5). Figure 2.3 shows the position of the critical point on a P-h diagram.

Figure 2.3: Critical point illustrated on carbon dioxide P-h diagram (Rasmussen, 2003).

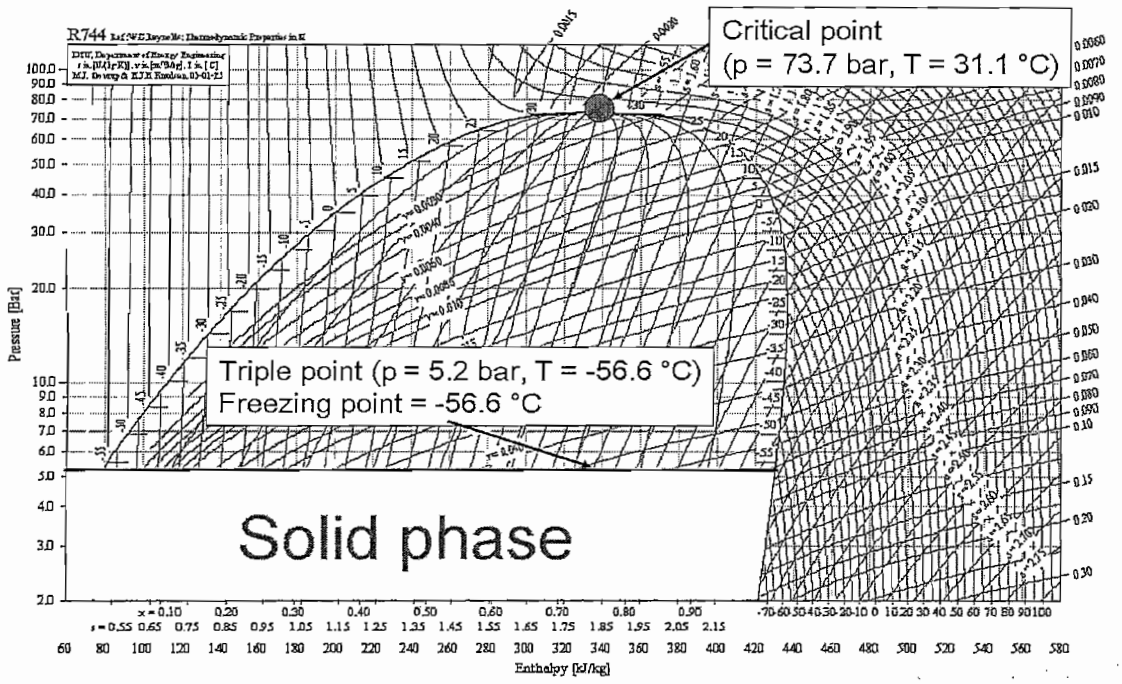


When the $CO_2$ system is operating above its critical point, the cycle takes on an additional degree of freedom relative to subcritical systems - which means the decoupling of the usual relationship between the normal pressure and temperature of conventional systems (Sienel, 2006). There are a few ways of controlling the operating pressure to give the acquired temperature gradient.

Table 2.2 shows some selected physical properties for Carbon Dioxide (Freund, s.a.).

Table 2.2: Physical Properties of Carbon Dioxide. (Freund, s.a.).

| Property | Value |
|---|---|
| Molecular weight | 44.01 |
| Critical temperature | 31.1°C |
| Critical pressure | 73.9 bar |
| Critical density | 467 kg $m^{-3}$ |
| Triple point temperature | -56.5 °C |
| Triple point pressure | 5.18 bar |
| Boiling (sublimation) point (1.013 bar) | -78.5 °C |
| *Gas Phase* | |
| Gas density (1.013 bar at boiling point) | 2.814 kg $m^{-3}$ |
| Gas density (@ STP) | 1.976 kg $m^{-3}$ |
| Specific volume (@ STP) | 0.506 $m^3$ $kg^{-1}$ |
| Cp (@ STP) | 0.0364 kJ ($mol^{-1}$ $K^{-1}$) |
| Cv (@ STP) | 0.0278 kJ ($mol^{-1}$ $K^{-1}$) |
| Cp/Cv (@ STP) | 1.308 |
| Viscosity (@ STP) | 13.72 μN.s $m^{-2}$ (or μPa.s) |
| Thermal conductivity (@ STP) | 14.65 mW (m $K^{-1}$) |
| Solubility in water (@ STP) | 1.716 vol $vol^{-1}$ |
| Enthalpy (@ STP) | 21.34 kJ $mol^{-1}$ |
| Entropy (@ STP) | 117.2 J mol $K^{-1}$ |
| Entropy of formation | 213.8 J mol $K^{-1}$ |
| *Liquid Phase* | |
| Vapour pressure (at 20 °C) | 58.5 bar |
| Liquid density (at -20 °C and 19.7 bar) | 1032 kg $m^{-3}$ |
| Viscosity (@ STP) | 99 μN.s $m^{-2}$ (or μPa.s) |
| *Solid Phase* | |
| Density of carbon dioxide snow at freezing point | 1562 kg $m^{-3}$ |
| Latent heat of vaporisation (1.013 bar at sublimation point) | 571.1 kJ $kg^{-1}$ |

Where STP stands for Standard Temperature and Pressure, which is 0°C and 1.013 bar.
Sources: Air Liquide gas data table; Kirk-Othmer (1985); NIST (2003).

Figure 2.4 shows the phase diagram for $CO_2$ and how its properties and its physical state changes by varying the pressure and temperature. Heat absorption or release takes place in each of its phase changes from solid-gas, solid-liquid and liquid-gas phases. However, if it changes phase from the transcritical condition to liquid or from transcritical to gas it does not require the release of heat. This is a useful design property for $CO_2$ compression facilities since it could avoid the heat handled associated with the liquid gas phase change (Freund, s.a). It could be seen that a low triple point is present, which means that the solid state could be reached under normal operating or pump down situations. This should be avoided since the forming of ice reduces the pressure and when the refrigerant returns back to a liquid or gas state the pressure will increase drastically and create a safety hazard.

Figure 2.4: Phase Diagram (Freund, s.a.).

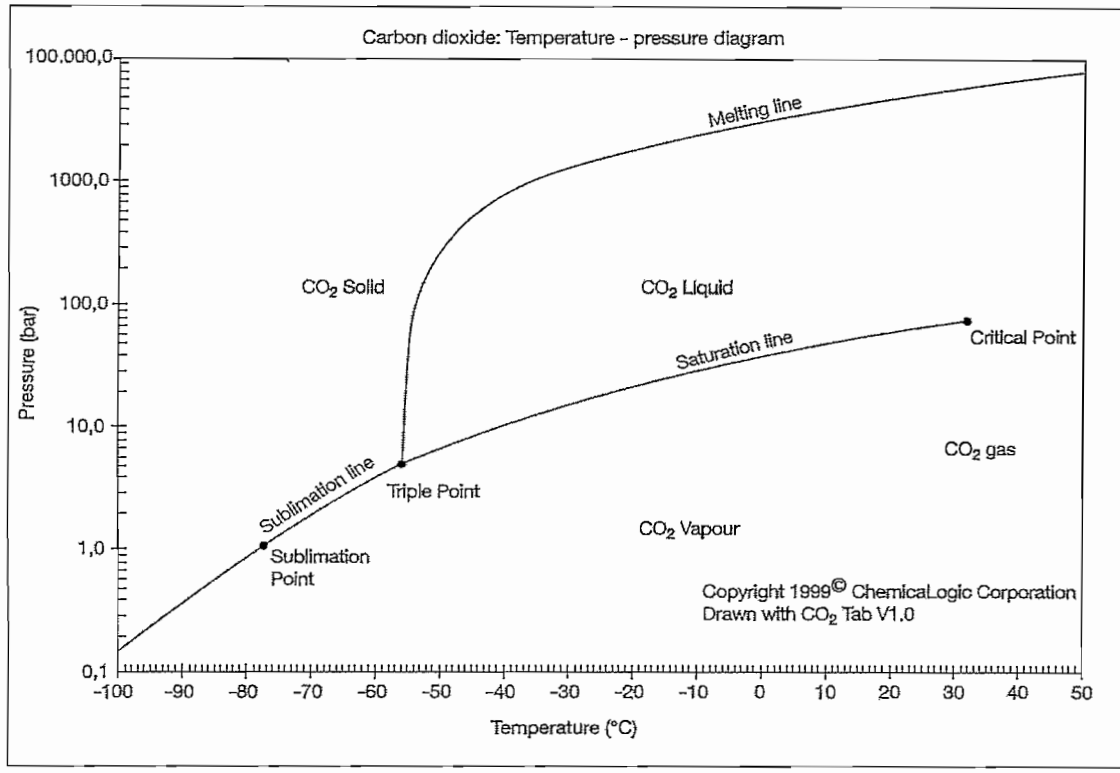


$CO_2$ has a much higher vapour pressure and volumetric refrigeration capacity than conventional fluids. Its volumetric capacity is 22,545kJ/m$^3$ at 0°C which is between 3 and 10 times higher compared to other fluids. The critical pressure and temperature for $CO_2$ is 73.8 bar and 31.1°C respectively, the pressure is very high compared to conventional systems. Therefore the operating pressure in the system will be 5 to 20 times higher than conventional systems. This is illustrated in figure 2.5, which compares the pressure-enthalpy diagrams of $CO_2$ and HFC-134a.

Above its critical point it is impossible for $CO_2$ to transfer heat to ambient conditions by condensation as in conventional vapour compression cycles. The heat transfer process for carbon dioxide takes place through gas cooling and this results in a system to be known as a transcritical system. In the supercritical region the high side pressure and temperatures are not connected and could be regulated independently to attain an optimum operating condition.

From the phase diagram shown in Figure 2.4 it could be seen that the temperature and pressure for the triple point is at -56.6°C and 5.2 bar respectively and its saturation at 0°C is at 35 bar. The triple point is known as the pressure temperature combination at which carbon dioxide can exist simultaneously in its three states. If

the pressure is reduced the liquid flashes to gas and ice. If the temperature is reduced the liquid will freeze. If the temperature is increased the liquid boils and forms a gas (ANON (a), s.a.). Its reduced pressure at 0°C is at 4.7 bar which is much higher than for conventional refrigerants. Because of its high reduced pressure and its low critical point, sub-critical operation will be much closer to the critical point than for conventional systems (Kim *et al.*, 2003). Carbon dioxide dissolves readily in most liquids. The higher the pressure the more $CO_2$ will dissolve in a certain liquid. When dissolved in water, carbonic acid ($H_2CO_3$) will form which is quite weak and unstable and will tend to revert back to $CO_2$ and $H_2O$. $CO_2$ is about 53% heavier than air and would settle on the ground if released freely, (ANON (a), s.a.).

Figure 2.5: Comparison of the P-h diagrams for R-134a and $CO_2$ (Stene, 2007).

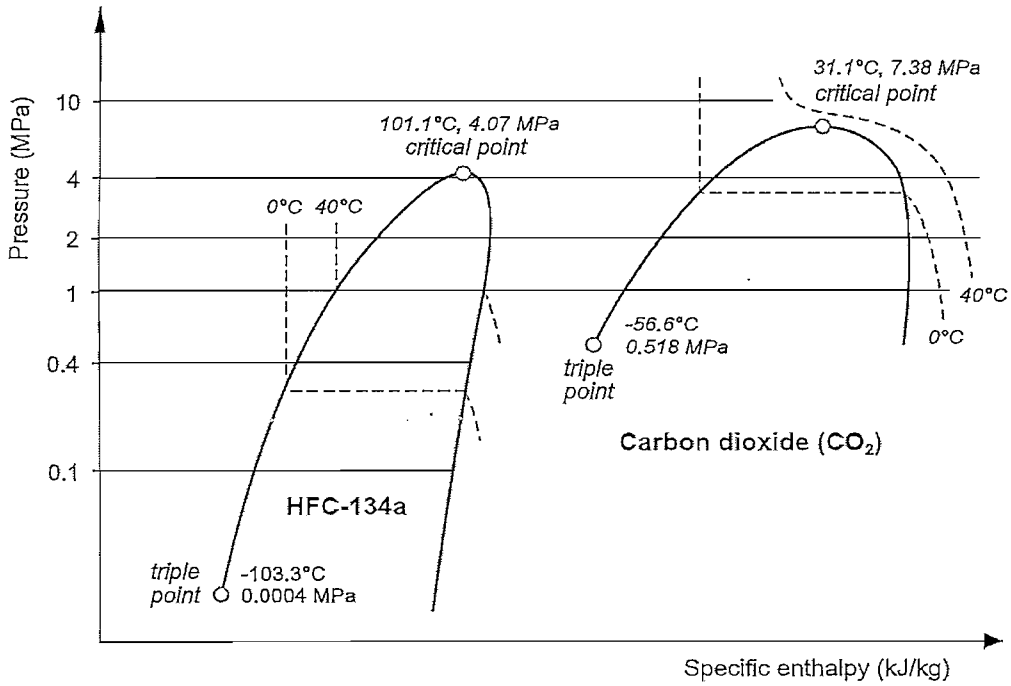

Figure 2.6: Enthalpy change of $CO_2$ in the gas cooling process. (Kim et al, 2003).

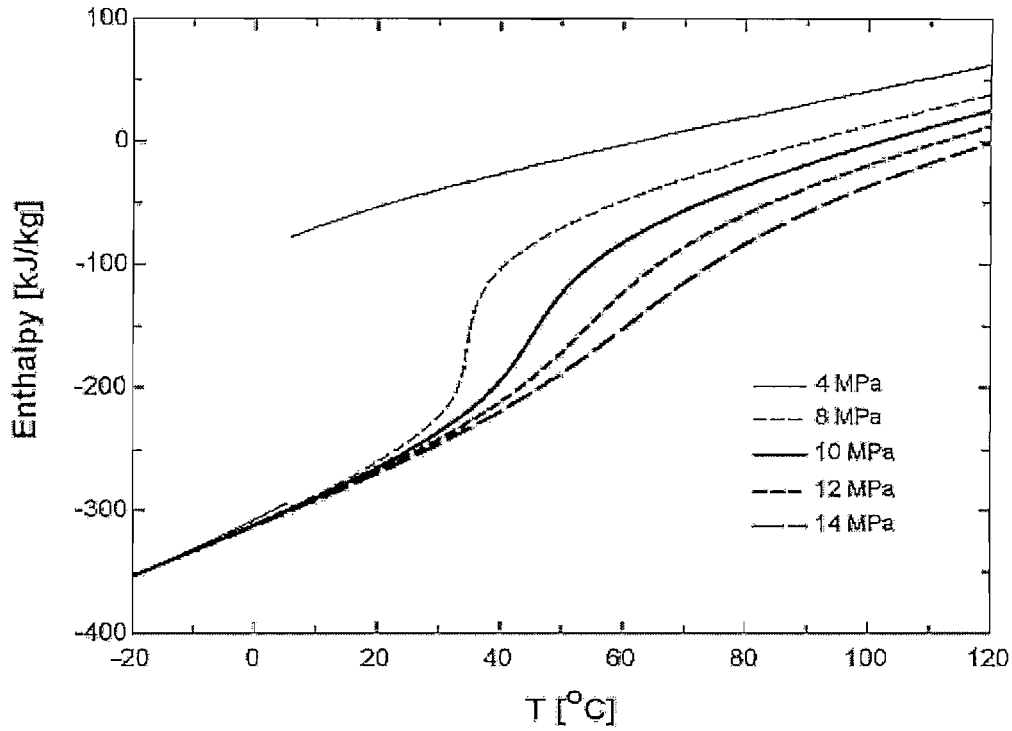


Figure 2.7: Entropy change of $CO_2$ in the gas cooling process. (Kim et al, 2003).

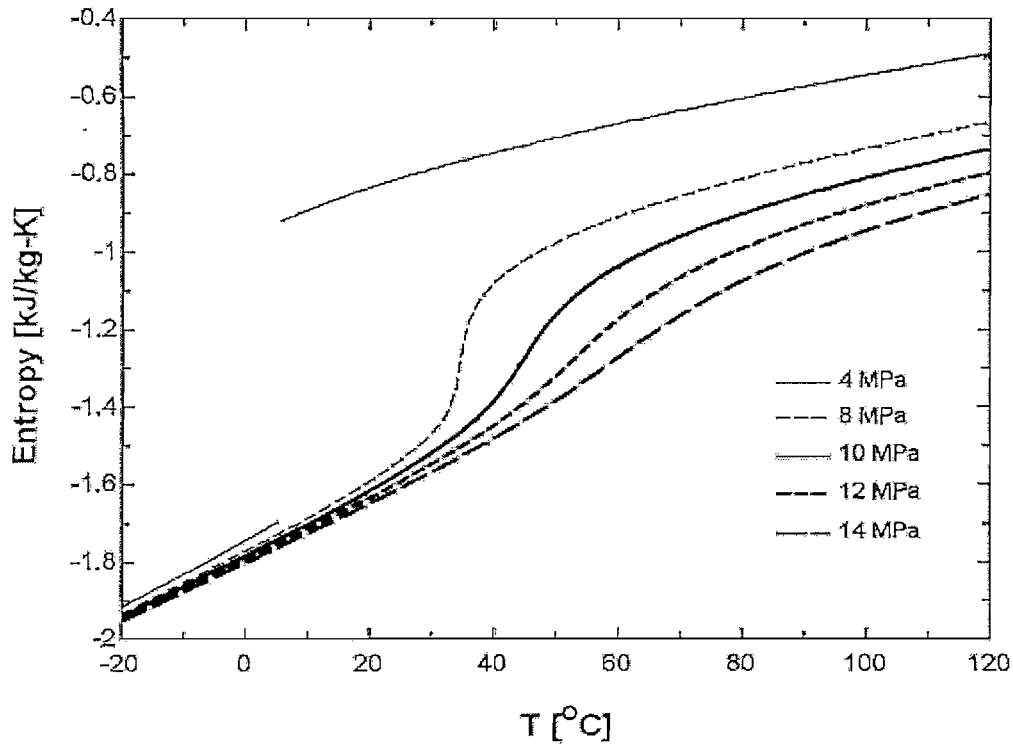


Figures 2.6 and 2.7 show how the enthalpy and entropy of $CO_2$ changes in the gas cooling process at constant pressures. The enthalpy and entropy decreases with temperature in the super-critical region. More distinct changes in enthalpy and

entropy take place near the critical point. Above the critical point pressure has an influence on the entropy and enthalpy but pressure has less effect on the entropy and enthalpy under the critical point because pressure drops may be allowed to be higher (Kim *et al.*, 2003). It could be seen that at higher pressures the entropy and enthalpy changes more linear because it is further away from the critical point. The change of enthalpy and entropy in the sub-critical region is represented by the 4MPa pressure line and it could be seen that change under the critical point is linear.

Figure 2.8: Vapour pressure for different refrigerants. (Kim et al, 2003).

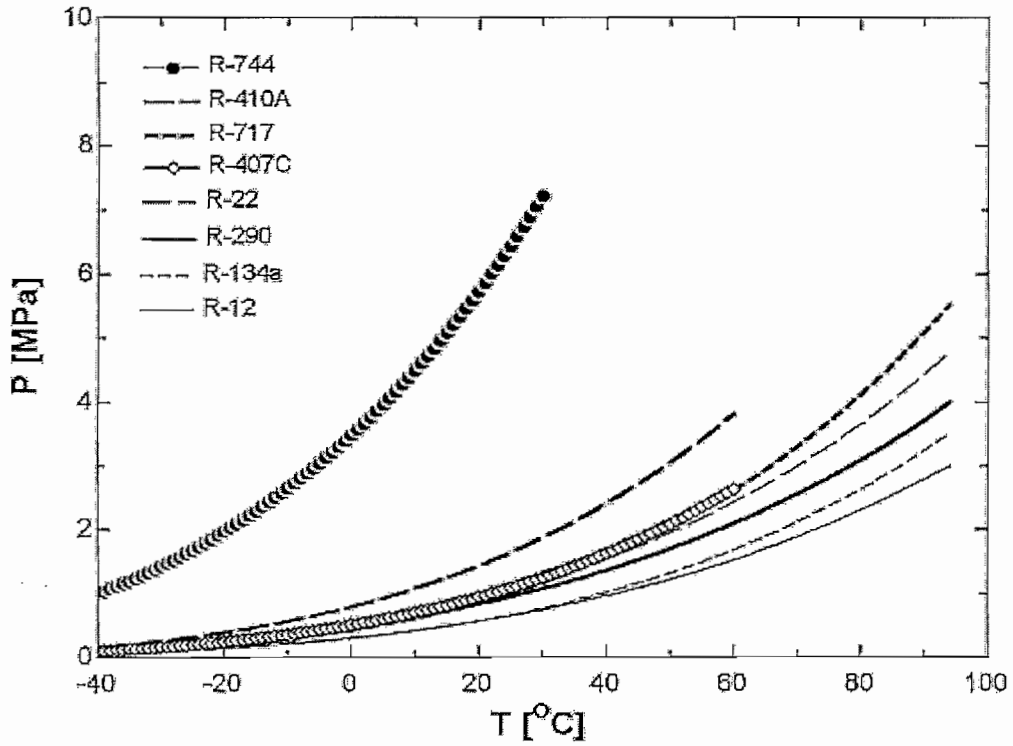


The vapour pressure and the slope of saturation pressure curves are shown in Figures 2.8 and 2.9 respectively for $CO_2$ and other refrigerants. Compared to other refrigerants the vapour pressure of $CO_2$ is between 4 and 10 times higher. Near its critical temperature (31.1°C) the vapour pressure curve for $CO_2$ gets very steep, resulting in a smaller temperature change for a given pressure change. This means that the temperature change associated with pressure drop in the evaporator will be smaller. Because of the high vapour pressure and its closeness to the critical point, the characteristics of the liquid and vapour densities of $CO_2$ is to a large extent different (Kim *et al.*, 2003).

Although $CO_2$ operates at very high pressures and the difference between the suction and discharge pressure is very high, the pressure difference to be overcome

is negligible because it is actually smaller than for conventional refrigerants. This leads to the possibility of designing compressors with a relatively larger efficiency than for conventional refrigerants.

Figure 2.9: Slope of saturation pressure curve for different refrigerants. (Kim et al, 2003).

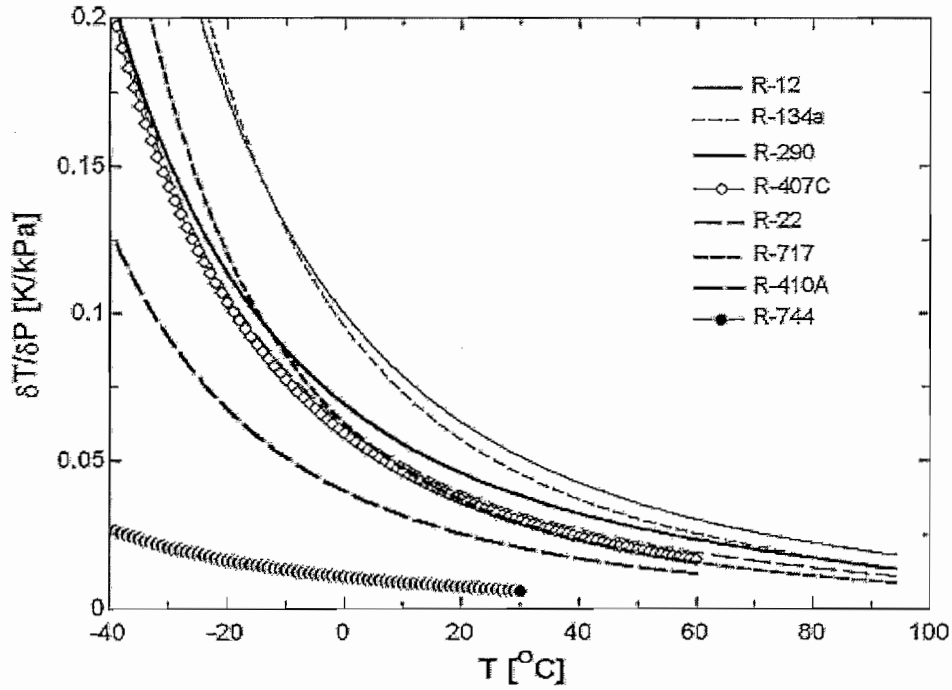


The density of $CO_2$ changes drastically near its critical point as a function of temperature and the density ratio is much less than for conventional refrigerants giving it a more homogenous two-phase flow. The above-mentioned is shown in figure 2.10. The density of $CO_2$ in its gas phase can be very large, approaching or even exceeding the density of water in its liquid phase (Freund, s.a.). The high vapour density of $CO_2$ gives it its unique high volumetric refrigeration capacity. The volumetric refrigeration capacity of $CO_2$ increases as the temperature increases, but reaches a maximum at 20°C and then starts to decrease again (Kim *et al.*, 2003). This is shown in Figure 2.11.

Figure 2.10: Variation of density as a function of temperature and pressure (Freund, s.a.).

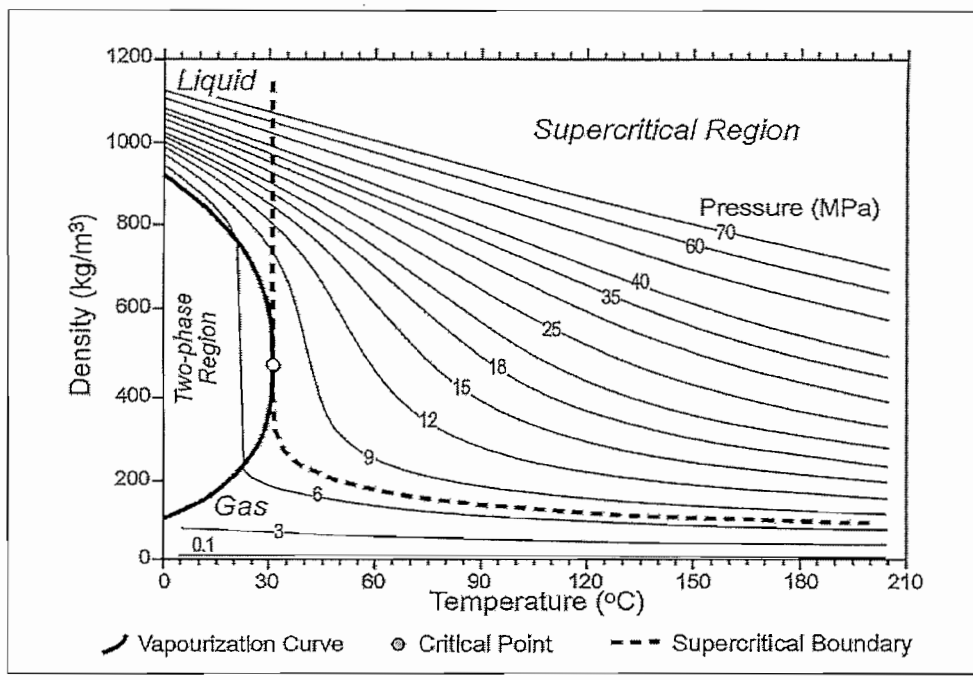


Figure 2.11: Variation of Volumetric refrigeration capacity for refrigerants (Kim *et al.*, 2003).

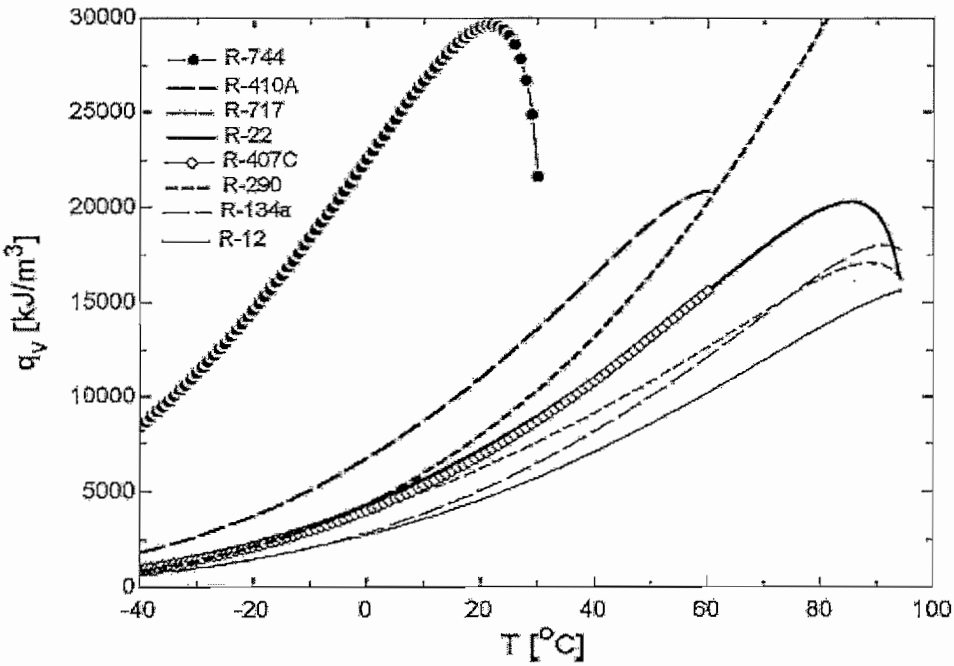


According to Kim *et al.* (2003), one of the most important characteristics of a super-critical fluid near its critical point is that the fluid properties change rapidly as the temperature changes in an isobaric process and especially near the pseudo-critical point (the temperature at which the specific heat becomes a maximum for a given pressure). This phenomenon is shown in Figures 2.12 and 2.13, where the isobaric

specific heat and pseudo-critical temperature is depicted. At different temperatures it could be seen that the specific heat (Cp) changes drastically as the temperature rises. The temperature at which the specific heat reaches a maximum is called the pseudo-critical temperature and the higher the pressure is, the higher the pseudo-critical temperature. The peak of the $CO_2$ specific heat also decreases as the pressure rises (Yang *et al.*, 2006).

Figure 2.12: Isobaric specific heat for $CO_2$ (Kim *et al.*, 2003).

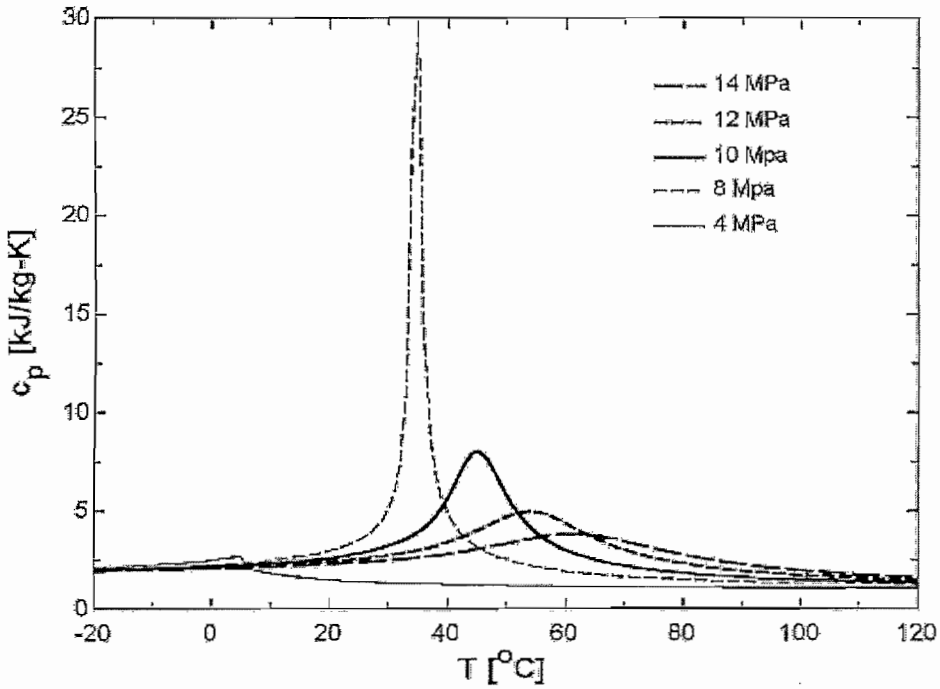


Should the ε-NTU or LMTD-method be used to attain data, one should find out whether the specific heat is constant, because these methods require the specific heat to be constant over the test section (Kim *et al.*, 2003).

Figure 2.13: Pseudo critical temperature and maximum isobaric specific heat for $CO_2$ (Kim *et al.*, 2003).

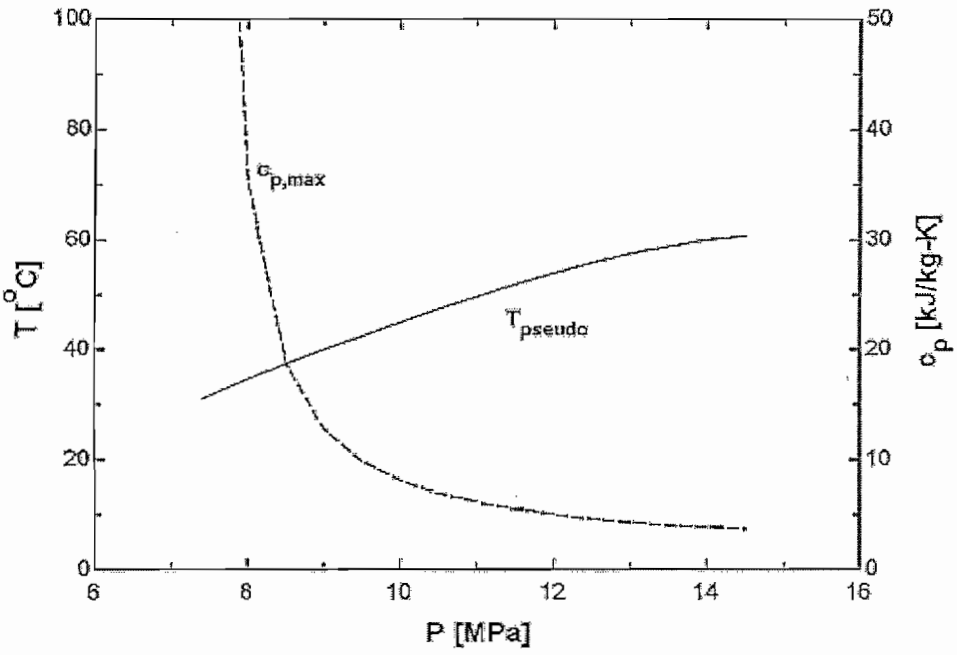


Transport properties of a refrigerant play an important role when it comes to the heat transfer and pressure drop characteristics. Figures 2.14 and 2.15 give schematics of the important transport properties *thermal conductivity* and *viscosity* at sub-and supercritical pressures.

Figure 2.14: Thermal conductivity of $CO_2$ (Kim *et al.*, 2003).

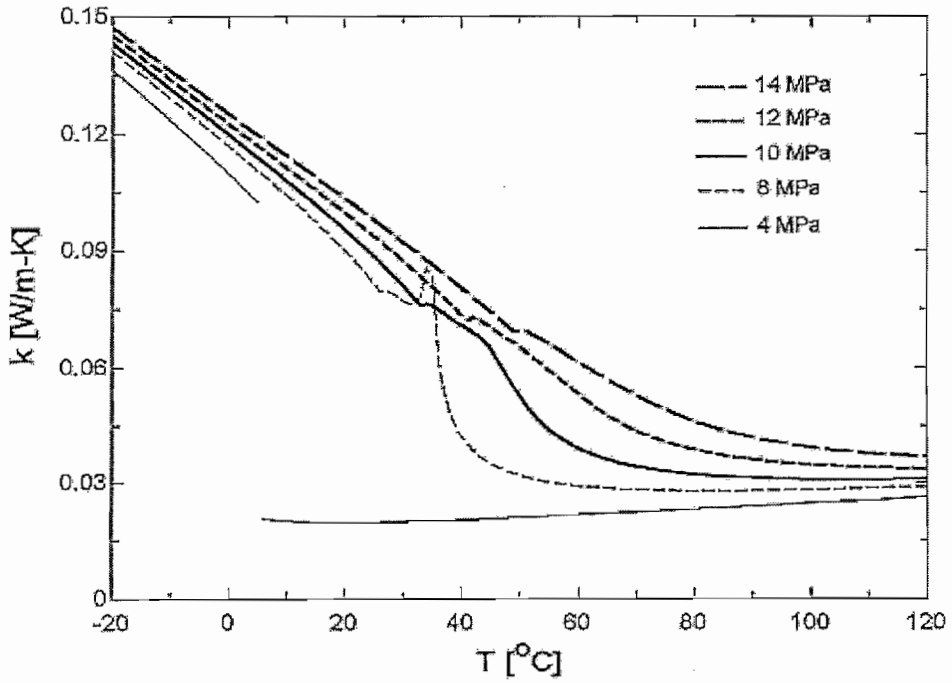

The conductivity of $CO_2$ is increased as the temperature of the refrigerant decreases. Therefore heat transfer is high near the pseudo-critical temperature (Yang *et al.*, 2006). For both single- and two-phase flow a high thermal conductivity is essential for the heat transfer coefficients. Viscosity and in particular that of the liquid phase and the ratio of liquid to vapour viscosity, are important parameters when it comes to the fluid flow behaviours, convection characteristics, two-phase heat transfer and the pressure drop. For saturated $CO_2$ liquid and vapour at 0°C the thermal conductivities are 20% to 60% higher than that of R-134a liquid and vapour. The viscosity of $CO_2$ liquid is 40% higher than the viscosity of R-134a liquid and the vapour viscosities of the two refrigerants are comparable.

Figure 2.15: Viscosity of $CO_2$ (Kim *et al.*, 2003).

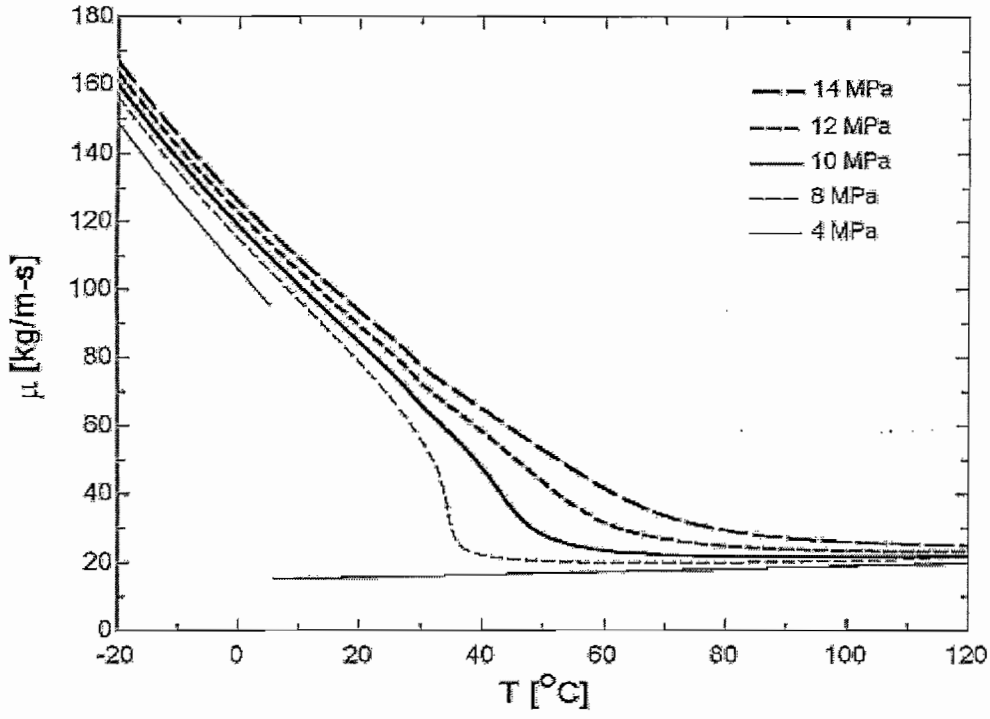


The Prandtl number plays an important role in the heat transfer coefficients. It is associated with the specific heat and thus has a maximum at the pseudo-critical temperature and the maximum value decreases with pressure. The Prandtl number gets higher at temperatures exceeding 60°C in the super-critical region.

It could be said that the thermodynamic and transport properties of $CO_2$ seem to be favourable in terms of heat transfer and pressure drop when taking in account other refrigerants (Kim *et al.*, 2003).

Figure 2.16: COP of a transcritical $CO_2$ heat pump as a function of the $CO_2$ outlet temperature from the gas cooler and the evaporation temperature (Stene, 2007).

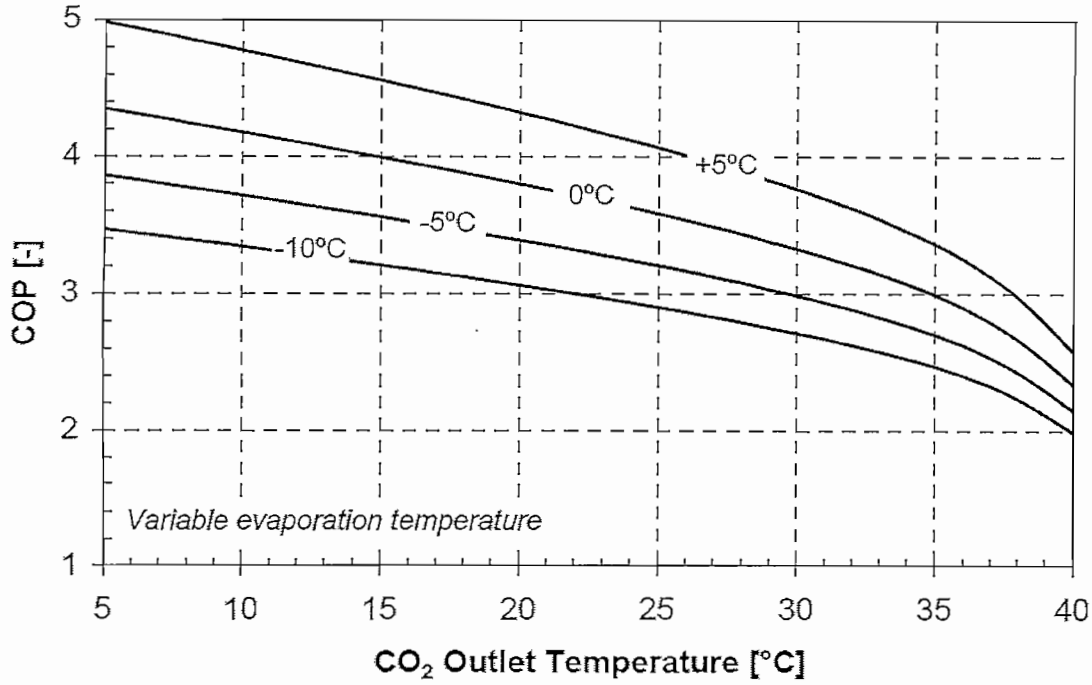


From Figure 2.16 it could be seen that the COP of the heat pump system is dependent on the evaporating and also the gas cooler outlet temperature. Studies made by Stene (2007) show that for a higher gas cooler outlet temperature the lower the COP will be, but for a higher evaporating temperature the higher the COP will be.

The heating capacity and COP of a transcritical $CO_2$ heat pump system are affected by the high-side pressure. Figure 2.17 illustrates the transcritical cycle in a temperature-enthalpy diagram for high-side pressures ranging from 8 to 11MPa. The evaporating temperature was kept constant at -5°C and the gas cooler outlet temperature was kept constant at 35°C.

It could be seen that the inlet enthalpy to the gas cooler increases and the outlet enthalpy decreases as the high-side pressure increases. The change of enthalpy due to the change in temperature is not proportional to the change in specific compressor work and for each fixed outlet temperature from the gas cooler there will be an optimum high-side pressure leading to a maximum COP (Stene, 2007).

Figure 2.17: The transcritical $CO_2$ heat pump cycle operated at four different high-side pressures. The $CO_2$ outlet temperature from the gas cooler is assumed to be constant at 35°C (Stene, 2007).

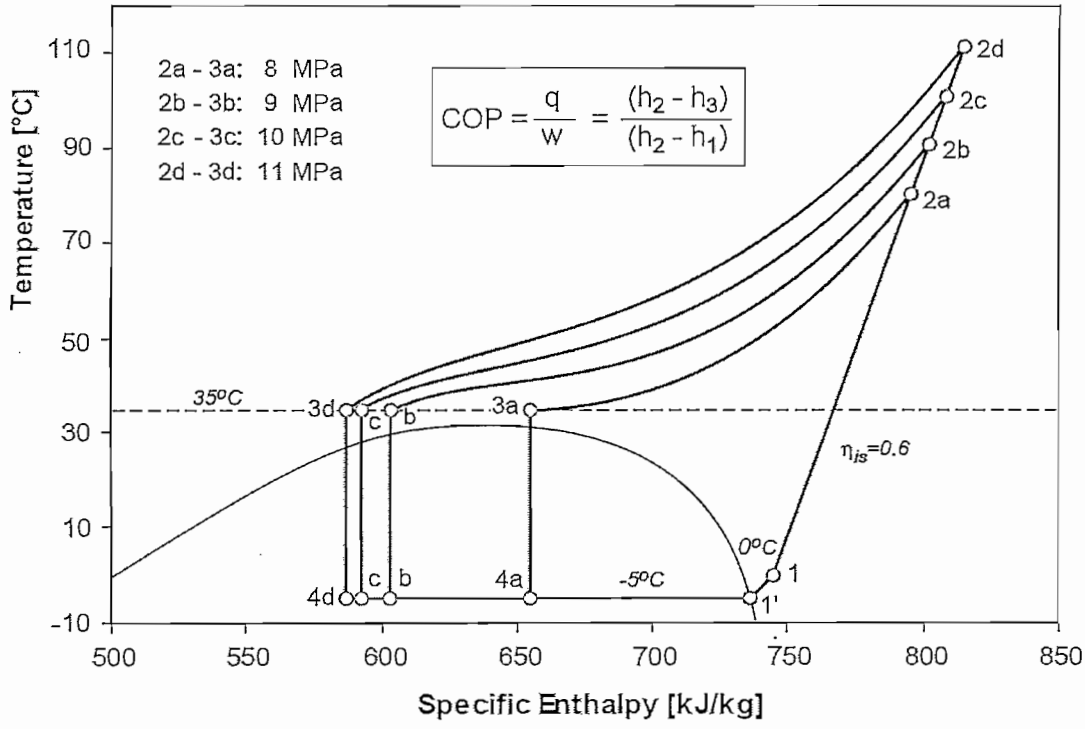

## 2.5 Applications of $CO_2$

This section provides a brief overview of some $CO_2$ applications.

### 2.5.1 Cascade systems

Cascade systems are widely used for commercial refrigeration in places like supermarkets. According to Palandre (2004) conventional commercial refrigeration has the largest emissions, contributing to about 37% within its sector. Leakage on these systems is reported to be up to 30% of the total refrigerant charge. This resulted in a need for a safe, efficient and environmentally friendly solution (Neksa *et al.*, 1998).

$CO_2$ is used in cascade systems operating at its sub-critical region with another refrigerant for the high temperature side. Recent studies are also looking at using $CO_2$ in the high temperature side in its transcritical state (Neksa, 2002). Figure 2.18 shows a Ph-diagram of a cascade system using $CO_2$ in the low-temperature region and R404A in the high-temperature region (Lukitobudi, s.a.).

Figure 2.18: P-h diagram for cascade system $CO_2$/R404A (Lukitobudi, s.a.).

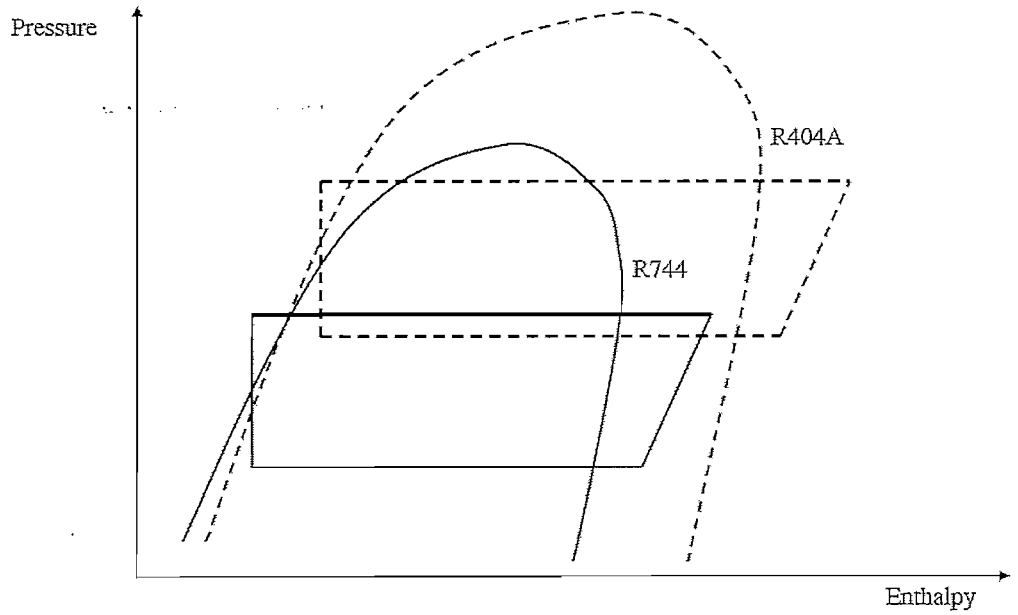


Some of the advantages about $CO_2$ cascade systems are the reduction in low-temperature compressor size, no liquid pump is necessary, fewer stages are

necessary for heat transfer, smaller pipe sizes are required and its safety aspect is advantageous (Neksa *et al.*, 1998).

By using $CO_2$ in the transcritical high temperature side of a cascade system a large temperature glide can be attained with a low volume flow rate resulting in small pipe dimensions. Waste heat from the high temperature side could be implemented towards the use of tap water heating. According to Neksa *et al.* (1998), a comparison of a $CO_2$ system and a conventional R-22 system has resulted in a decrease of up to 32% in energy consumption. The Coca Cola Company and McDonalds has also announced that $CO_2$ as refrigerant is a good alternative to HFCs in the use of their systems (Neksa *et al.*, 1998). Figure 2.19 shows the principle diagram for a cascade system used in supermarket refrigeration (Danfoss, 2002b).

**Figure 2.19: Principle diagram $CO_2$ cascade system with 2 temperature levels (Danfoss, 2002b).**

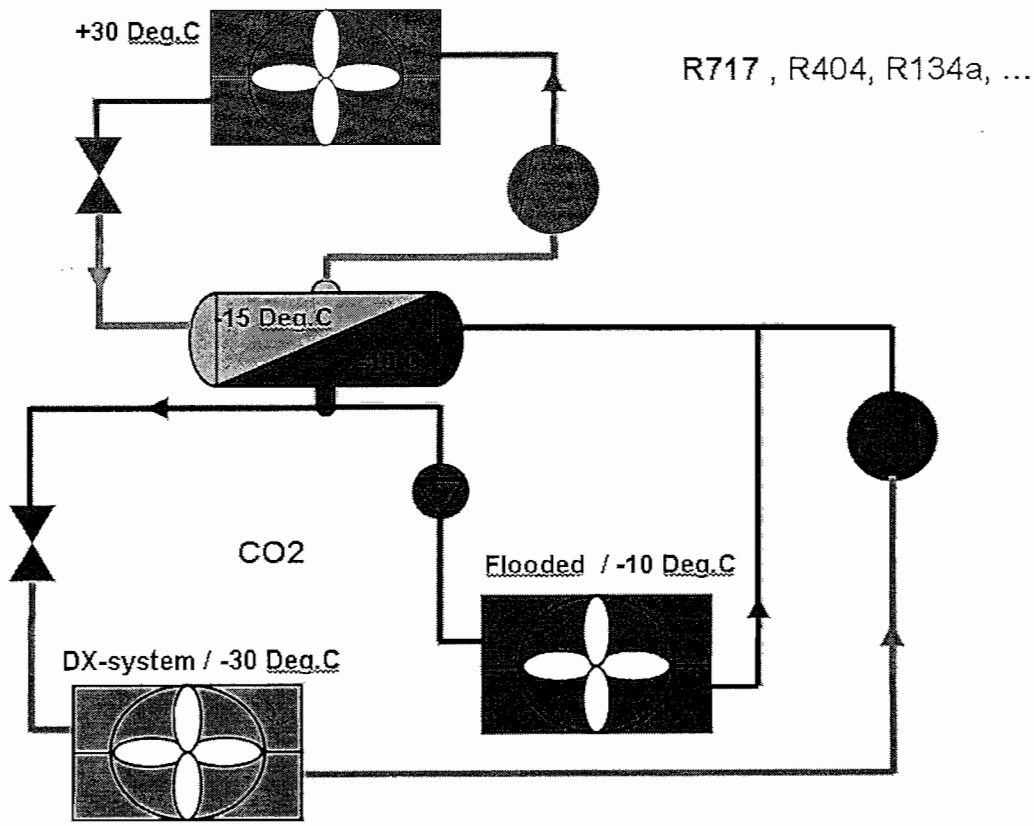


In 2008 Australia implemented their first full $CO_2$-based supermarket installation. The system was operated under the worst summer conditions in Australia having

temperatures of up to 40°C. After two months of operation it was shown that the $CO_2$ system used less electricity than the conventional R-404 systems. This implementation was the first big step in showing the viability of $CO_2$ in high climate conditions and not only in the cooler regions such as Europe where most tests on $CO_2$ usage are done. A big interest in implementation of these easy-to-install systems has been sparked under leading retail groups, according to R744.com (a).

### *2.5.2 Mobile air conditioning and heating*

A dominating source of refrigerant emissions into the atmosphere is mobile air conditioning; therefore reducing these emissions are necessary. According to Neksa (2002), the EU-commission is working on legislation to completely phase out HFC-134a in mobile air-conditioning. The current proposal is to completely ban the use of R-134a in all new vehicles from 2011. According to Wang (2006) it was planned to have more than a 1000 busses with $CO_2$ air conditioners for the 2008 Beijing Olympics and even more for the Shangai world expo in 2010. Lorentzen and Pettersen were the first to publish experimental results on $CO_2$ in mobile air conditioning. An interesting result that came from the data was the fact that $CO_2$ had a competitive COP compared to R-12. Because of the positive results obtained, the automobile industry initiated several development projects and launched further studies on carbon dioxide systems.

Because of its good volumetric efficiency, a smaller and more compact $CO_2$ compressor could be manufactured, which is essential to mobile air conditioning. This small compressor was first shown in a published article by Parsch (2002). $CO_2$ has a high heat rejection temperature and this enables manufacturers to design a more compact gas cooler (Kim *et al.*, 2003).

Further studies compared $CO_2$ to R-134a as refrigerant of which results are shown in Figure 2.20. Comparable cooling COPs were found at most operating conditions. Equal capacity was attained at high operating temperatures of up to 54.4°C when the car is in its idling condition. When operated at ambient temperatures of less than 40°C the $CO_2$ system showed a higher COP of up to 40% compared to the baseline R-134a system COP (Kim *et al.*, 2003).

Figure 2.20: Measured performance of mobile air-conditioning (Kim *et al.*, 2003).

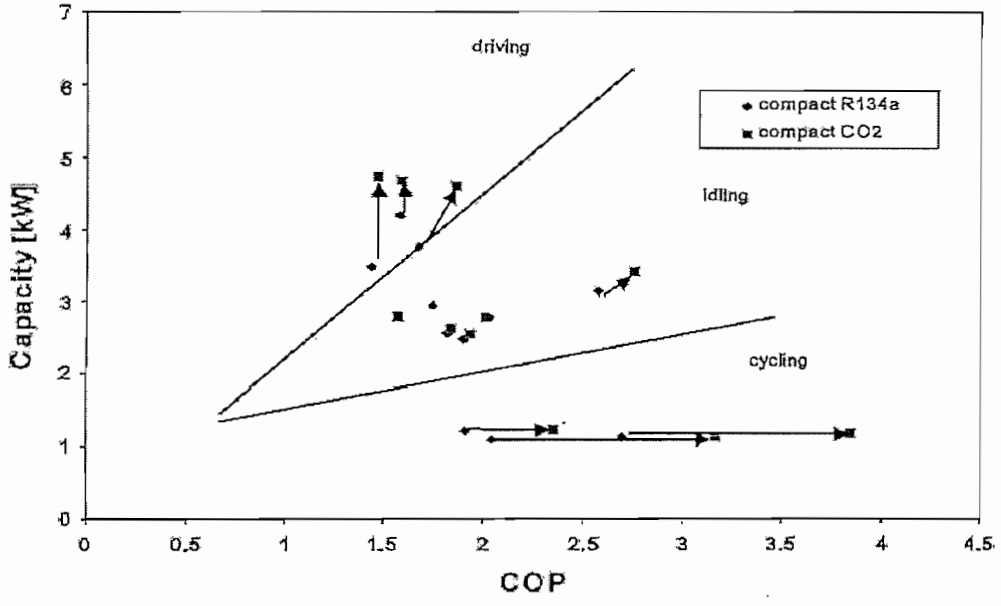


Conventional modern vehicles use waste heat for heating of the passenger compartment, which has a long heat-up period and slow defrost action. According to Neksa (2004) one possible solution could be to operate the air conditioning system as a heat pump. The heat pump systems could become an important factor for implementing $CO_2$ in mobile air conditioning applications. One problem anticipated in such an application is the freezing of the evaporator and defrosting thereof. There is a much greater heat up time than with conventional systems (Neksa, 2004).

### *2.5.3 Space heating*

The market for $CO_2$ heat pumps would be expanded to a great extent if the demand for space heating is investigated in-depth and implemented as is done with water heating. Systems that combine space heating with water heating are widely considered. This is also an efficient way of making use of the gliding gas cooler temperature for water heating (Neksa, 2002).

A comparison with a system using R-134a as a working fluid was made. It was shown that $CO_2$ had a more favourable seasonal performance for air heating applications than R-134a. A study done in Norway showed that larger buildings typically needed more than 50% of the total heat demand for the building in air heating applications and this is drastically increased as air quality demand is

increased. This makes $CO_2$ a promising candidate for use in these kinds of applications (Neksa, 2002).

Most studies on the use of heat pump technology for space heating concentrate on combining it with tap water heating. This contributes to a more efficient system where one application covers two heating demands. With the temperature glide found in the gas cooler it is made possible to make full use of heat pump applications for combined space heating and tap water heating (Neksa, 2002).

### *2.5.4 Heat pumps for Domestic Hot Water Heating*

#### *2.5.4.1 Conventional Heat Pumps for Domestic Hot Water Heating*

In a typical heat pump system as shown in figure 2.21, the evaporator extracts heat from a heat source at a low temperature. Through the evaporator, heat is absorbed by the low temperature fluid turning it into a low temperature gas as it absorbs the heat. The gas pressure is then increased by means of a compressor causing the fluid temperature to rise drastically, producing a heating effect which is exploited in heat pumps. The hot gas flows to the condenser where the heat is rejected from the working fluid and changes it from a gas to a liquid. As the working fluid is still at a high pressure it is passed through an expansion valve which reduces the pressure, producing a cooling effect which is used for refrigeration. By doing this the fluid returns to a liquid phase at low pressure. The working fluid then returns to the evaporator and the cycle starts over again (ANON (b), s.a.).

In conventional heat pump cycles which may use HFCs or HCFCs the liquefaction process occurs below the critical temperature of the refrigerant. The critical temperature is the point above which liquid cannot exist thus there it is referred to as a subcritical cycle. This cycle requires that the refrigerant critical temperature must be above the temperature at which the medium is rejecting its heat. Thus condensing of the refrigerant vapour yields a condensing pressure that is also below the critical pressure. The condensing pressure and temperature are linked by a unique relationship that depends on the nature of the refrigerant (Bensafi & Thonon, 2007).

A subcritical cycle using R-22 as refrigerant is discussed because it gives a good idea of a cycle operating in its subcritical region and because R-22 is the refrigerant

which will be used for comparison with $CO_2$ in the chapters to follow. Figure 2.22 gives the pressure-enthalpy diagram of a subcritical cycle using R-22 as refrigerant.

Figure 2.21: Principle schematic diagram of a heat pump water heater (ANON (b), s.a.).

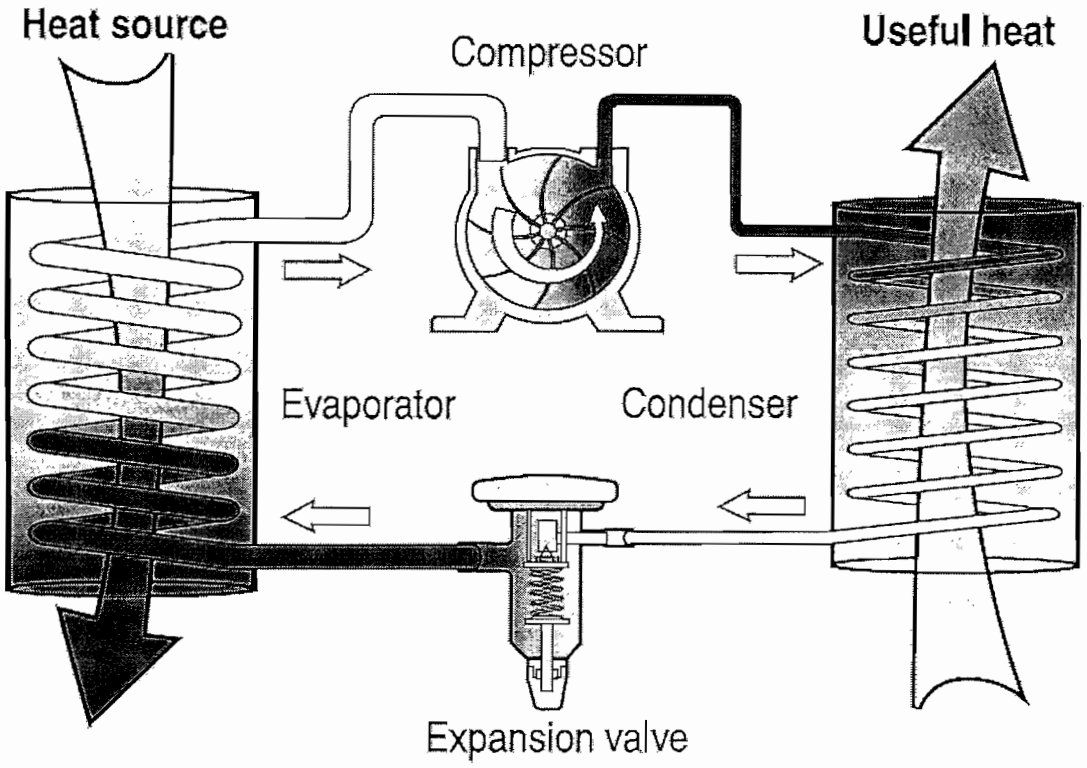

Figure 2.22: A subcritical cycle using R-22 as refrigerant (Bensafi & Thonon, 2007).

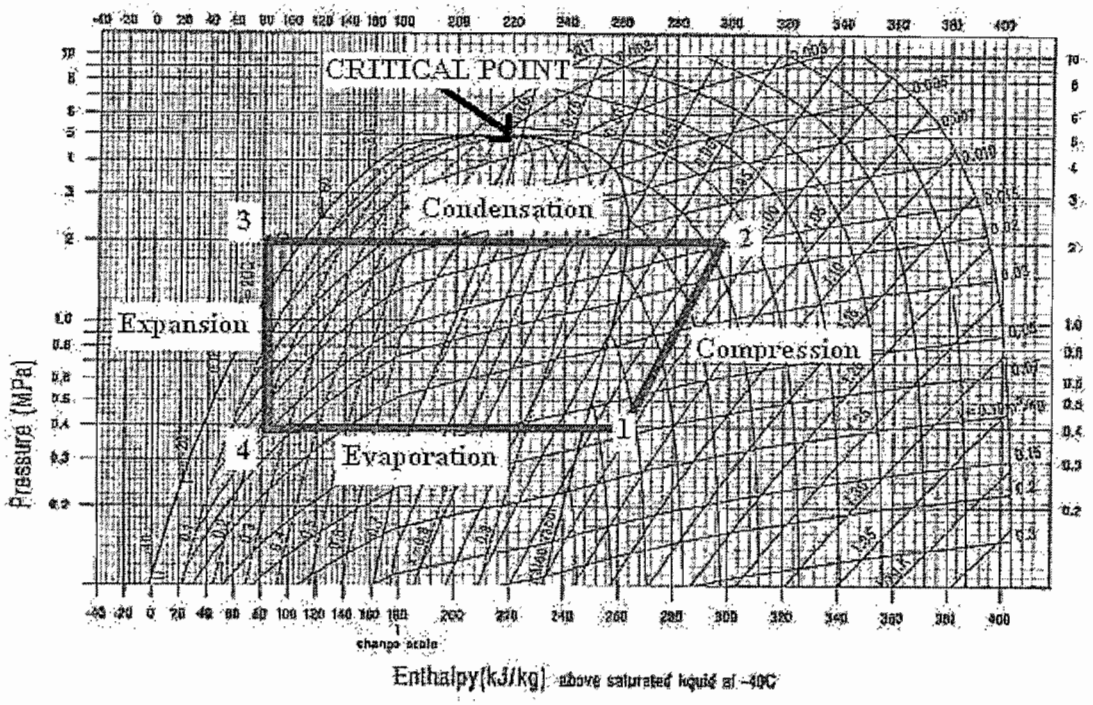


Conventional refrigerants have been chosen or designed to be condensed with an available medium such as air or water. This requires that their critical temperature must be above the temperature of the cooling medium. The critical temperature of R-22 is 96.2°C, which means that the available medium that will not go above 40°C, like the ambient air temperatures, will condense the R-22 at a temperature of about 55°C (Bensafi & Thonon, 2007).

Therefore it could be seen that heat pumps using conventional refrigerants such as R-22 will operate with a condensing pressure that depends only on the cooling medium conditions and on the refrigerant charge. The pressure at which the refrigerant will condense is much lower than the refrigerant critical pressure. The refrigerant flow rate is controlled by an expansion device in order to avoid the carry on of liquid droplets to the compressor (Bensafi & Thonon, 2007).

### *2.5.4.2 Transcritical Heat Pumps for Domestic Hot Water Heating*

In direct expansion vapour compression systems, $CO_2$ could be used as a refrigerant in its subcritical state if the medium temperature to be used is less than 20°C. Thus if the medium to be used is above 20°C, $CO_2$ will be used in its transcritical state. It is also found that a system that is working in its transcritical state can work just as

efficiently in subcritical operation. This means that a good seasonal COP is achievable with the use of $CO_2$ as refrigerant (Pisano, s.a.).

As mentioned earlier, the critical temperature of $CO_2$ is around 31°C therefore if ambient air is used to cool on the high pressure side and it is available at 30°C for example, it will not be able to condense the $CO_2$. Thus the refrigerant discharged from the compressor will be cooled as a supercritical fluid at a pressure higher than the critical pressure (Bensafi & Thonon, 2007). This cycle is illustrated in the Mollier diagram in figure 2.23.

Figure 2.23: A transcritical cycle using $CO_2$ as refrigerant (Bensafi & Thonon, 2007).

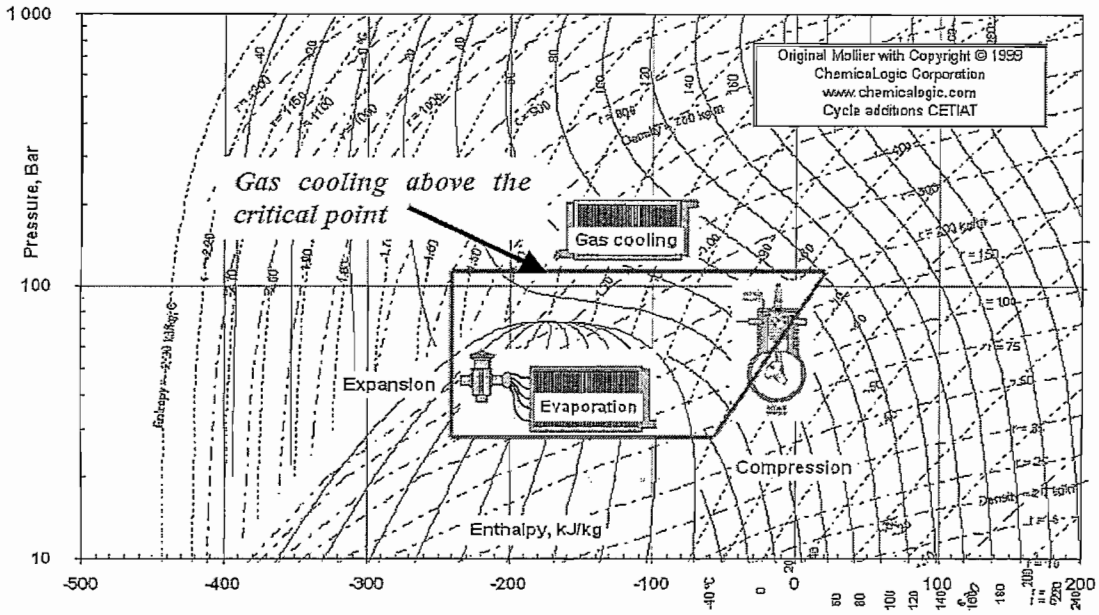


A transcritical cycle will therefore operate at pressures much higher than conventional systems. The high side pressure is no longer fixed by the cooling medium temperature or the flow rate of the refrigerant and therefore it is needed to control this parameter. It is also found that the more the refrigerant charge in the high pressure side, the higher the pressure will be (Bensafi & Thonon, 2007).

When using a transcritical cycle the gas cooler pressure is not a function of the $CO_2$ temperature because there is no relationship between temperature and pressure above the critical point. This means that the cycle can be operated at different values of high pressure which must be set by the control scheme i.e. the system pressure must be fixed by a control device so that the cycle can operate under its optimum condition (Bensafi & Thonon, 2007).

Table 2.3 gives the main differences between a transcritical $CO_2$ cycle and conventional systems.

Table 2.3: Main differences between Transcritical $CO_2$ cycle and subcritical cycle (Bensafi & Thonon, 2007).

| Cycle Parameters | Subcritical | Transcritical $CO_2$ |
|---|---|---|
| High pressure cooling - heat rejection device | Condenser - vapour condenses at constant temperature | Gas cooler - $CO_2$ undergoes large temperature change |
| Discharge pressure | HFCs : From 10 to 40 bars | From 90 to 130 bars |
| Suction pressure | HFCs : From 2 to 9 bars | From 25 to 50 bars |
| Refrigerant discharge temperature | Usually less than 95°C. | Up to 140°C. |
| Expansion device controls | By superheat set point or fixed flow expansion device. | Usually used to control high pressure of $CO_2$. |
| High pressure controls (excluding safety shut down controls) | Not controlled - pressure is set by condensation temperature - usually 40 bars max | Required - up to 130 bars |
| Refrigerant state at standstill | Partly liquid and partly vapour. | Gas (supercritical) above 31°C ambient; vapour-liquid mixture below 31°C. Can become solid upon cooling below P<6 bars! |
| System pressure at standstil (T ambient >31°C) | Refrigerant vapour pressure at ambient air temperature. | At least 74 bars - can be higher, depending on charge and temperature. |

Because of the high critical temperature value of conventional refrigerants, the pressure standstill is a function of the ambient temperature. Even under severe ambient temperatures most of the HFC and HCFC refrigerants used have pressures of lower than 40 bar at standstill. For $CO_2$ systems at ambient temperatures less than 31°C the pressure is equal to the saturation pressure of $CO_2$. Therefore at a temperature of 31°C the standstill pressure will be up to 75 bar. When ambient temperatures reach a temperature of higher than 31°C all the $CO_2$ contained in the system will be under supercritical conditions. This means that the standstill pressure will be more than 75 bar depending on the ambient temperature, the mass of the refrigerant charged and the internal volume of the system (Bensafi & Thonon, 2007).

Thermal expansion of $CO_2$ is also an important factor to take into account when designing and planning to maintain a $CO_2$ heat pump cycle. Thermal expansion is the means at which $CO_2$ will expand from its liquid or its gas state as the ambient temperatures rise. Liquid $CO_2$ will expand from around 80 bar at a temperature of 10°C to a pressure of around 200 bar and higher, ranging from a change of ambient

temperatures between 10-50°C. Thermal expansion of $CO_2$ in its gas state is not as severe as from its liquid state, but should still be taken note of (Madsen, 2008).

According to Sarkar *et al.* (2004), it is found that $CO_2$ heat pumps can successfully be used for medium and high temperature processes. For heating applications, $CO_2$ is superior to other alternative refrigerant choices because of its good heat transfer capabilities. For process heat application $CO_2$ seems to have better performance than other alternative refrigerants.

According to ANON (b) (s.a.) heat pumps can save up to 1.8 billion tonnes of $CO_2$ emissions per year resulting in a saving of up to 8% in global $CO_2$ emissions This is the equivalent of planting 50 million hectares of trees. In hotels, hospitals, apartment buildings etc. the annual energy demand for heating water typically range between 25% - 60%, (Stene, 2004).

Due to the demand for hot water heaters in Japan, a $CO_2$ heat pump water heater was developed under the brand name "Eco-Cute" and sale thereof started in February 2002. It is able to generate hot water up to 90°C with an average annual COP of above 3 (Kasai & Shibata, 2003).

The high energy efficiency of the $CO_2$ heat pump is due to the good temperature fit between $CO_2$ and the water in the gas cooler, the excellent heat transfer properties of $CO_2$ and due to the high compressor efficiency (Stene, 2004). A schematic representation of a principle $CO_2$ heat pump water heater is given in Fig 2.24.

Stene (2004) did a study where he compared four different kinds of heat pump designs with each other. The four designs were:

1) Heat pump with condenser and desuperheater;
2) Heat pump with sub-cooler, condenser and desuperheater;
3) Heat pump with suction gas heat exchanger, condenser and desuperheater; and
4) $CO_2$ heat pump with a single counter-flow gas cooler.

The first three designs were tested with R-134a and R290 and the last heat pump design used $CO_2$ as a refrigerant. All of the above-mentioned designs were tested at the same conditions and the results were compared.

Figure 2.24: Principle schematic of a $CO_2$ heat pump water heater (Stene, 2004).

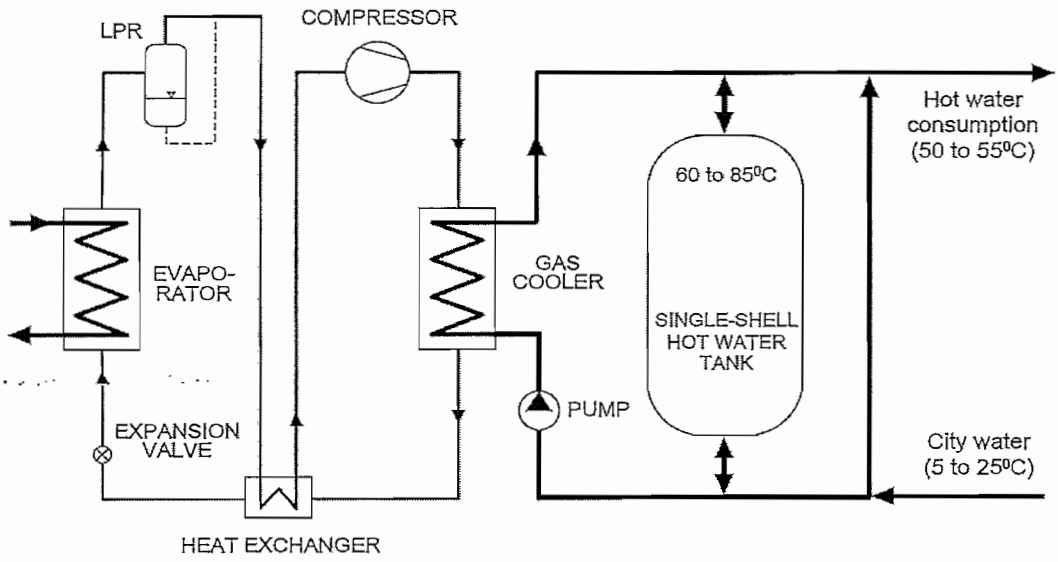


From Stene's results it was evident that the $CO_2$ system had on average a 20% higher COP than the best performed system between systems 1 – 3. This is most likely due to the higher compressor efficiency and the good temperature fit in the gas cooler between the water and $CO_2$. Figure 2.25 shows the calculated COP values for the different heat pump water heating systems as a function of the evaporation temperature. The calculations were based on the assumptions of a total UA-value of 2100 *W.K* for the gas cooler/condensers and evaporators, 5°C inlet water temperature and an outlet water temperature of 70°C (Stene, 2007).

Figure 2.25: Calculated COP as a function of evaporation temperature. (Stene, 2007).

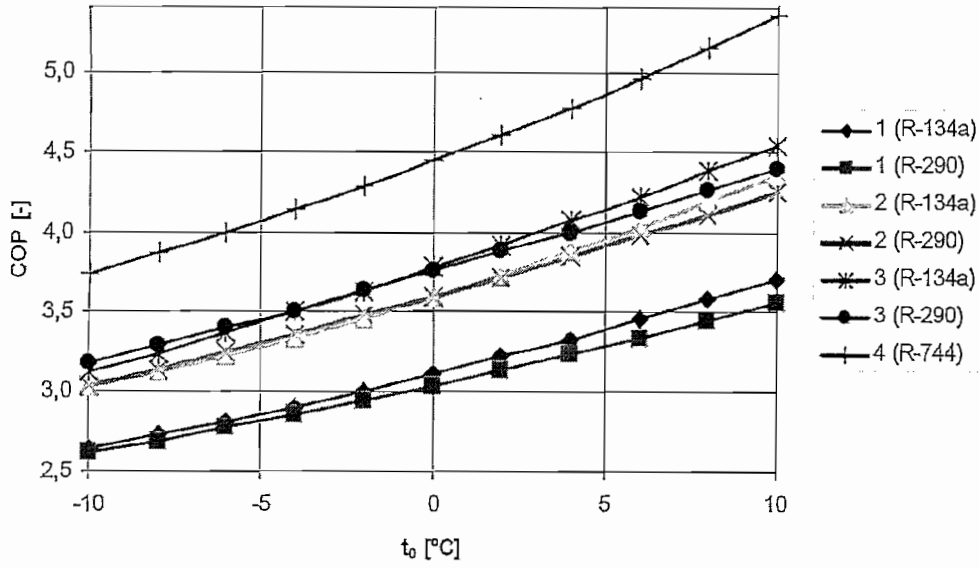


According to the results from Stene (2007), profitability was determined. It was found that when groundwater at a temperature of 7°C was used as the heat source, the calculated seasonal performance factor was approximately 3.8 for the $CO_2$ heat pump water heater, resulting in an approximate annual energy saving of 70-75% compared to conventional domestic hot water systems that uses electric immersion heaters. It also corresponds to an approximate 20-35% higher saving than that of the Scandinavian domestic hot water systems which use high efficient solar based collectors with electric immersion heaters as backup (Stene, 2007). Figure 2.26 illustrates this schematically.

Figure 2.26: Primary energy demand and utilization of renewable heat for different hot water heating systems (electric immersion heaters, heat pump and solar heating) (Stene, 2007).

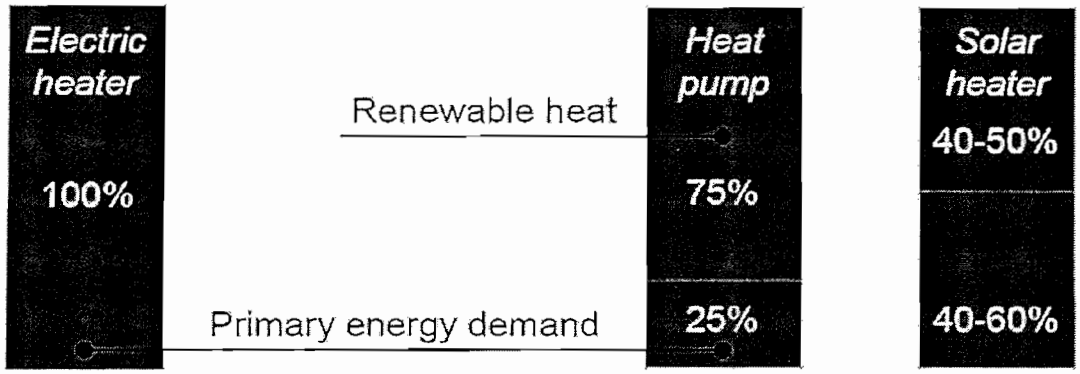


According to Chen *et al.* (2006), $CO_2$ has no pinch limitations in the heat exchanger and therefore the delta temperature between the refrigerant and the medium can

come close to one another. This also contributes to the fact that high temperature water outlet temperatures are attainable because of the temperature glide found in the transcritical heat exchanger. Conventional refrigeration systems are compared by operating the systems at the same boiling and condensing temperatures. Because $CO_2$ transfers heat through a gliding temperature, the mean temperature could be used to compare such a system with conventional systems (Chen *et al.*, 2006).

$CO_2$ systems have the same effect as conventional systems as far as the decrease in heating capacity is concerned, since the surrounding ambient temperatures also decrease (Zha *et al.*, 2006). This makes $CO_2$ a favourable option for South African applications where the ambient temperatures are high.
The rise in temperature for water heating matches the temperature glide of the refrigerant well, enabling the ability to provide hot water temperatures with a relatively small compressor ratio. Conventional systems are very efficient at low heating temperatures, but $CO_2$ systems show that the COP of the cycle decreases more slowly with increasing temperatures (White *et al.*, 2002). According to White *et al.* the maximum heating capacity to be gained from a $CO_2$ system decreased with about 33% and the heating COP decreased with about 21% as the hot water outlet temperature was increased from 65 to 120°C, yet the COP was found to be still close to 3 even at low evaporating temperatures and high water outlet temperatures. These studies were done at an evaporation temperature of -6.5°C. The reductions observed in the system performance and COP is relatively small compared to conventional systems, whereas conventional systems would have to make use of a multi stage system and will still have a COP of less than 2 (White *et al.*, 2002).

The properties of supercritical $CO_2$ vary rapidly at high inlet water temperatures making the design of the gas cooler very important (Fartaj *et al.*, 2004). The main components of the $CO_2$ system are the compressor, gas cooler, internal heat exchanger, evaporator and expansion valve. Figure 2.24 shows the typical layout of these components. The high temperature $CO_2$ enters the gas cooler where it rejects its heat to the water, in the gas cooler the heat is rejected with a glide at constant pressure. The high pressure $CO_2$ exiting the gas cooler is cooled by the low pressure $CO_2$ coming from the evaporator through the use of an internal heat exchanger. The cooled $CO_2$ expands through the expansion valve to a state of low pressure and low temperature refrigerant. Entering the evaporator it absorbs heat from the surrounding air causing the refrigerant to vaporize. Finally the low pressure $CO_2$ enters the

compressor where it is compressed to a high temperature and high pressure gas before entering the gas cooler (Fartaj *et al.*, 2004).

From the results of Sarkar (2007) it was noted that there is an increase in system COP of up to 75% when the evaporation temperature is varied from -10°C to 10°C. It was also found that the system COP increases sharply as the gas cooler outlet temperature decreases. For an evaporating temperature of 0°C the system COP almost doubles as the gas cooler exit temperature decreases from 50 to 35°C, (Sarkar, 2007). Therefore it could be seen that the system COP is dependent on the evaporation temperature, compressor efficiency, gas cooler outlet temperature, compressor discharge temperature and the heat exchanger effectiveness, and as a result attention should be given to these factors. From the results mentioned above the two factors that a designer has to take in account is to design a $CO_2$ system with the lowest possible gas cooler outlet temperature and the highest possible evaporation temperature. This is highly relevant for South African conditions since the ambient temperatures are usually high resulting in heat pump systems having a high evaporation temperature. It is only the gas cooler outlet temperature that would have to be looked at closely since the water inlet temperatures are also usually higher because of the high ambient temperatures. According to findings made by Sarkar *et al.* (2006), $CO_2$ systems can effectively be used in plants where temperatures of between 100°C and 140°C are required. Typically other refrigerants are not capable of reaching these temperatures. Although reaching these temperatures would lead to less efficient cycles, the high temperatures reached are worthwhile for some applications.

Constraints that arise from the very high operating pressure make it hard to design and manufacture basic components, but the industry is starting to solve these problems. The high density of $CO_2$ helps manufacturers to find solutions since the high density allows the use of smaller components (Cecchinato *et al.*, 2005). The storage tank for the hot water is also an important factor with regard to system efficiency. Good stratification is difficult to be obtained and this increases the inlet water temperature to the system thus decreasing system performance and also increasing the water flow rate, as illustrated in Figure 2.27. Therefore stratification becomes mandatory when high energy efficiency is required for heat pumps using $CO_2$ as refrigerant (Cecchinato *et al.*, 2005). Because of the high operating pressures the pressure drop in the heat exchangers of a $CO_2$ system is lower than for a conventional refrigerating system (Cecchinato *et al.*, 2005).

Figure 2.27: Simulated relative COPs for a $CO_2$ heat pump water heater as a function of the inlet water temperature to the gas cooler at 60 and 80°C set point temperature for domestic hot water. (Stene, 2007).

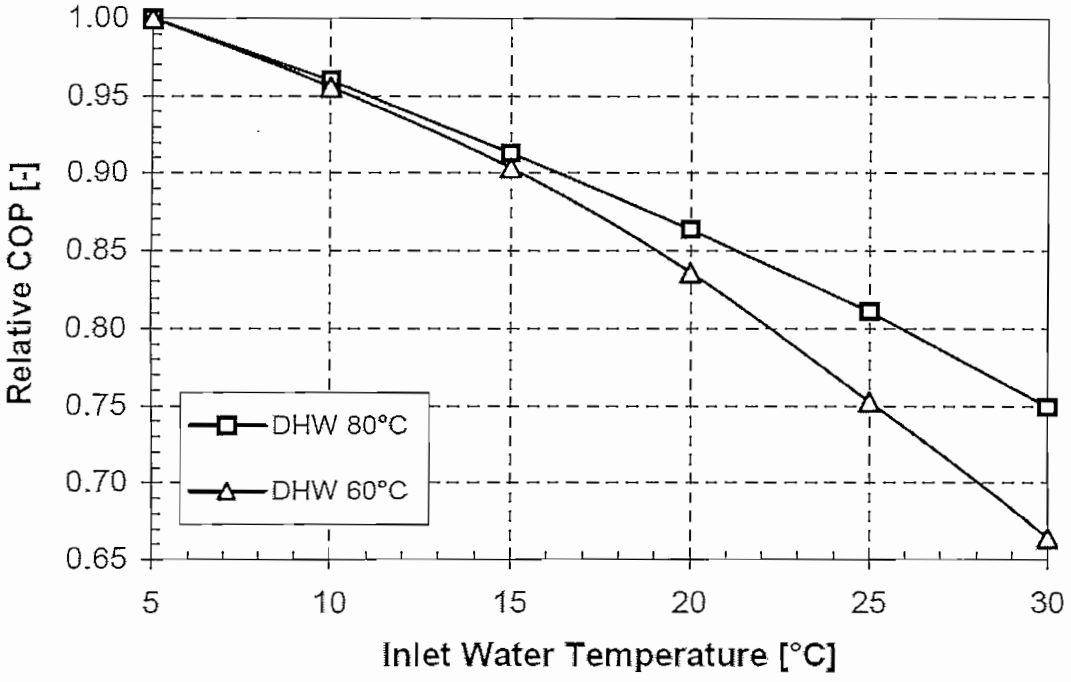


The optimum gas cooler pressure was found to be between 9 and 11MPa. $CO_2$ heat pumps for domestic hot water production ranging between 5 to 20 kW have since been tested by various researchers including Rieberer and Halozen, Hwang and Radermacher and Saikawa and Hashimoto. These systems had the same typical measured COPs than for the 50kW machine built by Neksa (2004) which will be discussed later on. According to Stene (2007) the Denso Corporation Ltd. in Japan was the first company to start production of a residential air source heat pump water heater in 2001. This machine is a 4.5kW system able to produce hot water at temperatures of up to 85°C.

There are three specific distinctions favouring a $CO_2$ system above systems using HCFC and CFC refrigerants. The first is the fact that heat is rejected at a supercritical pressure. This classifies the system as a transcritical system because it operates above the critical point of the refrigerant. In a transcritical system the high side pressure is determined by the refrigerant charge and not the saturation pressure as with conventional systems. This means that the systems design should take into account the possibility of controlling the high side pressure to ensure a good COP. An example of the importance of manipulating the discharge pressure is given in Figure 2.28 (Neksa *et al.*, 1998). Figure 2.28 shows how the heating capacity,

heating COP and compressor shaft power vary with the compressor discharge pressure. The heating capacity tends to increase steeply in the beginning but as the discharge pressure increases the heating capacity evens out. The compressor shaft power increases linearly as the discharge pressure increases. The heating COP of a system is determined by the ratio of the heating capacity and the power input with the maximum COP found as indicated on Figure 2.28. It could also be seen that the COP evens out a little around its optimum area (Neksa, 2006). Therefore the maximum COP of a system is said to be around discharge pressures of 90 – 110 bar depending on the surrounding conditions. When operating in a subcritical state, the COP is dependent on the heat sink temperature.

Figure 2.28: Variation of discharge pressure and the effect thereof (Neksa *et al.*, 1998).

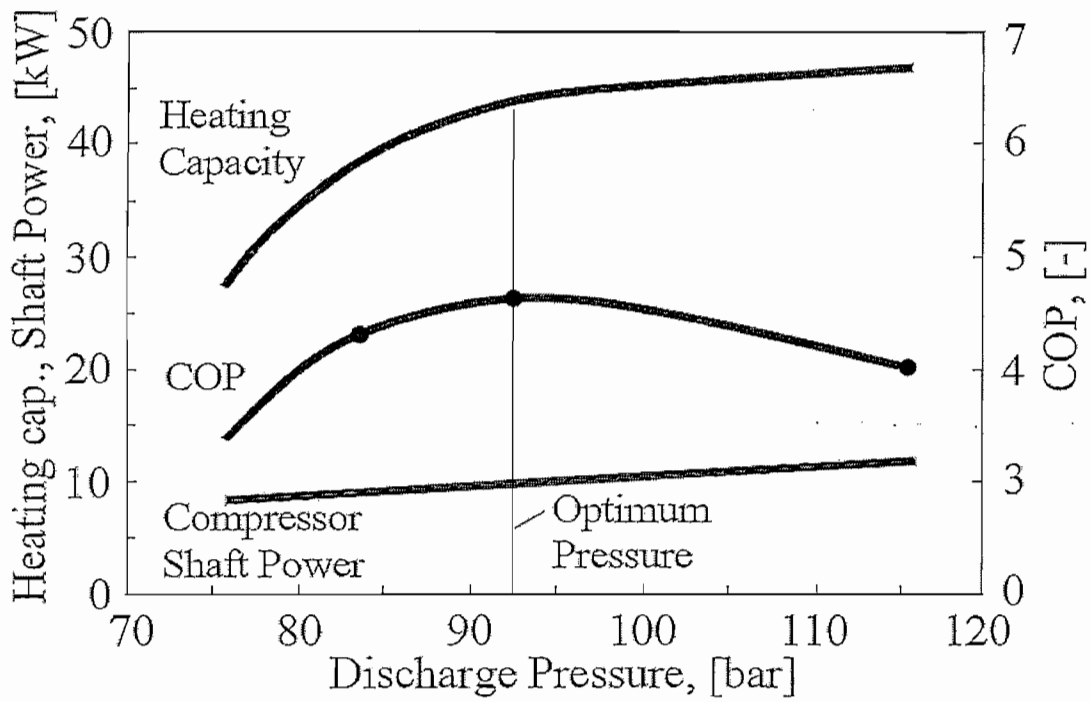


Secondly the pressure level inside a $CO_2$ system is remarkably higher than conventional refrigerant systems, able to reach operating pressures of 130 bar and higher. Because of the smaller size of the components and piping the explosive energy inside a $CO_2$ system is not much different from conventional systems. One of the benefits from the high pressure is the effect it has on the compressor displacement needed for a given capacity; it could be up to 80-90% smaller. Thirdly it has a large refrigerant temperature glide during heat rejection. At supercritical

conditions most of or even all of the heat rejection from the refrigerant takes place by cooling the compressed gas, therefore the heat exchanger is known as a gas cooler. Having a proper gas cooler the refrigerant can be cooled to a few degrees above the entering coolant temperature, contributing to a high COP of the system (Neksa *et al.*, 1998).

Figure 2.29: T-s diagram, including a diagram of a transcritical heat pump system commonly used for water heating (Neksa *et al.*, 1998).

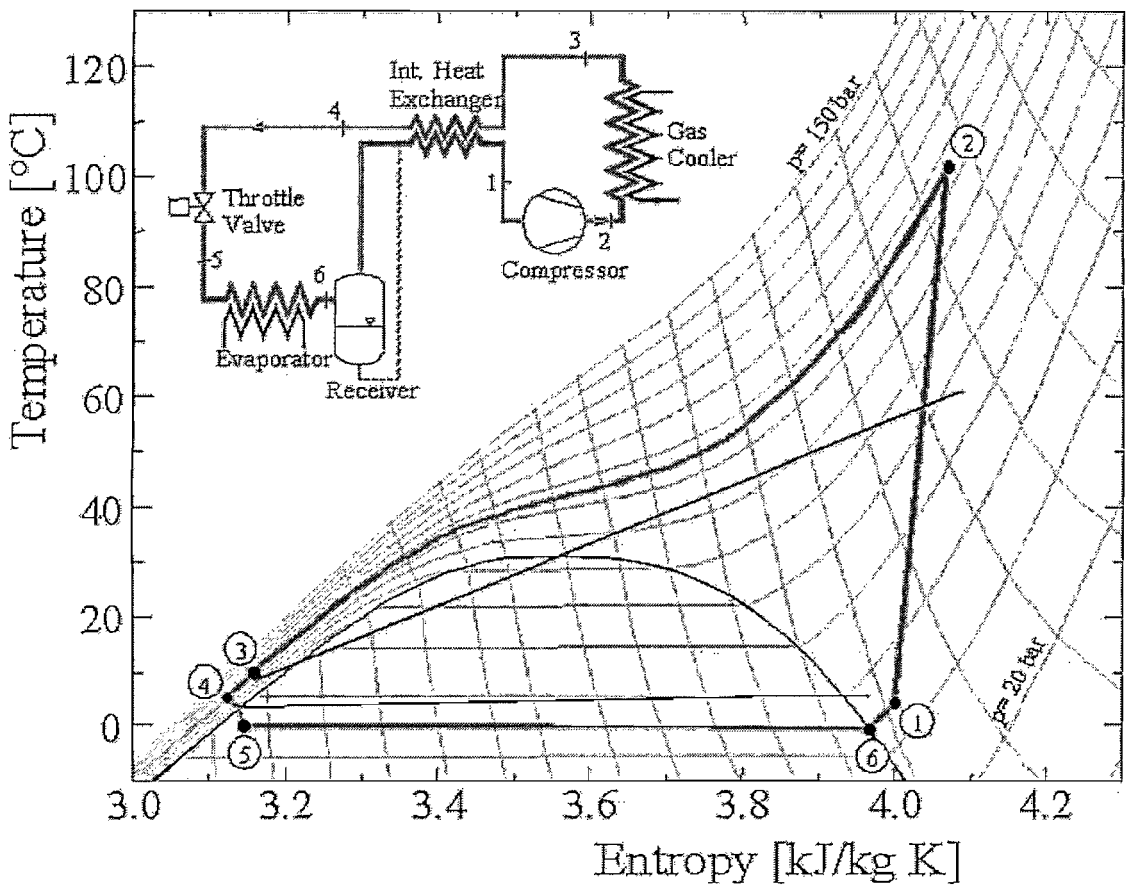


According to Neksa (2002), the first $CO_2$ systems on the market were heat pump systems for water heating because of the favourable thermodynamic properties. Figure 2.29 shows a Temperature-Entropy diagram for a $CO_2$ heat pump system. Studies relating to $CO_2$ heat pump water heaters have been initiated in the early eighties by SINTEF/NTNU and a first full scale 50kW lab prototype heat pump water heater was built in 1996 (Neksa, 2002). Results attained from the prototype showed that a COP of above 4 was achievable even for a hot water outlet temperature of above 60°C. These results are shown in Figure 2.30. It was noted that water temperatures of up to 90°C and higher are achievable with a $CO_2$ heat pump water

heater without operational problems and only a small loss in the systems efficiency (Neksa, 2002). Measured results from the lab prototype heat pump showed that increasing the water outlet temperature from 60°C to 80°C resulted in a decrease in the heating COP from 4.3 to 3.6 at an evaporating temperature of 0°C. This lead to one of the biggest advantages of a $CO_2$ heat pump system running at supercritical conditions, namely the ability to produce high temperature water with a good COP (Neksa *et al.*, 1998). This made $CO_2$ a feasible possibility as refrigerant in heat pump water heaters for domestic use including hotels and restaurants.

According to Neksa *et al.* (1998) the temperature difference between the outlet of the gas cooler and the secondary fluid is determined by the high-side pressure. When operating at high compressor outlet pressures the temperature difference is small and stays more or less the same but as the pressure decreases the temperature difference increases. This is because of a temperature pinch point occurring in the gas cooler. The reason for the pinch point occurring at lower operating temperatures is because of the fact that the temperature glide becomes more curvaceous as it reaches the critical point (Neksa *et al.*, 1998).

**Figure 2.30: Measured heating COP of prototype system with an inlet water temperature of 10°C (Neksa et al, 1998).**

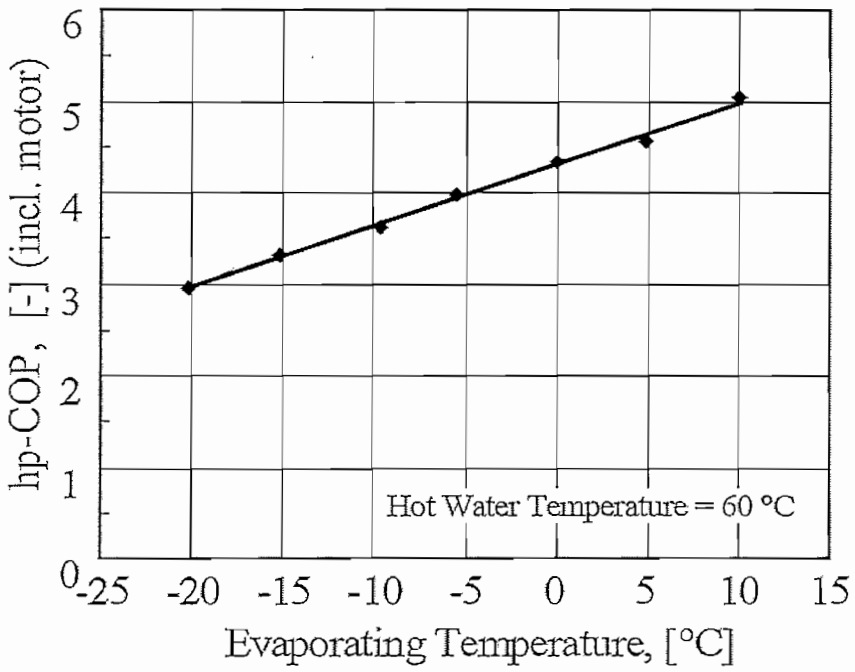


The implementation of an internal heat exchanger is for further cooling down the high pressure $CO_2$ and to vaporise any $CO_2$ liquid entering the low pressure receiver (if

installed) from the evaporator (Kern *et al.*, 2006). According to Aprea and Maiorino (2008), the thermodynamic efficiency of a $CO_2$ system could be improved by implementing an internal heat exchanger. The specific volume of the refrigerant vapour entering the compressor increases and thus increases specific compressor work too. Figure 2.31 shows the difference in operating pressures between a transcritical and subcritical system. Here the big difference between the two operating cycles can be seen.

**Figure 2.31: Comparison of transcritical cycle to subcritical cycle. (Endoh et al, 2006).**

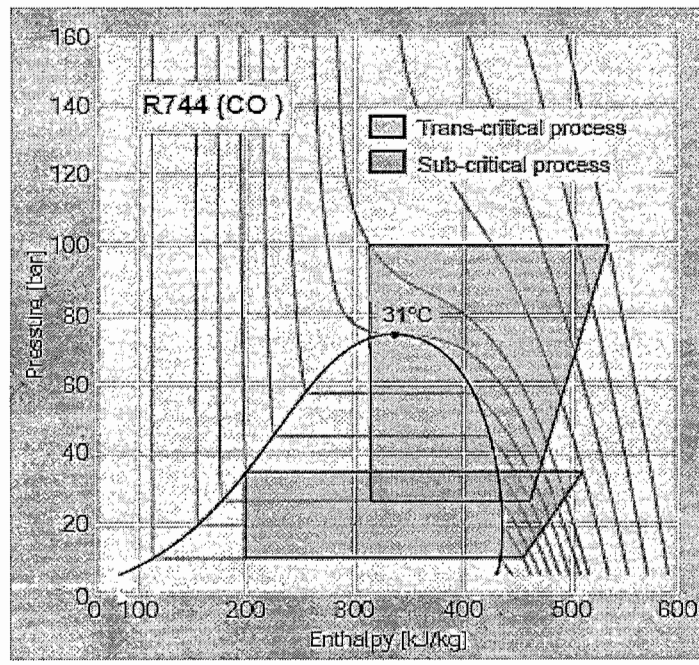


According to Wolf *et al.* (2006), Japan plans to have 5.2 million $CO_2$ hot water heat pumps installed by 2010. Endoh *et al.* (2006) developed a $CO_2$ heat pump that gives instant hot water. $CO_2$ systems developed before this one used storage tanks of up to 300-480L capacity and were constantly kept at temperature by means of a 4.5-6kW heat pump system. Endoh's heat pump supplies the hot water at exactly the required temperature. To realize this they had to develop a 23kW heat pump system. They included a support tank that has a capacity of 45L and so doing, combined the heat pump and storage tank into a single unit. A picture of this heat pump is given in Figure 2.32.

The system has a COP of 4.6 rated at water inlet and outlet temperatures of 12°C and 42°C respectively and with dry bulb and wet bulb temperatures of 16°C and 12°C respectively (Endoh *et al.*, 2006).

Figure 2.32: Instant hot water supply heat pump (Endoh *et al.*, 2006).

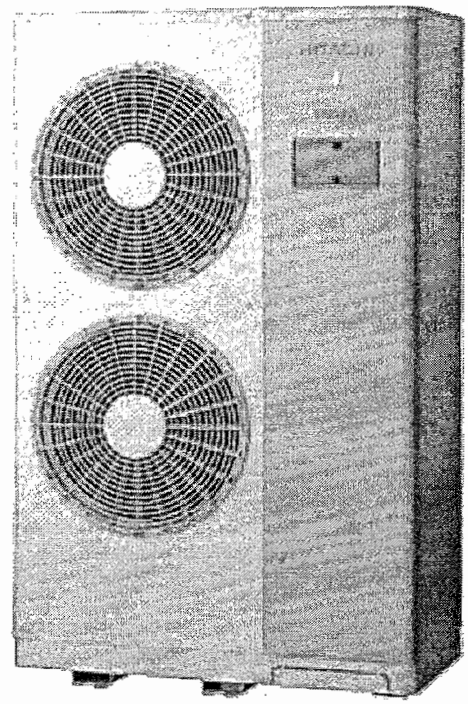

Experiments done by Kuwabara et al. (2006) showed that the higher the gas cooler inlet temperature or the lower the air temperature was, the lower the COP and heating capacity were as a result, although the water outlet temperature was reasonably unaffected by these changes. Figure 2.33 shows the P-h diagram for a $CO_2$ heat pump cycle with different water inlet temperatures. From the diagram it can be seen that as the water inlet temperature is increased the compressor discharge pressure will be higher. The effect on the gas cooler directly affects the system COP. As the water inlet temperature is higher so will the gas cooler outlet temperature be higher which plays a role in the COP of the system (Kuwabara *et al.*, 2006).

According to Huff and Sienel (2006), eight commercial-sized $CO_2$ heat pump water heaters have been developed and installed in the North American market under diverse conditions. These systems have already been working for over 8000 hours. From the performance results obtained, a considerable benefit over conventional systems was showed as the $CO_2$ systems provided between US$4000 and US$10000 saving in annual energy cost compared to the other refrigerants used.

Figure 2.33: P-h diagram of $CO_2$ heat pump cycle (Kuwabara *et al.*, 2006).

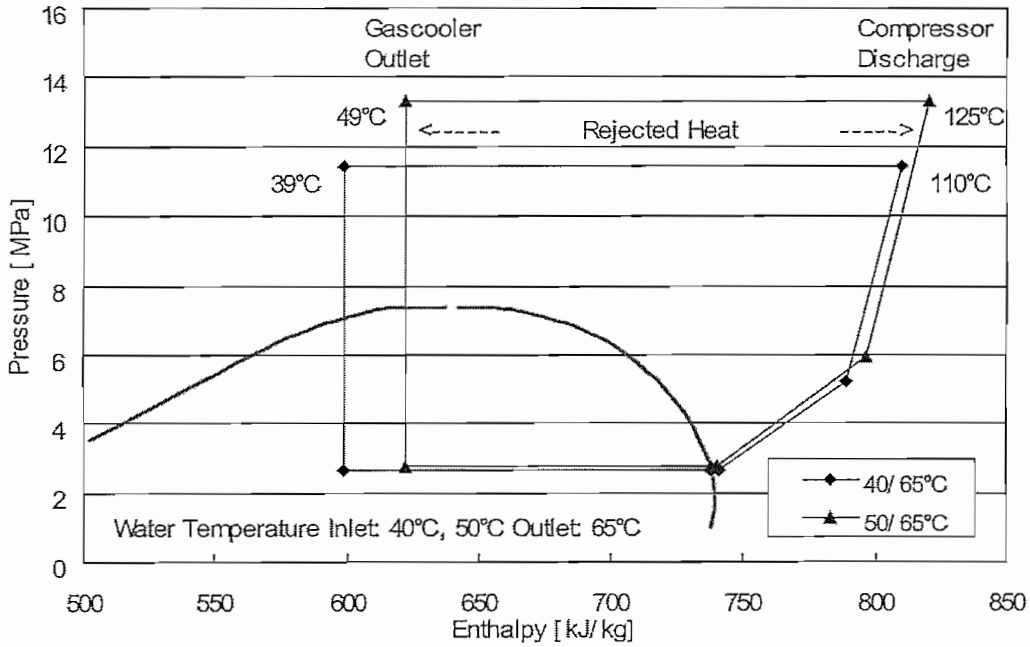


The pinch point, which is the smallest temperature difference to be reached in a heat exchanger between the refrigerant and the secondary fluid, occurs at the outlet of the gas cooler because of the temperature glide that occurs. Therefore it is able to cool the refrigerant to the lowest possible temperature before entering the expansion device. It also means that the water entering the gas cooler could be close to the temperature at which the refrigerant is leaving the gas cooler (Huff & Sienel, 2006).

In conclusion it could be seen that $CO_2$ has great potential to be used as a refrigerant for future refrigeration and heating systems. From the literature study one is able to see that the properties of $CO_2$ are to its advantage when used as a refrigerant. The disadvantages of $CO_2$ are relatively easy to overcome. Therefore $CO_2$ will make a feasible replacement as a natural refrigerant.

# CHAPTER 3

# HEAT PUMP SIMULATION MODEL

# CHAPTER 3

## 3. HEAT PUMP SIMULATION MODEL

The aim of this chapter is to give background on the development of the simulation model of a transcritical water heating heat pump system. It includes the steps taken to formulate a simulation system model as well as the results obtained using the model.

In short, to develop the transcritical heat pump model the first step was to identify a compressor for which a performance chart was available in order to characterize the compressor. The characterized compressor was implemented into a heat pump simulation model from which the system could be characterized. The heat pump cycle was finally expressed by two formulas that can be used for comparison studies with a conventional R-22 system. In the sections to follow this process will be discussed in more detail.

- Compressor characterization.
- System simulation.
- Characterization of compressor.
- Updating the EES program.
- Characterization of the $CO_2$ system.

## 3.1 Compressor Characterization

DORIN (s.a.) presents a wide range of $CO_2$ compressors, satisfying nearly every application of $CO_2$ in the field, as can be seen from Figure 3.1.

Figure 3.1: DORIN compressor range. (DORIN, s.a.).

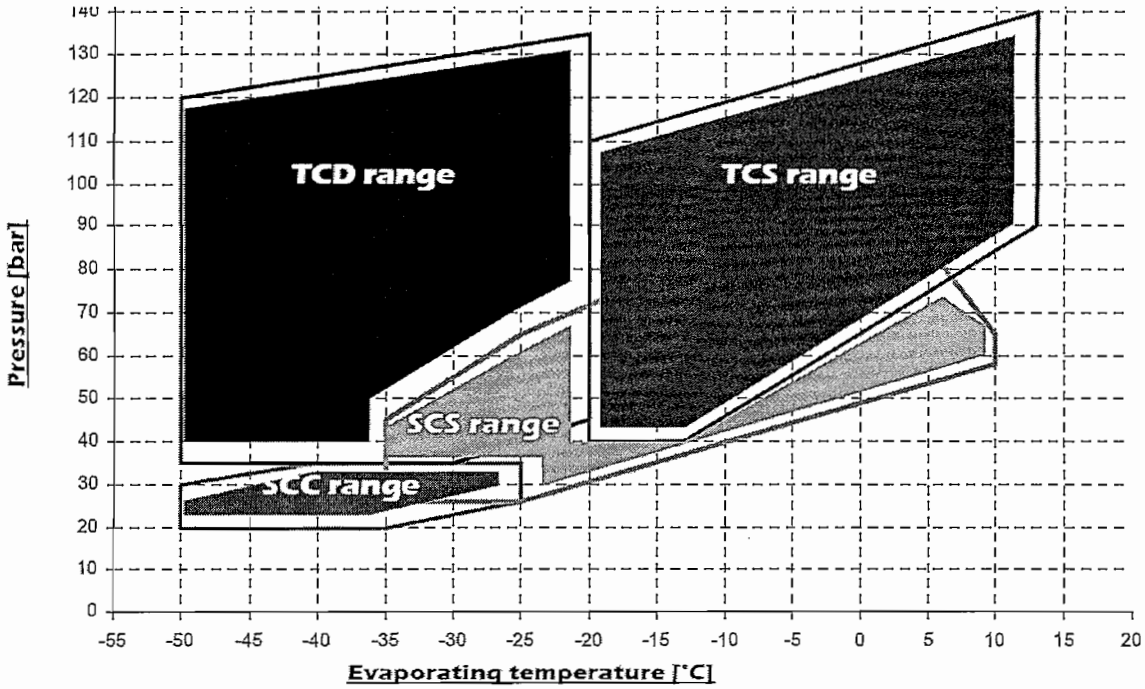


It was decided to use the TCS362-D compressor from the range. This compressor was chosen because it could be compared to an R-22 heat pump of the same heating capacity of on average 50kW. It is a transcritical compressor suitable for the following applications:

- Commercial refrigeration for medium to low evaporating temperature.
- Refrigerated transport.
- Sanitary hot water heat pump and ambient heating systems.
- Chillers.
- HVAC systems.

Figure 3.2 shows a picture of a typical DORIN compressor similar to the one selected for the purpose of this study.

Figure 3.2: DORIN compressor (DORIN, s.a.).

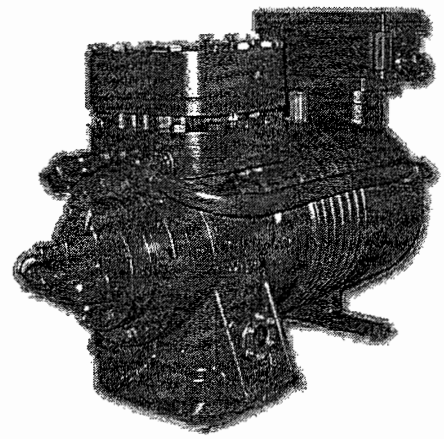

The TCS362-D compressor has the following specifications:

- Operating pressures of up to 130 bar.
- Operates under transcritical conditions.
- Can operate under high evaporating temperatures.
- It has an average heating capacity of about 50kW.

The application envelope shown in Figure 3.3 for the TCS-compressor range is valid for values lower than $10K$ for suction superheat.

Figure 3.3: DORIN compressor TCS range main features (DORIN, s.a.).

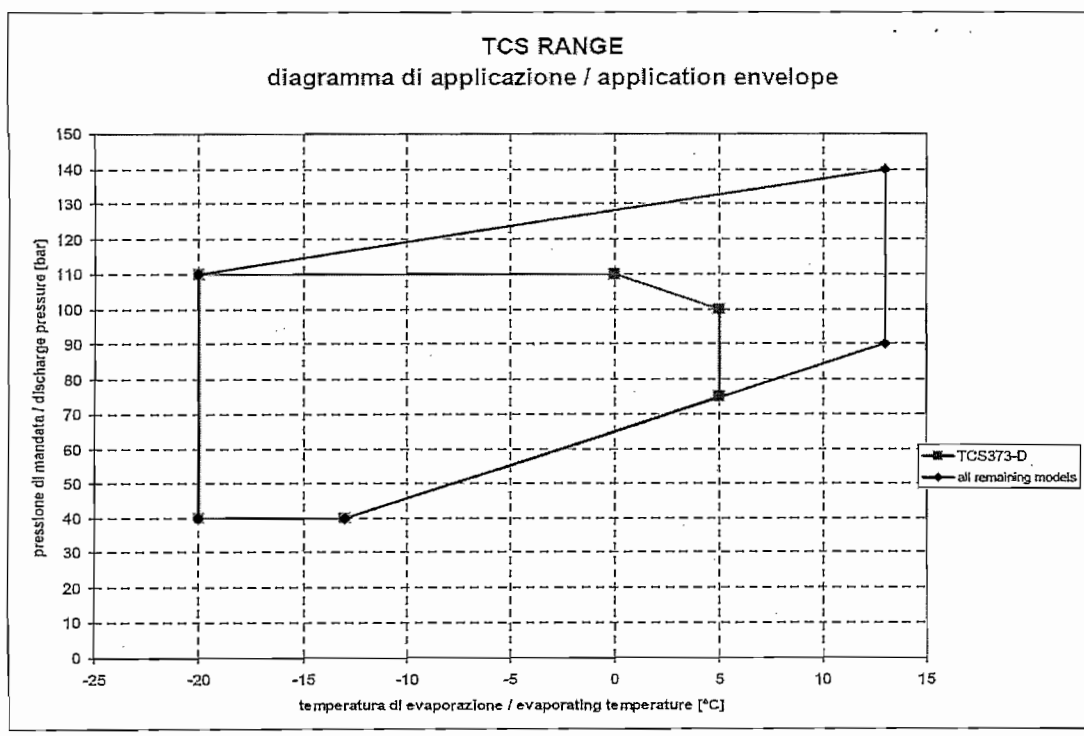

A system working with a transcritical $CO_2$ compressor won't have a conventional condenser but will rather have a gas cooler that cools down the compressed $CO_2$ (Dorin, s.a.). Therefore it must be known that the global efficiency of the system will depend on how good the heat transfer is in the gas cooler and thus the gas cooler should be designed accordingly. A higher refrigerating capacity will be found for a lower gas cooler outlet temperature.

Table 3.1 shows the compressor performance for the TCS362-D compressor that will be used in the system simulation.

**Table 3.1: Performance chart for the TCS362-D compressor (DORIN, s.a.).**

| TRANSCRITICO MONOSTADIO / TRANSCRITICAL SINGLE STAGE | | | | | | | |
|---|---|---|---|---|---|---|---|
| modello / model type | t_ev | p_suc | tgc_out | p_dis | beta | Q | P |
| TCS362-D | -20 | 19,72 | 15 | 75 | 3,803 | 21,9 | 9,9 |
| | | | 25 | 75 | 3,803 | 18,8 | 9,9 |
| | | | 35 | 90 | 4,564 | 13,7 | 10,3 |
| | | | 40 | 110 | 5,578 | 11,0 | 11,6 |
| | -15 | 22,93 | 15 | 75 | 3,271 | 27,0 | 10,4 |
| | | | 25 | 75 | 3,271 | 23,1 | 10,4 |
| | | | 35 | 90 | 3,925 | 17,6 | 11,2 |
| | | | 40 | 110 | 4,797 | 14,5 | 12,8 |
| | -10 | 26,50 | 15 | 75 | 2,830 | 33,3 | 10,5 |
| | | | 25 | 75 | 2,830 | 28,5 | 10,5 |
| | | | 35 | 90 | 3,396 | 21,8 | 11,7 |
| | | | 45 | 120 | 4,528 | 18,4 | 15,3 |
| | 0 | 34,86 | 15 | 75 | 2,151 | 47,9 | 12,2 |
| | | | 25 | 75 | 2,151 | 41,0 | 12,2 |
| | | | 35 | 90 | 2,582 | 31,4 | 14,1 |
| | | | 15 | 100 | 2,869 | 44,5 | 14,9 |
| | | | 25 | 100 | 2,869 | 39,1 | 14,9 |
| | | | 45 | 120 | 3,442 | 25,5 | 16,5 |
| | 5 | 39,69 | 15 | 75 | 1,890 | 56,7 | 12,4 |
| | | | 25 | 75 | 1,890 | 48,5 | 12,4 |
| | | | 35 | 90 | 2,268 | 37,7 | 14,9 |
| | | | 15 | 120 | 3,023 | 50,4 | 17,4 |
| | | | 25 | 120 | 3,023 | 45,0 | 17,4 |
| | | | 35 | 120 | 3,023 | 38,4 | 17,4 |
| | | | 45 | 120 | 3,023 | 30,4 | 17,4 |
| | 10 | 45,01 | 15 | 75 | 1,666 | 68,0 | 11,7 |
| | | | 25 | 75 | 1,666 | 57,9 | 11,7 |
| | | | 35 | 90 | 2,000 | 45,7 | 14,7 |
| | | | 15 | 120 | 2,666 | 60,7 | 17,9 |
| | | | 25 | 120 | 2,666 | 54,3 | 17,9 |
| | | | 35 | 120 | 2,666 | 46,3 | 17,9 |
| | | | 45 | 120 | 2,666 | 36,5 | 17,9 |
| | | | 15 | 130 | 2,888 | 59,1 | 19,5 |
| | | | 25 | 130 | 2,888 | 52,7 | 19,5 |

Beta = pressure ratio.
Data is valid for a 10*K* suction gas temperature.
Q = refrigeration capacity [kW]
Tgc_out = gas cooler outlet temperature [°C]
P_dis = discharge pressure [bar]
P_suc = suction pressure [bar]
T_ev = evaporating temperature [°C]
P = power

$CO_2$ compressors can work at higher pressure levels than HFC and HCFC compressors, which have two main benefits:

- The pressure drop inside the system is less important because of the lower pressure difference that needs to be overcome.
- The heat transfer coefficient is very high in both the gas cooler and the evaporator.

Therefore if the system is kept at the same refrigeration capacity and the same ambient temperature, the mean $\Delta T$ inside the evaporator and gas cooler can be kept smaller compared to conventional systems. A $\Delta T$ of $2K$ is possible inside the gas cooler.

## 3.2 System Simulation

In the previous section the reasons for choosing a suitable compressor were discussed. This section describes the system simulation of the transcritical heat pump and determines the unknown variables needed to describe a heat pump cycle. After the system has been simulated, the chosen compressor will be implemented.

Figure 3.5 shows the system diagram layout and the positioning of the components making up the heat pump system. The $CO_2$ heat pump system consists of the DORIN compressor, pressure relieve valve, gas cooler, internal heat exchanger, expansion valve, air to refrigerant evaporator and liquid receiver. For the characterization of the compressor the internal heat exchanger was not taken into account seeing that the compressor chart was obtained with sub-cooling being added.

Figure 3.4: T-s diagram showing certain points for simulation description.

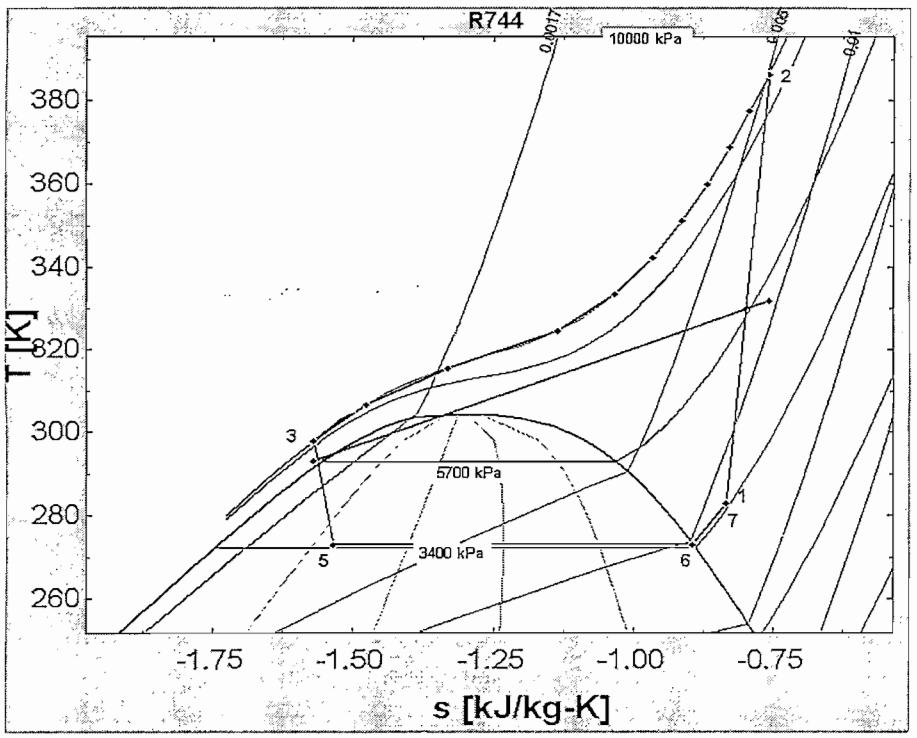

Figure 3.5: $CO_2$ heat pump diagram.

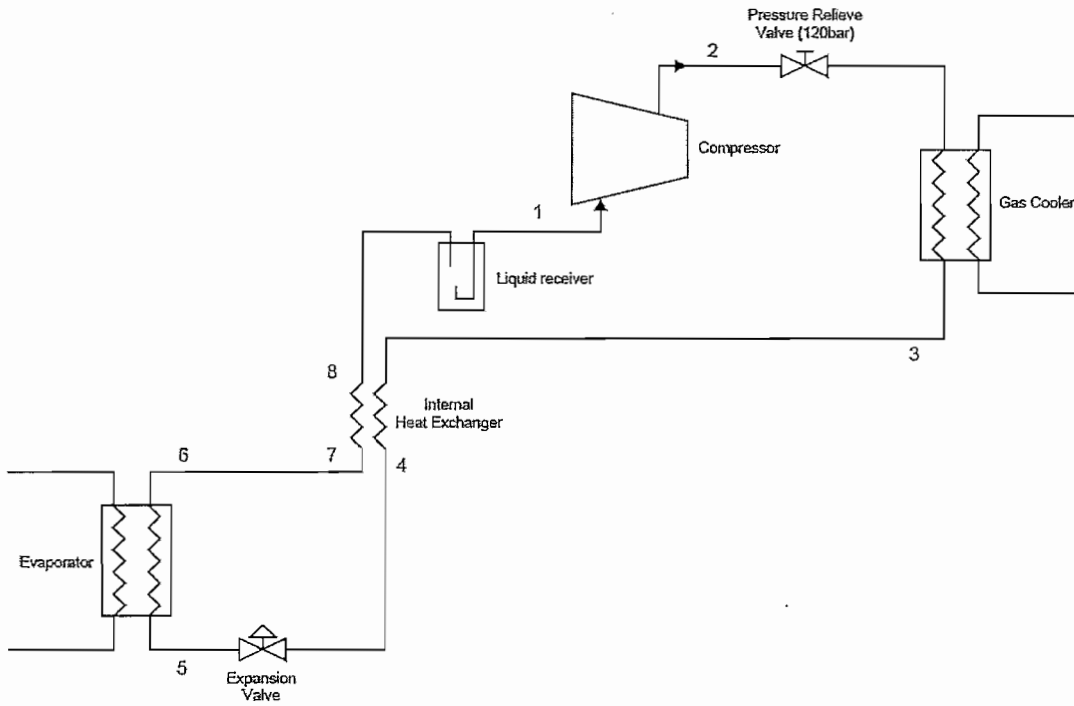


A simple cycle simulation has been done using Engineering Equation Solver (EES). The data used for this simulation can be found in table 3.1 The EES programming code and results are found in Appendix A.

The methodology behind the cycle simulation is given below, while Figure 3.4 shows a T-s diagram indicating some critical points to refer to the methodology of the cycle simulation:

- (5) The suction pressure, evaporating temperature and refrigeration capacity are known variables found in table 3.1.
- A constant enthalpy is assumed over the expansion valve.
- The quality of the refrigerant at the inlet to the evaporator is calculated in terms of enthalpy and suction pressure.
- The entropy is determined in terms of the quality of the refrigerant and the suction pressure.
- (6) It is assumed that evaporation takes place at a constant pressure through the evaporator.
- It is also assumed that there is no pressure drop through the liquid receiver and internal heat exchanger.
- A superheat of $10K$ is assumed in the evaporator.

- The refrigerant leaving the evaporator is assumed to be a gas at all times.
- The enthalpy of the refrigerant after it has left the evaporator is determined in terms of the outlet temperature and the suction pressure.
- Since the cooling capacity is known and the enthalpy is calculated before and after the evaporator the mass flow of the refrigerant can be calculated with the following formula:

$$Q\_e = \dot{m} \cdot (h_7 - h_5) \quad [3.1]$$

- The entropy of the refrigerant after the evaporator is calculated in terms of the temperature of the refrigerant after the evaporator and the suction pressure.
- (1) The temperature, pressure, entropy and enthalpy entering the compressor are now known.
- (2) The discharge pressure and compressor power are given in the compressor chart of Table 3.1.
- With the compressor power known and the mass flow of the refrigerant already calculated, the enthalpy exiting the compressor can be calculated with the following formula:

$$Q\_p = \dot{m} \cdot (h_2 - h_1) \quad [3.2]$$

- The isentropic enthalpy of the refrigerant after the compressor can be calculated in terms of the discharge pressure and the entropy entering the compressor.
- With the isentropic enthalpy and the enthalpy leaving the compressor known, the compressor efficiency can be calculated as follows:

$$eta\_c = \frac{h_{s2} - h_1}{h_2 - h_1} \quad [3.3]$$

- The compressor efficiency is known and with the compressor power known the heating capacity can be calculated:

$$Q\_h = Q\_e + Q\_p \cdot eta\_c \quad [3.4]$$

- From all the known factors, the heating coefficient of performance (COP) of the system can now be calculated with the following formula:

$$COP = \frac{Q\_h}{Q\_p} \quad [3.5]$$

- (3) The gas cooler outlet temperature is known from the compressor chart and a constant pressure over the gas cooler is assumed.

- The enthalpy and entropy of the refrigerant leaving the gas cooler can be calculated in terms of the gas cooler outlet temperature and the discharge pressure.
- The cycle is completed and all the variables required were calculated.

The important variables calculated in the cycle simulation mentioned above are the COP, heating capacity, mass flow and compressor efficiency of the cycle. The results are given in table 3.2 for the conditions in table 3.1.

The average heating COP obtained from the results is 3.3, which is in accordance with the literature and with what is expected from a heat pump system. As expected it can be seen that the COP is higher for a higher evaporating temperature, lower for a higher gas cooler outlet temperature and lower for a higher discharge pressure. This corresponds well with what was found in the literature.

The average heating capacity obtained from the results is 46kW, which is about the same as that of the R-22 heat pump system it will be compared to later.
The average compressor efficiency obtained from the results is 63%.

Table 3.2: Results for the cycle simulation.

| P_suc (kPa) | P_dis (kPa) | T_ev (K) | Tgc_out (K) | mass flow | Q (kW) | P (kW) | COP | Qh | eta_c |
|---|---|---|---|---|---|---|---|---|---|
| 1972 | 7500 | 253 | 288 | 0.1016 | 21.9 | 9.9 | 2.865 | 28.36 | 0.6526 |
| 1972 | 7500 | 253 | 298 | 0.1022 | 18.8 | 9.9 | 2.555 | 25.3 | 0.6565 |
| 1972 | 9000 | 253 | 308 | 0.09068 | 13.7 | 10.3 | 1.98 | 20.39 | 0.6498 |
| 1972 | 11000 | 253 | 313 | 0.07467 | 11 | 11.6 | 1.499 | 17.39 | 0.551 |
| 2293 | 7500 | 258 | 288 | 0.1252 | 27 | 10.4 | 3.261 | 33.91 | 0.6645 |
| 2293 | 7500 | 258 | 298 | 0.1255 | 23.1 | 10.4 | 2.887 | 30.03 | 0.6662 |
| 2293 | 9000 | 258 | 308 | 0.1164 | 17.6 | 11.2 | 2.248 | 25.17 | 0.6762 |
| 2293 | 11000 | 258 | 313 | 0.09832 | 14.5 | 12.8 | 1.72 | 22.02 | 0.5873 |
| 2650 | 7500 | 263 | 288 | 0.1545 | 33.3 | 10.5 | 3.869 | 40.62 | 0.6973 |
| 2650 | 7500 | 263 | 298 | 0.155 | 28.5 | 10.5 | 3.414 | 35.84 | 0.6994 |
| 2650 | 9000 | 263 | 308 | 0.1443 | 21.8 | 11.7 | 2.565 | 30.01 | 0.7018 |
| 2650 | 12000 | 263 | 313 | 0.12 | 18.4 | 15.3 | 1.773 | 27.13 | 0.5708 |
| 3486 | 7500 | 273 | 288 | 0.2241 | 47.9 | 12.2 | 4.535 | 55.33 | 0.6088 |
| 3486 | 7500 | 273 | 298 | 0.2251 | 41 | 12.2 | 3.972 | 48.46 | 0.6115 |
| 3486 | 9000 | 273 | 308 | 0.2103 | 31.4 | 14.1 | 2.852 | 40.22 | 0.6255 |
| 3486 | 10000 | 273 | 288 | 0.2046 | 44.5 | 14.9 | 3.635 | 54.16 | 0.6483 |
| 3486 | 10000 | 273 | 298 | 0.2045 | 39.1 | 14.9 | 3.272 | 48.75 | 0.648 |
| 3486 | 12000 | 273 | 313 | 0.1681 | 25.5 | 16.5 | 2.123 | 35.03 | 0.5776 |
| 3969 | 7500 | 278 | 288 | 0.2672 | 56.7 | 12.4 | 5.149 | 63.85 | 0.5764 |
| 3969 | 7500 | 278 | 298 | 0.2686 | 48.5 | 12.4 | 4.491 | 55.68 | 0.5794 |
| 3969 | 9000 | 278 | 308 | 0.2525 | 37.3 | 14.9 | 3.099 | 46.18 | 0.5961 |
| 3969 | 12000 | 278 | 288 | 0.2313 | 50.4 | 17.4 | 3.552 | 61.81 | 0.6558 |

| P_suc (kPa) | P_dis (kPa) | T_ev (K) | Tgc_out (K) | mass flow | Q (kW) | P (kW) | COP | Qh | eta_c |
|---|---|---|---|---|---|---|---|---|---|
| 3969 | 12000 | 278 | 298 | 0.2324 | 45 | 17.4 | 3.245 | 56.47 | 0.659 |
| 3969 | 12000 | 278 | 308 | 0.2313 | 38.4 | 17.4 | 2.863 | 49.81 | 0.6559 |
| 3969 | 12000 | 278 | 313 | 0.2026 | 30.4 | 17.4 | 2.322 | 40.39 | 0.5744 |
| 4501 | 7500 | 283 | 288 | 0.3238 | 68 | 11.7 | 6.387 | 74.73 | 0.5752 |
| 4501 | 7500 | 283 | 298 | 0.3246 | 57.9 | 11.7 | 5.525 | 64.65 | 0.5766 |
| 4501 | 9000 | 283 | 308 | 0.3141 | 45.7 | 14.7 | 3.725 | 54.76 | 0.6162 |
| 4501 | 12000 | 283 | 288 | 0.2814 | 60.7 | 17.9 | 4.058 | 72.63 | 0.6666 |
| 4501 | 12000 | 283 | 298 | 0.2837 | 54.3 | 17.9 | 3.705 | 66.33 | 0.6719 |
| 4501 | 12000 | 283 | 308 | 0.2826 | 46.3 | 17.9 | 3.256 | 58.28 | 0.6695 |
| 4501 | 12000 | 283 | 313 | 0.2468 | 36.5 | 17.9 | 2.624 | 46.97 | 0.5847 |
| 4501 | 13000 | 283 | 288 | 0.2729 | 59.1 | 19.5 | 3.68 | 71.76 | 0.6493 |
| 4501 | 13000 | 283 | 298 | 0.2731 | 52.7 | 19.5 | 3.352 | 65.37 | 0.6497 |

## 3.3 Characterization of Compressor

This section uses the results obtained from the simulation above to characterize the compressor. Characterizing the compressor into only two [3.23,3.24] formulas both in terms of evaporation pressure and discharge pressure, enables the manipulation of the first cycle simulation so that results can be obtained for any evaporation temperature, gas cooler outlet temperature and discharge pressure.

With all the variables known and from the compressor chart the following plots can be made;

1. evaporating capacity against evaporation temperature,
2. mass flow against evaporating pressure and
3. compressor efficiency against evaporating pressure.

These plots are shown in Figures 3.6, 3.7 and 3.8 respectively and will be discussed in more detail in the section to follow. All the variables used were attained from the results as shown in Table 3.2.

Figure 3.6 shows cooling capacity against evaporation temperature in terms of the discharge pressure and the gas cooler outlet temperature.

- Plot 1 is at a discharge pressure of 7500kPa and a gas cooler outlet temperature of 288*K*.
- Plot 2 is at a discharge pressure of 7500kPa and a gas cooler outlet temperature of 298*K*.
- Plot 3 is at a discharge pressure of 9000kPa and a gas cooler outlet temperature of 308*K*.
- Plot 4 is at a discharge pressure varying between 11000 to 12000kPa and a gas cooler outlet temperature of 313*K*.

Plot 4 is made up of varying pressures because of the compressor chart being used. This may have an affect on the accuracy of the plot but it is done at a constant gas cooler outlet temperature. Results found from the plots in table 3.2 depicts that the accuracy is still good enough.

Figure 3.6: Cooling capacity against evaporation pressure.

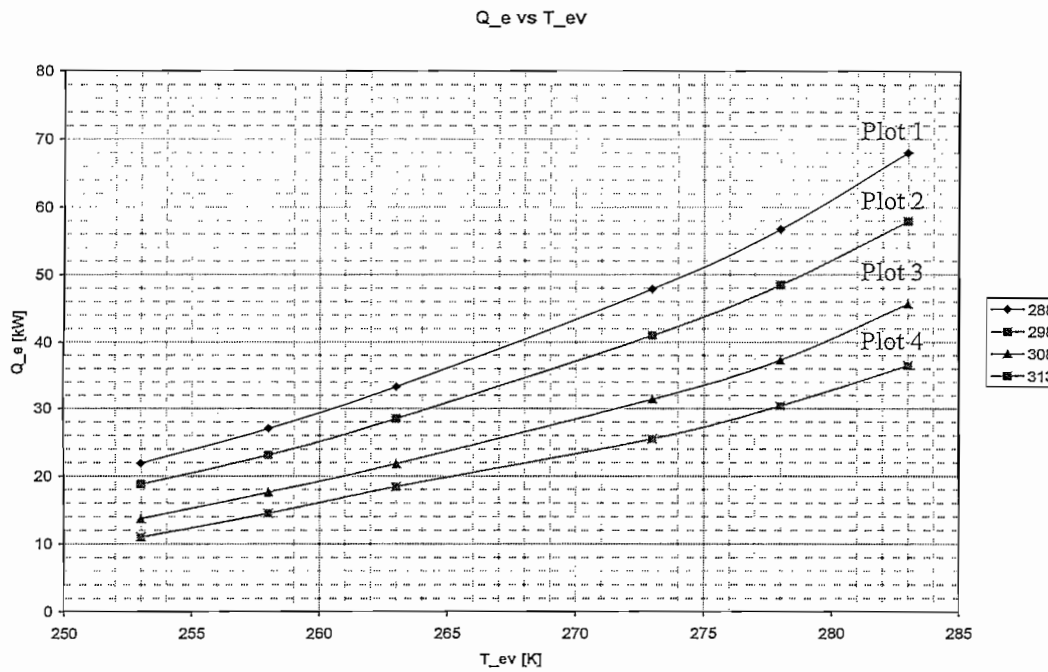


From figure 3.6 it could be seen that as the gas cooler outlet temperature increases there is a loss in the evaporating capacity because less heat is rejected in the gas cooler which affects the amount of heat to be absorbed in the evaporator. It is also clear that as the evaporating temperature increases, the cooling capacity increases because there is a lot more energy in the surrounding medium to be extracted.

The evaporating temperature is directly linked to the ambient wet bulb temperature since the cycle simulated consists of an air to refrigerant evaporator. Therefore from figure 3.8 it can be clearly seen that a better system performance will be attained at high wet bulb ambient temperatures and a low gas cooler outlet temperature which is directly linked to the water inlet temperature because the system simulated consists of a refrigerant to water gas cooler. This is because the warmer the ambient temperature the more heat there is for the refrigerant to extract from the ambient air. For the gas cooler, the lower the water inlet temperature is the more heat could be rejected into water. These both lead to a highly efficient system with a good COP.

Figure 3.7 shows the mass flow against evaporation pressure in terms of the discharge pressure and the gas cooler outlet temperature.

- Plot 1 is at a discharge pressure of 7500kPa and a gas cooler outlet temperature of 288*K*.
- Plot 2 is at a discharge pressure of 7500kPa and a gas cooler outlet temperature of 298*K*.
- Plot 3 is at a discharge pressure of 9000kPa and a gas cooler outlet temperature of 308*K*.
- Plot 4 is at a discharge pressure varying between 11000 to 12000kPa and a gas cooler outlet temperature of 313*K*.

Figure 3.7: Mass flow against evaporation pressure.

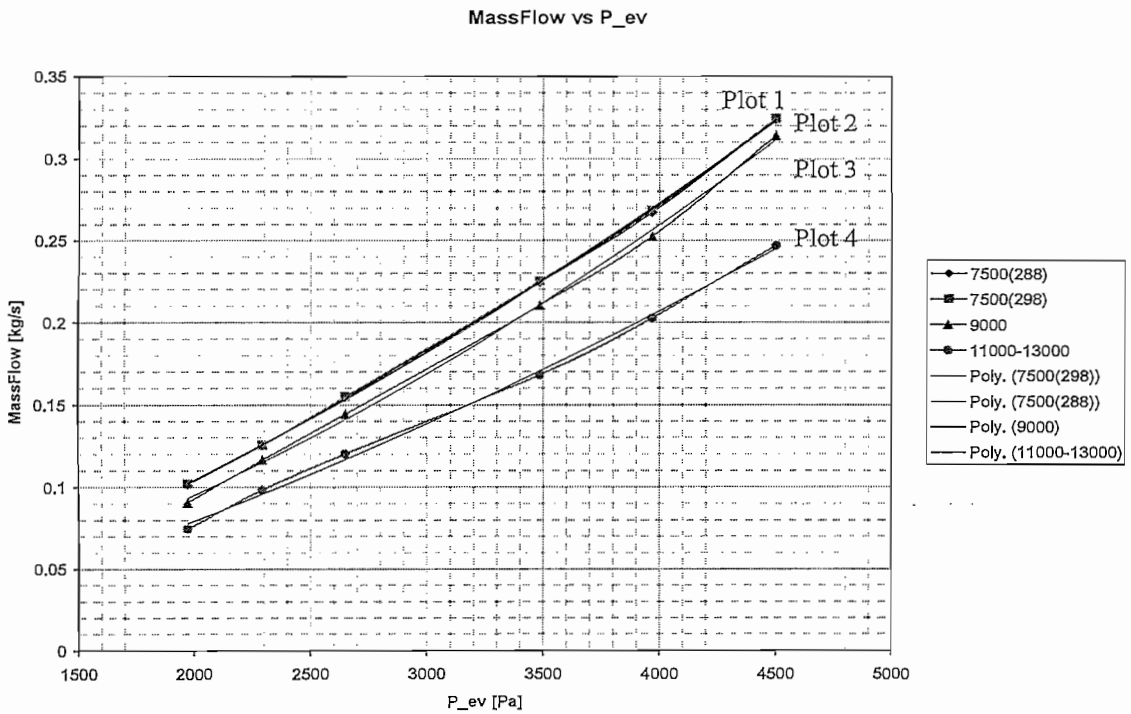


From figure 3.7 it can be seen that there is a near linear increase in the mass flow through the system as the evaporating pressure increases. As the discharge pressure and the gas cooler outlet temperature increases the mass flow through the system decreases. This is a result of the mass flow compensating, by means of the expansion valve, for a constant evaporating capacity in the system which is determined by the evaporating pressure and gas cooler outlet temperature as mentioned earlier.

The plot made for figure 3.8 is made up out of compressor efficiency against evaporating pressure in terms of the discharge pressure and the gas cooler outlet temperature.

- Plot 1 is at a discharge pressure of 7500 kPa and a gas cooler outlet temperature of 288*K*.
- Plot 2 is at a discharge pressure of 7500 kPa and a gas cooler outlet temperature of 298*K*.
- Plot 3 is at a discharge pressure of 9000 kPa and a gas cooler outlet temperature of 308*K*.
- Plot 4 is at a discharge pressure varying between 11000 to 12000 kPa and a gas cooler outlet temperature of 313*K*.

Figure 3.8: Compressor efficiency against evaporation pressure.

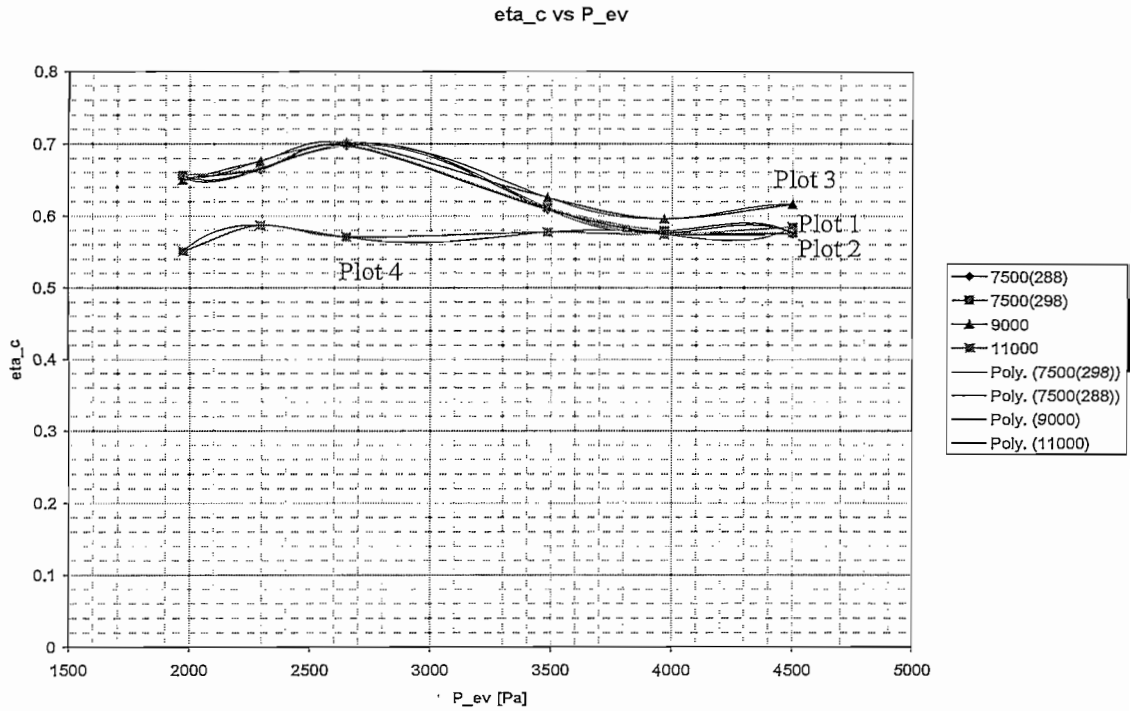


From figure 3.8 it can be seen that the compressor efficiency stays reasonably unaffected with the change in evaporating pressure, discharge pressure and gas cooler outlet temperature. This is because the compressor efficiency is directly linked to the manufacturing of the compressor and is only slightly influenced by the discharge pressure and suction pressure.

In figures 3.7 and 3.8 a polynomial equation is fitted to the profiles attained from the plots made. The polynomial fitted through the mass flow resulted in a 3rd order polynomial equation describing the mass flow of the system in terms of evaporating pressure. The polynomial fitted through the compressor efficiency resulted in a 6th order polynomial equation describing the compressor efficiency in terms of the evaporating pressure. The $R^2$-equation shows the accuracy of the equations obtained from the polynomials fitted through the plots, 1 being a good fit and 0 being a bad fit. The equations obtained are given below:

The 3rd order polynomial equations describing the mass flow in terms of the evaporating pressure are as follow:

- $y = 6.7164\times10^{-9}x^2 + 4.372\times10^{-5}x - 1.0121\times10^{-2}$ [3.6]

  $R^2 = 9.9978\times10^{-1}$
- $y = 6.5642\times10^{-9}x^2 + 4.4975\times10^{-5}x - 1.167\times10^{-2}$ [3.7]

  $R^2 = 9.9985\times10^{-1}$
- $y = 8.58\times10^{-9}x^2 + 3.0797\times10^{-5}x - 8.1267\times10^{-4}$ [3.8]

  $R^2 = 9.99885\times10^{-1}$
- $y = 4.777\times10^{-9}x^2 + 3.5101\times10^{-5}x - 9.8689\times10^{-3}$ [3.9]

  $R^2 = 9.9805\times10^{-1}$

The 6th order polynomial equations describing the compressor efficiency in terms of the evaporating pressure are given below:

- $y = -7.2821\times10^{-17}x^5 + 1.1863\times10^{-12}x^4 - 7.5315\times10^{-9}x^3 + 2.3222\times10^{-5}x^2 - 3.4725\times10^{-2}x + 2.0812\times10^{1}$

  $R^2 = 1$ [3.10]
- $y = -7.4802\times10^{-17}x^5 + 1.2188\times10^{-12}x^4 - 7.7427\times10^{-9}x^3 + 2.3899\times10^{-5}x^2 - 3.5793\times10^{-2}x + 2.1477\times10^{1}$

  $R^2 = 1$ [3.11]
- $y = -4.4582\times10^{-17}x^5 + 7.2839\times10^{-13}x^4 - 4.6132\times10^{-9}x^3 + 1.41\times10^{-5}x^2 - 2.0752\times10^{-2}x + 1.2432\times10^{1}$

  $R^2 = 1$ [3.12]
- $y = 5.3014\times10^{-17}x^5 - 8.7155\times10^{-13}x^4 + 5.632\times10^{-9}x^3 - 1.7859\times10^{-5}x^2 + 2.7758\times10^{-2}x - 1.6328\times10^{1}$

  $R^2 = 1$ [3.13]

All of the above fitted equations are reasonable fittings and can now be used to describe the system mass flow and compressor efficiency in terms of evaporating

pressure for any given circumstance, 'x' being the common denominator for the evaporating pressure.

Because we want the mass flow and the compressor efficiency to be in terms of both evaporating pressure and discharge pressure and not only evaporating pressure, the above attained equations must be plotted against the discharge pressure in order to attain the required equations. The coefficients from the equation attained are plotted against the discharge pressures given in the compressor chart.

The coefficients from the equation describing the mass flow in terms of evaporating pressure is plotted against the corresponding discharge pressure as shown in table 3.3.

**Table 3.3: Coefficients from mass flow equation against the suitable discharge pressure.**

| P_dis | a2 | a1 | a0 |
|---|---|---|---|
| 7500 | -1.01E-02 | 4.37E-05 | 6.72E-09 |
| 7500 | -1.17E-02 | 4.50E-05 | 6.56E-09 |
| 9000 | -8.13E-04 | 3.08E-05 | 8.58E-09 |
| 12000 | -9.87E-03 | 3.51E-05 | 4.78E-09 |

The following plots are made according to table 3.3. The plots are shown in figures 3.9, 3.10 and 3.11.

**Figure 3.9: Coefficients a2 against discharge pressure.**

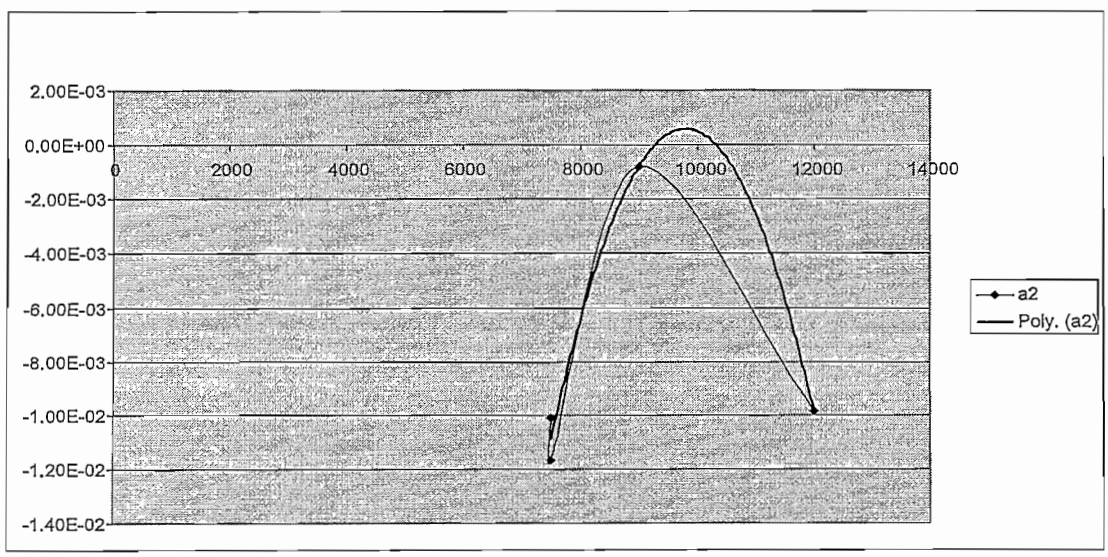

Figure 3.10: Coefficients a1 against discharge pressure.

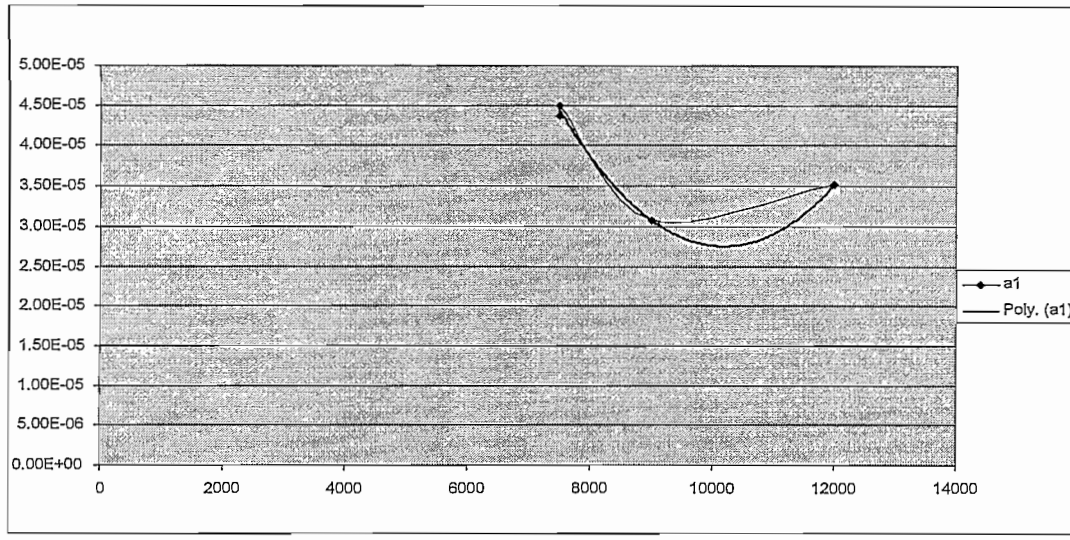


Figure 3.11: Coefficients a0 against discharge pressure.

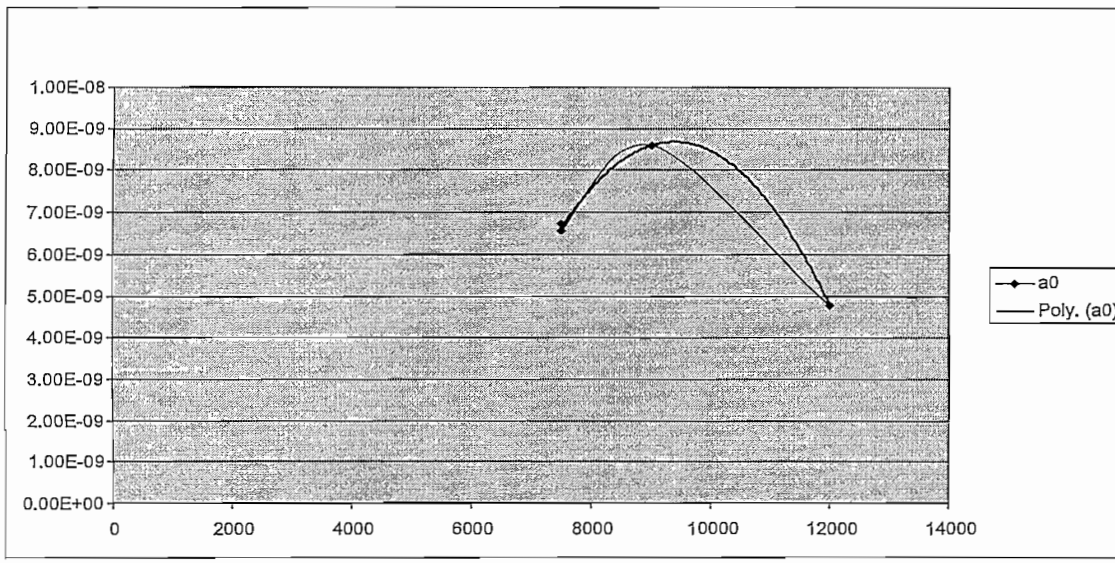


As in the first few plots, a polynomial equation is fitted through the different plots with $R^2$-equation showing the accuracy of the plot.

The polynomial equation resulted in 3rd order polynomial equations taking the discharge pressure into consideration as well.

The 3rd order polynomials taking the discharge pressure into account are given below:

- $$y = -2.1646\times10^{-9}x^2 + 4.2438\times10^{-5}x - 2.0742\times10^{-1} \qquad [3.14]$$

$$R^2 = 9.8358\times10^{-1}$$

- $y = 2.3263\times10^{-12}x^2 - 4.7418\times10^{-8}x + 2.6913\times10^{-4}$ [3.15]

  $R^2 = 9.8358\times10^{-1}$

- $y = -6907\times10^{-16}x^2 + 1.0683\times10^{-11}x - 4.147\times10^{-8}$ [3.16]

  $R^2 = 9.984\times10^{-1}$

All of the above fitted equations are reasonable fittings, with 'x' being the common denominator for the discharge pressure.

The coefficients from the equation describing the compressor efficiency in terms of evaporating pressure is plotted against the corresponding discharge pressure as shown in table 3.4.

Table 3.4: Coefficients from compressor efficiency equation against the suitable discharge pressure.

| P_dis | a5 | a4 | a3 | a2 | a1 | a0 |
|---|---|---|---|---|---|---|
| 7500 | 2.08E+01 | -3.47E-02 | 2.32E-05 | -7.53E-09 | 1.19E-12 | -7.28E-17 |
| 7500 | 2.15E+01 | -3.58E-02 | 2.39E-05 | -7.74E-09 | 1.22E-12 | -7.48E-17 |
| 9000 | 1.24E+01 | -2.08E-02 | 1.41E-05 | -4.61E-09 | 7.28E-13 | -4.46E-17 |
| 12000 | -1.63E+01 | 2.78E-02 | -1.79E-05 | 5.63E-09 | -8.72E-13 | 5.30E-17 |

The following plots are made according to table 3.4. The plots are shown in figures 3.12, 3.13, 3.14, 3.15, 3.16 and 3.17.

Figure 3.12: Coefficients a5 against discharge pressure.

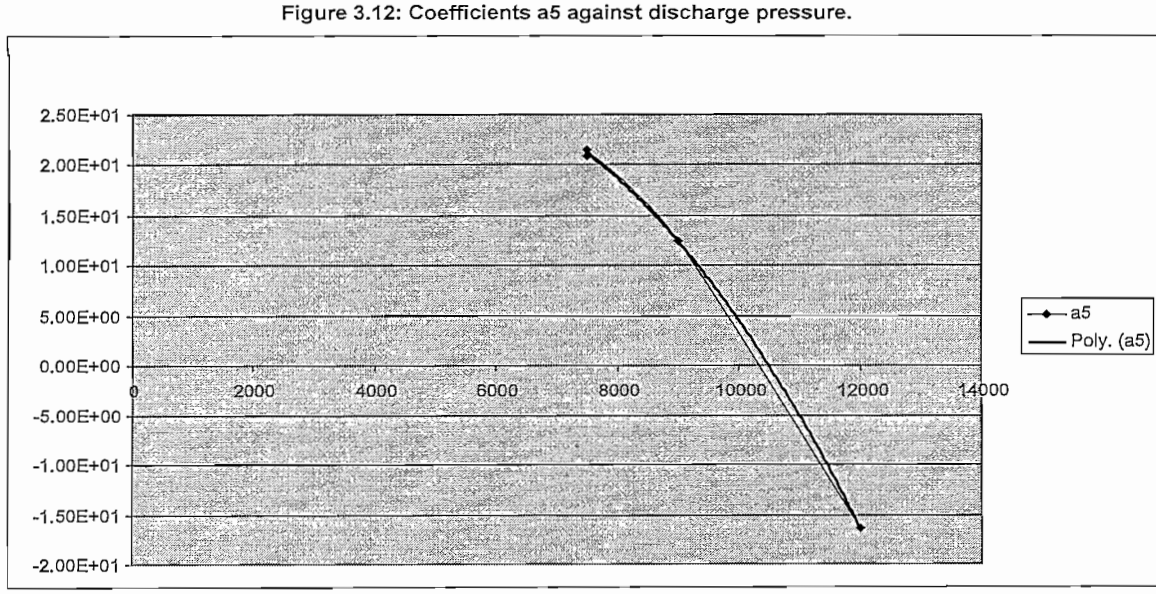

Figure 3.13: Coefficients a4 against discharge pressure.

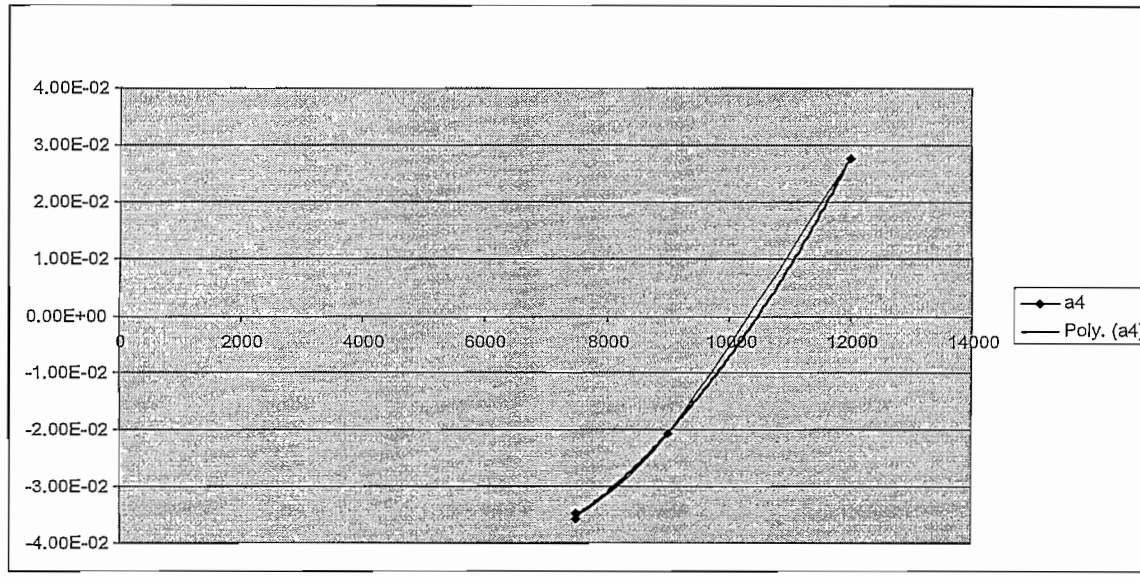


Figure 3.14: Coefficients a3 against discharge pressure.

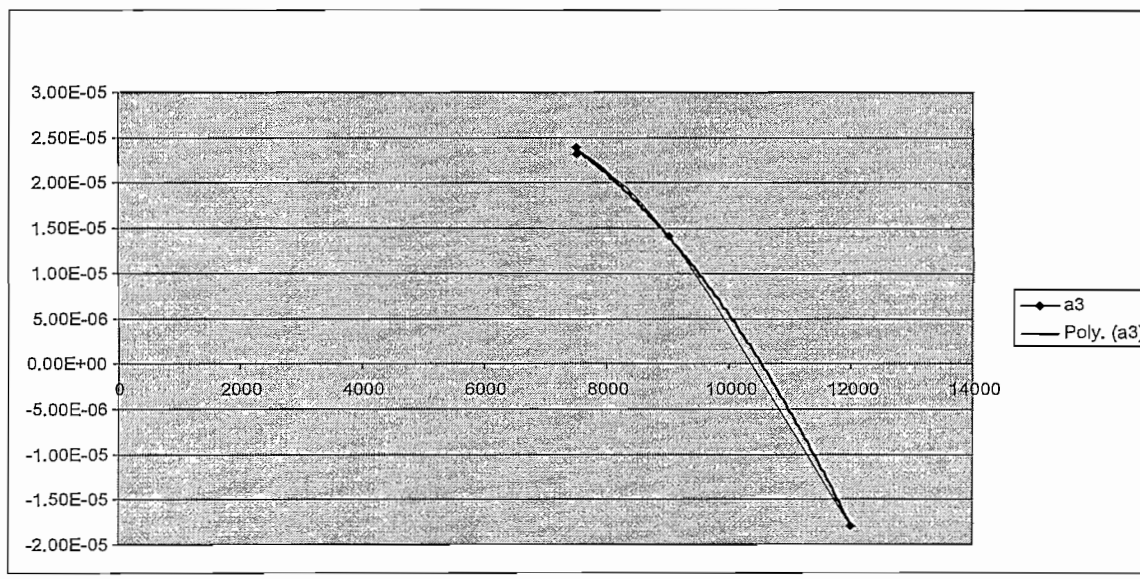

Figure 3.15: Coefficients a2 against discharge pressure.

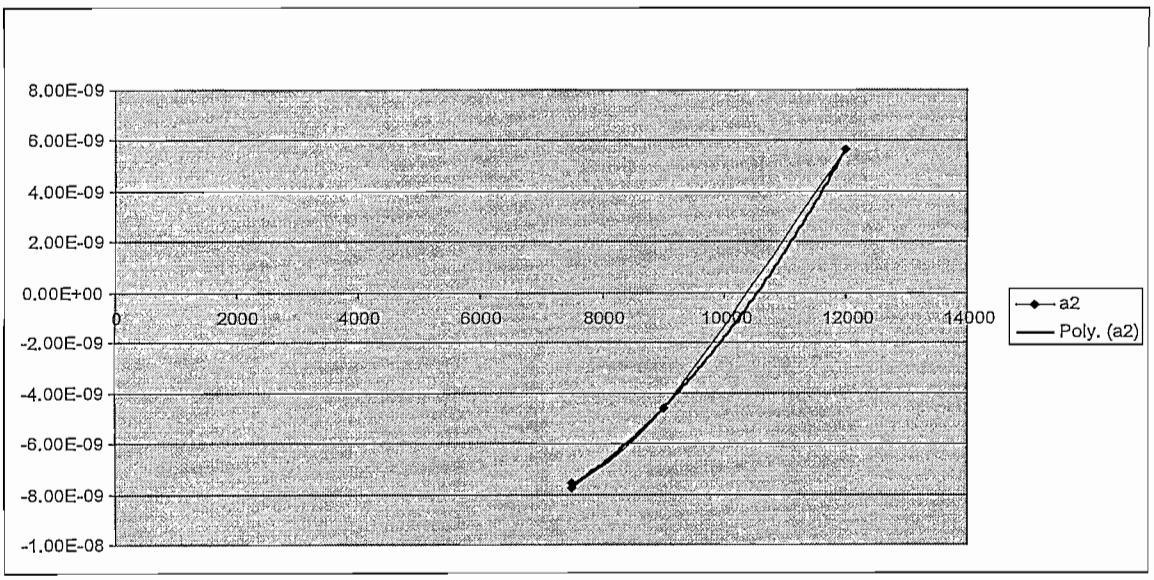


Figure 3.16: Coefficients a1 against discharge pressure.

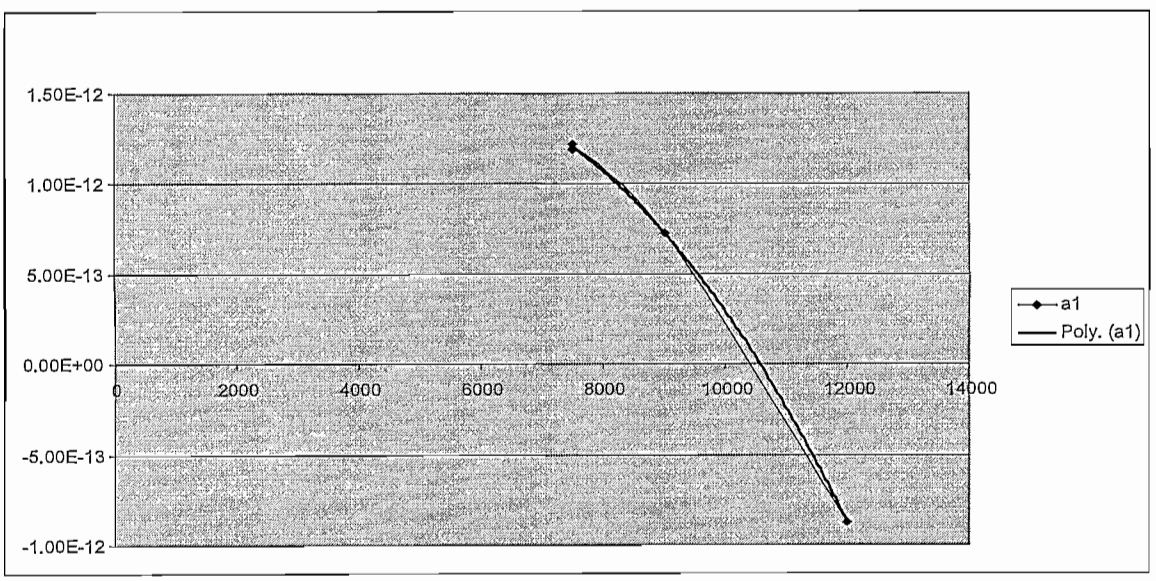

Figure 3.17: Coefficients a0 against discharge pressure.

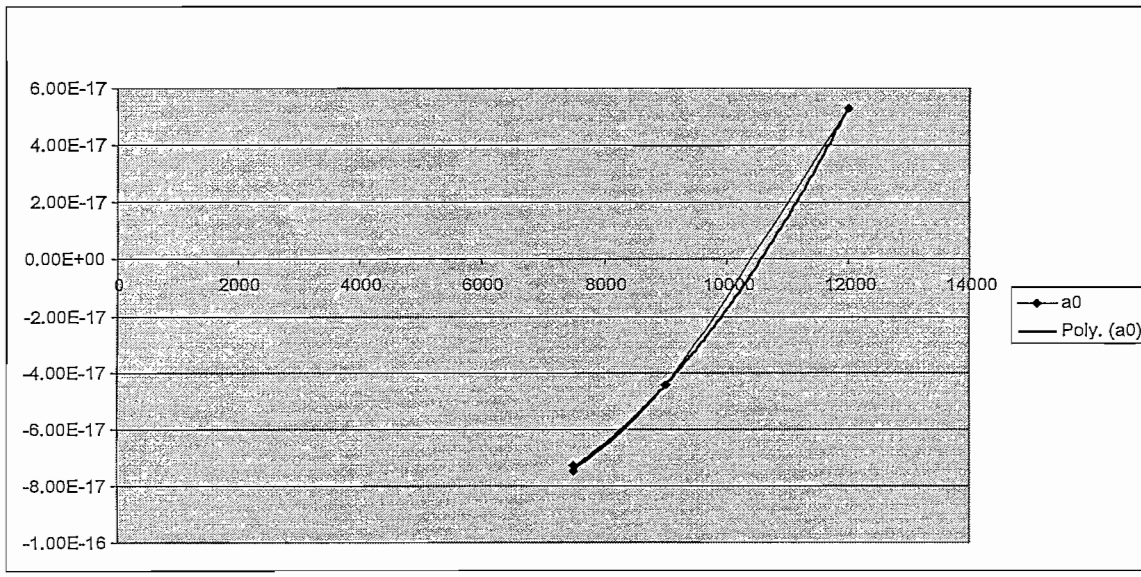


A polynomial equation is fitted through the different plots with $R^2$-equation showing the accuracy of the plot. The polynomial equation resulted in 3rd order polynomial equations taking the discharge pressure into consideration as well.

The 3rd order polynomials taking the discharge pressure into account are given below:

- $y = -8.3963\times10^{-7}x^2 + 8.0456\times10^{-3}x + 8.032$ [3.17]

  $R^2 = 9.9977\times10^{-1}$

- $y = 1.4441\times10^{-9}x^2 - 1.4157\times10^{-5x} - 1.0314\times10^{-2}$ [3.18]

  $R^2 = 9.9979\times10^{-1}$

- $y = -9.6578\times10^{-13}x^2 + 9.6283\times10^{-9}x + 5.673\times10^{-6}$ [3.19]

  $R^2 = 9.998\times10^{-1}$

- $y = 3.1092\times10^{-16}x^2 - 3.1142\times10^{-12}x - 1.7696\times10^{-9}$ [3.20]

  $R^2 = 9.9981\times10^{-1}$

- $y = -4.8268\times10^{-20}x^2 + 4.8032\times10^{16}x + 3.1525\times10^{-13}$ [3.21]

  $R^2 = 9.9982\times10^{-1}$

- $y = 2.899\times10^{-24}x^2 - 2.8348\times10^{-20}x - 2.4274\times10^{-17}$ [3.22]

  $R^2 = 9.9982\times10^{-1}$

All of the above fitted equations are reasonable fittings, 'x' being the common denominator for the discharge pressure.

From all of the above generated polynomial equations the mass flow through the system and the compressor efficiency can be described in terms of evaporating pressure and discharge pressure. All the polynomial equations can now be combined into two final equations - one equation describing the mass flow in terms of evaporating pressure and discharge pressure and the other describing the compressor efficiency in terms of evaporating pressure and discharge pressure.

The two formulas attained are as follows:

- $$\dot{m} = (-2.1646\times10^{-9}\cdot P_{dis}{}^{2} + 4.2438\times10^{-5}\cdot P_{dis} - 2.0742\times10^{-1}) + (2.3263\times10^{-12}\cdot P_{dis}{}^{2} - 4.7418\times10^{-8}\cdot P_{dis} + 2.6913\times10^{-4})\cdot P_{suc} + (-5.6907\times10^{-16}\cdot P_{dis}{}^{2} + 1.0683\times10^{-11}\cdot P_{dis} - 4.147\times10^{-8})\cdot P_{suc}{}^{2} \quad [3.23]$$

- $$eta\_c = (-8.3963\times10^{-7}\cdot P_{dis}{}^{2} + 8.0456\times10^{-3}\cdot P_{dis} - 8.032) + (1.4441\times10^{-9}\cdot P_{dis}{}^{2} - 1.4157\times10^{-5}\cdot P_{dis} - 1.0314\times10^{-2})\cdot P_{suc} + (-9.6578\times10^{-13}\cdot P_{dis}{}^{2} + 9.6283\times10^{-9}\cdot P_{dis} + 5.673\times10^{-6})\cdot P_{suc}{}^{2} + (3.1092\times10^{-16}\cdot P_{dis}{}^{2} - 3.1142\times10^{-12}\cdot P_{dis} - 1.7696\times10^{-9})\cdot P_{suc}{}^{3} + (-4.8268\times10^{-20}\cdot P_{dis}{}^{2} + 4.8032\times10^{-16}\cdot P_{dis} + 3.1525\times10^{-13})\cdot P_{suc}{}^{4} + (2.899\times10^{-24}\cdot P_{dis}{}^{2} - 2.8348\times10^{-20}\cdot P_{dis} - 2.4274\times10^{-17})\cdot P_{suc}{}^{5} \quad [3.24]$$

## 3.4 Updating the EES program

The formula for the compressor efficiency and the formula for the mass flow system are now implemented into the first EES equation. The EES program containing the two formulas is given in Appendix A. With the implementation of the two formulas all the heat pump system variables could be determined for any evaporating temperature, gas cooler outlet temperature and discharge pressure combination.

For the first run all the known variables for evaporating temperature, gas cooler outlet temperature and discharge pressure found from the compressor chart is kept as the known variables. This is done so that the unknown variables of the system can be determined and compared to the values of the compressor chart where the determined variables were known. This is to establish whether the characterizing of the compressor was successful. The results after implementing the equations into the EES program are shown in table 3.5 with the error compared to the given variables found in table 3.2.

**Table 3.5: Results after implementation of equations into EES and the errors compared to known variables.**

| T_ev (K) | Tgc_out(K) | P_dis (kPa) | P_suc (kPa) | P_suc_err | mass flow | m_doterr | Qe (kW) | Qe_err |
|---|---|---|---|---|---|---|---|---|
| 253 | 288 | 7500 | 1961 | 0.56 | 0.1016 | 0.00 | 21.92 | 0.09 |
| 253 | 298 | 7500 | 1961 | 0.56 | 0.1016 | 0.59 | 18.71 | 0.48 |
| 253 | 308 | 9000 | 1961 | 0.56 | 0.09254 | 2.05 | 14 | 2.19 |
| 253 | 313 | 11000 | 1961 | 0.56 | 0.08037 | 7.63 | 11.86 | 7.82 |
| 258 | 288 | 7500 | 2281 | 0.52 | 0.1248 | 0.32 | 26.94 | 0.22 |
| 258 | 298 | 7500 | 2281 | 0.52 | 0.1248 | 0.56 | 23 | 0.43 |
| 258 | 308 | 9000 | 2281 | 0.52 | 0.114 | 2.06 | 17.27 | 1.88 |
| 258 | 313 | 11000 | 2281 | 0.52 | 0.09894 | 0.63 | 14.61 | 0.76 |
| 263 | 288 | 7500 | 2637 | 0.49 | 0.1522 | 1.49 | 32.84 | 1.38 |
| 263 | 298 | 7500 | 2637 | 0.49 | 0.1522 | 1.81 | 28.03 | 1.65 |
| 263 | 308 | 9000 | 2637 | 0.49 | 0.1401 | 2.91 | 21.19 | 2.80 |
| 263 | 313 | 12000 | 2637 | 0.49 | 0.1105 | 7.92 | 16.98 | 7.72 |
| 273 | 288 | 7500 | 3471 | 0.43 | 0.2231 | 0.45 | 47.74 | 0.33 |
| 273 | 298 | 7500 | 3471 | 0.43 | 0.2231 | 0.89 | 40.7 | 0.73 |
| 273 | 308 | 9000 | 3471 | 0.43 | 0.2095 | 0.38 | 31.33 | 0.22 |
| 273 | 288 | 10000 | 3471 | 0.43 | 0.1961 | 4.15 | 42.7 | 4.04 |
| 273 | 298 | 10000 | 3471 | 0.43 | 0.1961 | 4.11 | 37.54 | 3.99 |
| 273 | 313 | 12000 | 3471 | 0.43 | 0.1589 | 5.47 | 24.15 | 5.29 |
| 278 | 288 | 7500 | 3954 | 0.38 | 0.2683 | 0.41 | 57 | 0.53 |
| 278 | 298 | 7500 | 3954 | 0.38 | 0.2683 | 0.11 | 48.52 | 0.04 |
| 278 | 308 | 9000 | 3954 | 0.38 | 0.2551 | 1.03 | 37.76 | 1.23 |
| 278 | 288 | 12000 | 3954 | 0.38 | 0.1889 | 18.33 | 41.21 | 18.23 |
| 278 | 298 | 12000 | 3954 | 0.38 | 0.1889 | 18.72 | 36.62 | 18.62 |
| 278 | 308 | 12000 | 3954 | 0.38 | 0.1889 | 18.33 | 31.41 | 18.20 |
| 278 | 313 | 12000 | 3954 | 0.38 | 0.1889 | 6.76 | 28.4 | 6.58 |

| T_ev (K) | Tgc_out(K) | P_dis (kPa) | P_suc (kPa) | P_suc_err | mass flow | m_doterr | Qe (kW) | Qe_err |
|---|---|---|---|---|---|---|---|---|
| 283 | 288 | 7500 | 4485 | 0.36 | 0.3216 | 0.68 | 67.63 | 0.54 |
| 283 | 298 | 7500 | 4485 | 0.36 | 0.3216 | 0.92 | 57.47 | 0.74 |
| 283 | 308 | 9000 | 4485 | 0.36 | 0.3099 | 1.34 | 45.2 | 1.09 |
| 283 | 288 | 12000 | 4485 | 0.36 | 0.2234 | 20.61 | 48.26 | 20.49 |
| 283 | 298 | 12000 | 4485 | 0.36 | 0.2234 | 21.25 | 42.83 | 21.12 |
| 283 | 308 | 12000 | 4485 | 0.36 | 0.2234 | 20.95 | 36.66 | 20.82 |
| 283 | 313 | 12000 | 4485 | 0.36 | 0.2234 | 9.48 | 33.1 | 9.32 |
| 283 | 288 | 13000 | 4485 | 0.36 | 0.1758 | 35.58 | 38.12 | 35.50 |
| 283 | 298 | 13000 | 4485 | 0.36 | 0.1758 | 35.63 | 33.98 | 35.52 |

Table 3.5 cont.: Results after implementation of equations into EES and the errors compared to known variables.

| P (kW) | P_err | COP | COP_err | Qh | Qh_err | Tcomp_out | Tihx_out | eta_c | eta_err |
|---|---|---|---|---|---|---|---|---|---|
| 9.896 | 0.04 | 2.872 | 0.24 | 28.42 | 0.21 | 263 | 391.3 | 0.657 | 0.67 |
| 9.896 | 0.04 | 2.547 | 0.31 | 25.21 | 0.36 | 263 | 391.3 | 0.657 | 0.08 |
| 10.57 | 2.62 | 1.974 | 0.30 | 20.87 | 2.35 | 263 | 412.1 | 0.6499 | 0.02 |
| 12.01 | 3.53 | 1.563 | 4.27 | 18.78 | 7.99 | 263 | 448.3 | 0.576 | 4.54 |
| 10.37 | 0.29 | 3.267 | 0.18 | 33.88 | 0.09 | 268 | 380 | 0.6688 | 0.65 |
| 10.37 | 0.29 | 2.887 | 0.00 | 29.94 | 0.30 | 268 | 380 | 0.6688 | 0.39 |
| 10.99 | 1.87 | 2.251 | 0.13 | 24.74 | 1.71 | 268 | 398.1 | 0.6794 | 0.47 |
| 12.29 | 3.98 | 1.808 | 5.12 | 22.22 | 0.91 | 268 | 428.3 | 0.6189 | 5.38 |
| 10.22 | 2.67 | 3.925 | 1.45 | 40.11 | 1.26 | 273 | 367.5 | 0.7107 | 1.92 |
| 10.22 | 2.67 | 3.454 | 1.17 | 35.3 | 1.51 | 273 | 367.5 | 0.7107 | 1.62 |
| 11.21 | 4.19 | 2.604 | 1.52 | 29.21 | 2.67 | 273 | 385.5 | 0.7149 | 1.87 |
| 15.05 | 1.63 | 1.665 | 6.09 | 25.06 | 7.63 | 273 | 441.2 | 0.5373 | 5.87 |
| 11.23 | 7.95 | 4.917 | 8.42 | 55.2 | 0.23 | 283 | 354 | 0.6639 | 9.05 |
| 11.23 | 7.95 | 4.289 | 7.98 | 48.15 | 0.64 | 283 | 354 | 0.6639 | 8.57 |
| 12.9 | 8.51 | 3.114 | 9.19 | 40.18 | 0.10 | 283 | 371 | 0.6856 | 9.61 |
| 13.69 | 8.12 | 3.799 | 4.51 | 52.01 | 3.97 | 283 | 382 | 0.6804 | 4.95 |
| 13.69 | 8.12 | 3.422 | 4.58 | 46.86 | 3.88 | 283 | 382 | 0.6804 | 5.00 |
| 14.56 | 11.76 | 2.282 | 7.49 | 33.21 | 5.20 | 283 | 406.4 | 0.6226 | 7.79 |
| 10.79 | 12.98 | 5.951 | 15.58 | 64.24 | 0.61 | 288 | 346.1 | 0.6703 | 16.29 |
| 10.79 | 12.98 | 5.165 | 15.01 | 55.76 | 0.14 | 288 | 346.1 | 0.6703 | 15.69 |
| 12.86 | 13.69 | 3.64 | 17.46 | 46.79 | 1.32 | 288 | 362.3 | 0.7028 | 17.90 |
| 13.58 | 21.95 | 3.725 | 4.87 | 50.58 | 18.17 | 288 | 391.9 | 0.6901 | 5.23 |
| 13.58 | 21.95 | 3.387 | 4.38 | 45.99 | 18.56 | 288 | 391.9 | 0.6901 | 4.72 |
| 13.58 | 21.95 | 3.003 | 4.89 | 40.78 | 18.13 | 288 | 391.9 | 0.6901 | 5.21 |
| 13.58 | 21.95 | 2.781 | 19.77 | 37.77 | 6.49 | 288 | 391.9 | 0.6901 | 20.14 |
| 9.147 | 21.82 | 8.131 | 27.31 | 74.38 | 0.47 | 293 | 337.3 | 0.7375 | 28.22 |
| 9.147 | 21.82 | 7.02 | 27.06 | 64.21 | 0.68 | 293 | 337.3 | 0.7375 | 27.90 |
| 11.22 | 23.67 | 4.832 | 29.72 | 54.2 | 1.02 | 293 | 352.1 | 0.8029 | 30.30 |
| 12.09 | 32.46 | 4.78 | 17.79 | 57.78 | 20.45 | 293 | 379.2 | 0.7882 | 18.24 |
| 12.09 | 32.46 | 4.331 | 16.90 | 52.36 | 21.06 | 293 | 379.2 | 0.7882 | 17.31 |
| 12.09 | 32.46 | 3.821 | 17.35 | 46.19 | 20.74 | 293 | 379.2 | 0.7882 | 17.73 |
| 12.09 | 32.46 | 3.527 | 34.41 | 42.63 | 9.24 | 293 | 379.2 | 0.7882 | 34.80 |
| 11.08 | 43.18 | 4.181 | 13.61 | 46.32 | 35.45 | 293 | 389.2 | 0.7402 | 14.00 |
| 11.08 | 43.18 | 3.807 | 13.57 | 42.18 | 35.47 | 293 | 389.2 | 0.7402 | 13.93 |

From the results found in table 3.5 the following conclusions could be made. The error for the determination of the suction pressure is on average less than 1% which indicates a very good correlation. Because of the way that the compressor chart is put together, seeing that not all of the pressures are kept constant throughout the DORIN simulation, the pressures implemented into the equations could not be constant throughout the correlation. Values in the original compressor chart are given for a constant pressure of 7500 and 9000kPa throughout the compressor chart but with higher pressures it varies between 10000, 11000 and 12000kPa. To get a plot for all the given evaporating temperatures a plot had to be prepared which consisted of both pressures - 11000kPa at a lower evaporating temperature and 12000kPa for a higher evaporating temperature.

This could be determined from the errors displayed in table 3.5. The purpose of the polynomial equations determined earlier is to interpolate between given pressures. Therefore, for pressures at 7500 and 9000kPa the errors are small, not exceeding 5%, this is because these values are well within the boundaries and the equations have been correlated from a plot that used these pressures for all evaporating temperatures. A more significant error is seen for pressures 11000 and 12000kPa, this is because of the fact that one plot had to be made containing both pressures for certain evaporating temperatures. These values are still considered acceptable reaching only a 20% error at most.

The most positive result found from the correlation is the error for the correlations at 10000kPa. There are only two results found for 10000kPa in the compressor chart initially given and therefore they were not implemented into the determination of the polynomial equations. The errors at a pressure of 10000kPa do not exceed 5%. This is satisfactory because this is exactly what is expected from the polynomial equations, to determine the values needed at any given discharge pressure, evaporating temperature and gas cooler outlet temperature.

From the above results we can now determine the unknown variables for any evaporating temperature, gas cooler outlet temperature and discharge pressure keeping in mind that we should stay within the boundaries of the determined polynomials. From the literature it was found that best performance of a $CO_2$ system was for discharge pressures between 8000 and 11000kPa. Knowing that the gas cooler outlet temperature depends on the water inlet temperature and knowing that

the evaporation temperature cannot exceed the gas cooler outlet temperature this also has to be kept in mind.

The following section is to determine at which discharge pressure the system will operate at its best for certain evaporating and gas cooler outlet temperatures. A water temperature gradient was built into the EES simulation which is given in Appendix A. The gradient was made for a certain inlet water temperature and a fixed outlet water temperature of 60 °C. From this we could see whether or not the water profile fits with the temperature slope in the gas cooler.

The simulations were done with the gas cooler temperatures and evaporating temperatures as given in the compressor chart. The simulations were done for discharge pressures of 8000,9000,10000 and 11000kPa respectively.

The following is the comparison between the results at different discharge pressures. The average COP, heating capacity and compressor efficiency was used to compare the system at different types of discharge pressures. This is given in Table 3.6.

Table 3.6: Average COP, heating capacity and compressor efficiency at different discharge pressures.

| P_dis | Avg COP | Avg Q_h | Avg eta_c |
|---|---|---|---|
| 8000 | 3.3 | 40.9 | 0.63 |
| 9000 | 3.320 | 45.3 | 0.63 |
| 10000 | 3.100 | 45.5 | 0.63 |
| 11000 | 2.800 | 43.99 | 0.61 |

From Table 3.6 it could be seen that the average values does not differ that much. At 8000kPa and 11000kPa they start to deviate from the results found in the simulations done at 9000 and 10000kPa, this could be because they are close to the boundaries from which the polynomials were derived. At 9000 and 10000kPa the results are satisfactory, the average COP being very good and the average heating capacity being what is needed to compare it to the R-22 system later on. Thus it could be seen that for discharge pressures of 9000 and 10000kPa the system results are satisfactory.

The water temperature gradient should not exceed the gas cooler gradient and the water inlet should also not be higher than the gas cooler outlet temperature. Therefore a discharge pressure and gas cooler outlet temperature should be chosen

so that the inlet water temperature is not higher than the gas cooler outlet temperature and also that the water temperature gradient does not exceed the gas cooler's decreasing temperature gradient. Secondly, for certain inlet water temperatures and evaporating temperatures it had to be determined at which gas cooler outlet temperature and discharge pressure the system will have to operate. This was done by bringing into account the water profile.

The water inlet temperatures were implemented at 10, 20 and 30 °C. The system was simulated with gas cooler outlet temperatures of 288, 298 and 308*K* respectively at the different water inlet temperatures. These were all simulated at evaporating temperatures of 273,278 and 283K and at discharge pressures of 9000 and 10000kPa. All the runs were plotted on a temperature-entropy (T-s) diagram and are shown in the following figures.

The routine followed was as follow:

- For an evaporating temperature of 0 degrees and water inlet temperature of 10 degrees the gas cooler outlet temperature were changed between 288, 298 and 308*K*.
- For an evaporating temperature of 0 degrees and water inlet temperature of 20 degrees the gas cooler outlet temperature were changed between 288, 298 and 308*K*.
- For an evaporating temperature of 0 degrees and water inlet temperature of 30 degrees the gas cooler outlet temperature were changed between 288, 298 and 308*K*.
- The same was done for an evaporating temperature of 5 and 10 degrees.

The results for 10000kPa, an evaporating temperature of 0 degrees and the gas cooler outlet temperature being changed from 288*K*, to 298*K* and to 308*K* are shown.

Figure 3.18: T-s diagram: T_wi = 10°C; T_gc = 288K and P_dis = 10000kPa.

Figure 3.19: T-s diagram: T_wi = 10°C; T_gc = 298K and P_dis = 10000kPa.

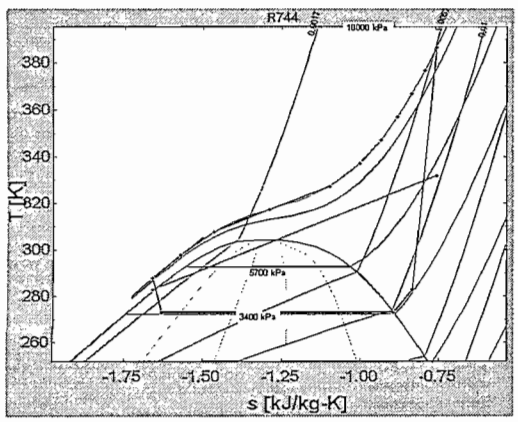


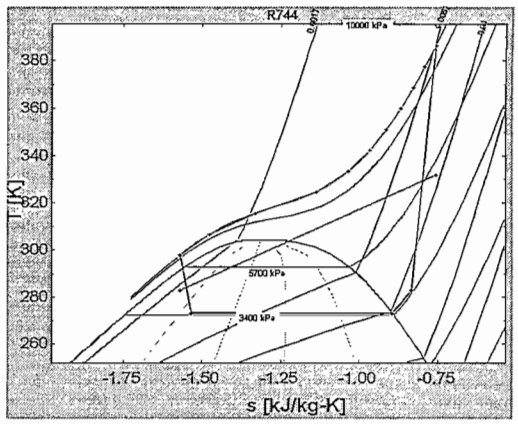


Figure 3.20: T-s diagram: T_wi = 10°C; T_gc = 308K and P_dis = 10000kPa.

Figure 3.21: T-s diagram: T_wi = 20°C; T_gc = 288K and P_dis = 10000kPa.

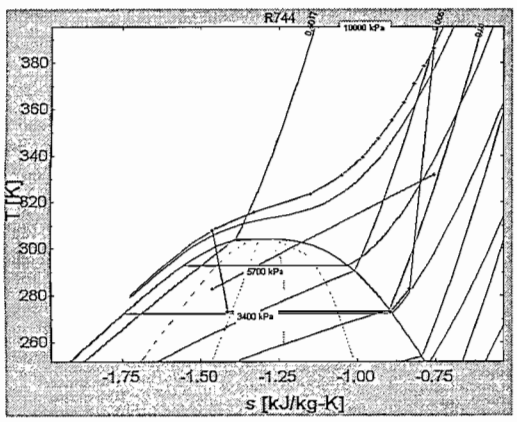


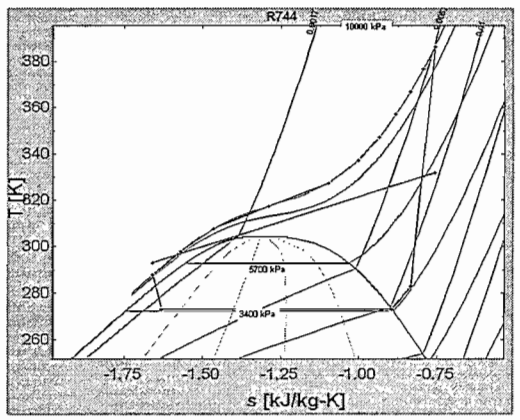


Figure 3.22: T-s diagram: T_wi = 20°C; T_gc = 298K and P_dis = 10000kPa.

Figure 3.23: T-s diagram: T_wi = 20°C; T_gc = 308K and P_dis = 10000kPa.

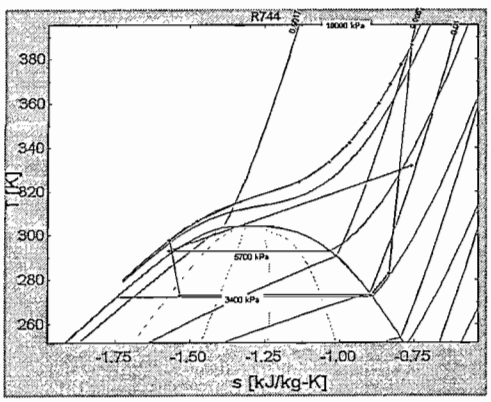


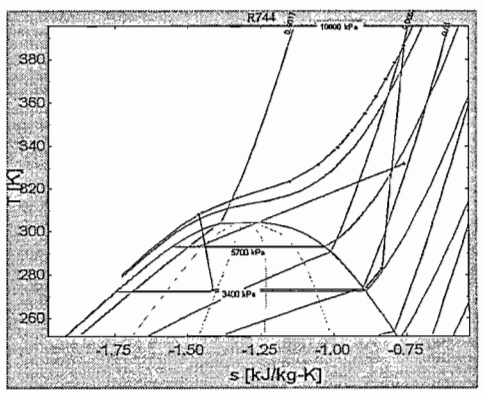

From Figures 3.18 to 3.23 the effect of the gas cooler outlet temperature on the T-s diagram of the $CO_2$ cycle could be seen. We know that the gas cooler outlet temperature cannot be lower than the water inlet temperature and the reason for this can be seen in Figures 3.18 to 3.23. Where if the water inlet temperature is higher than the gas cooler outlet temperature, the two profiles (refrigerant temperature and water temperature profile) will cross and that is impossible in practice.

Because the refrigerant cools down with a temperature glide in the gas cooler, it was also a concern whether or not the water profile will cross the refrigerant profile as the refrigerant cools down in a glide. It could be seen that as long as the water inlet temperature is kept lower than the gas cooler outlet temperature that these two profiles won't cross each other. This could be a problem for lower discharge pressures since the refrigerant also cools down with a temperature glide but at a constant pressure.

Therefore from Figures 3.18 to 3.23 it could be seen that as the water inlet temperature rises the gas cooler temperature will have to rise as well. This corresponds with what was found in the literature and this is the reason why the water inlet temperature is directly linked to the system's performance. If the water inlet temperature rises the gas cooler temperature will have to rise causing the heat that is available to be extracted from the ambient air to be less and this decreases the system's cooling capacity which decreases the systems heating capacity and therefore results in a less efficient system.

Figure 3.24: T-s diagram: T_wi = 30°C; T_gc = 308K and P_dis = 9000kPa.

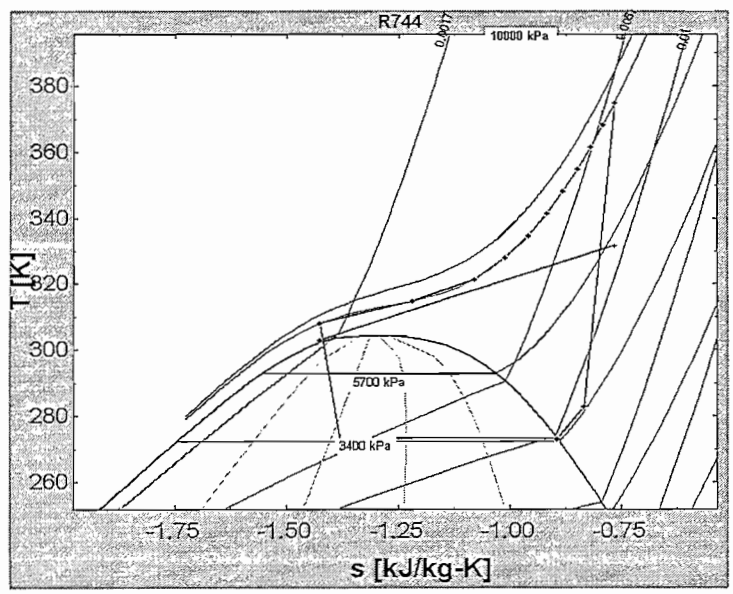

Figure 3.24 shows the T-s diagram for a discharge pressure of 9000kPa, water inlet temperature of 30 degrees and gas cooler outlet temperature of 308*K* and evaporating temperature of 273*K*. From this it could be seen that in the centre of the gas cooler temperature glide the water profile gets very close to the temperature glide within the gas cooler. From the literature it is known that the delta temperature between the refrigerant and medium could be as close as 2*K*, but this is for a highly efficient gas cooler and can potentially cause problems in practice. Therefore one of the reasons that lead to 10000kPa to be the preferred discharge pressure at which to operate is because the delta temperature between the medium and refrigerant is much more likely in practice at a discharge pressure of 10000kPa.

From the simulations made to attain Figures 3.18 to 3.23 the heating capacity, COP and power was determined. These results were compared with each other and are shown in Table 3.7.

Table 3.7: Comparison of COP, Q_h and P at different T_ev, T_wi, T_gc and discharge pressures.

| | | P_dis | | | | | |
|---|---|---|---|---|---|---|---|
| | | 9000 | | 10000 | | 11000 | |
| | | T_wi | T_gc | T_wi | T_gc | T_wi | T_gc |
| T_ev | 0 (273) | 10 | 288 | 10 | 288 | 10 | 288 |
| | | 20 | 298 | 20 | 298 | 20 | 298 |
| | | 30 | 308 | 30 | 308 | 30 | 308 |
| | 5 (278) | 10 | 288 | 10 | 288 | 10 | 288 |
| | | 20 | 298 | 20 | 298 | 20 | 298 |
| | | 30 | 308 | 30 | 308 | 30 | 308 |
| | 10 (283) | 10 | 288 | 10 | 288 | 10 | 288 |
| | | 20 | 298 | 20 | 298 | 20 | 298 |
| | | 30 | 308 | 30 | 308 | 30 | 308 |

Table 3.7 cont.: Comparison of COP, Q_h and P at different T_ev, T_wi, T_gc and discharge pressures.

| P_dis | | | | | | | | |
|---|---|---|---|---|---|---|---|---|
| 9000 | | | 10000 | | | 11000 | | |
| P | Q_h | COP | P | Q_h | COP | P | Q_h | COP |
| 14.11 | 59.46 | 4.013 | 15.87 | 58.25 | 3.67 | 16.79 | 56.43 | 3.361 |
| 14.82 | 53.63 | 3.62 | 15.87 | 53.04 | 3.342 | 16.79 | 51.78 | 3.084 |
| 14.82 | 45.45 | 3.068 | 15.87 | 46.54 | 2.932 | 16.79 | 46.3 | 2.758 |
| 15.83 | 69.9 | 4.416 | 17.05 | 68.49 | 4.016 | 17.87 | 65.81 | 3.682 |
| 15.83 | 62.81 | 3.968 | 17.05 | 62.14 | 3.644 | 17.87 | 60.16 | 3.366 |
| 15.83 | 52.84 | 3.338 | 17.05 | 54.2 | 3.178 | 17.87 | 53.5 | 2.993 |
| 15.12 | 80.34 | 5.313 | 16.53 | 78.71 | 4.763 | 17.58 | 75.29 | 4.282 |
| 15.12 | 71.72 | 4.743 | 16.53 | 70.98 | 4.294 | 17.58 | 68.44 | 3.892 |
| 15.12 | 59.61 | 3.942 | 16.53 | 61.32 | 3.71 | 17.58 | 60.37 | 3.433 |

Table 3.7 gives a very good indication of how the system is affected by the evaporating temperature, water inlet temperature, gas cooler outlet temperature and discharge pressure.

It could be clearly seen that as the water inlet temperature increases the gas cooler outlet temperature has to increases as well and this causes a decrease in the COP of the system and the heating capacity available. This was predicted and can now be seen from the data that was found.

For a higher discharge pressure the COP decreases, this is because the power that is needed to reach the higher discharge pressure increases and therefore reduces the system's COP. On the other hand as the discharge pressure increases so does the heating capacity, this is because more energy is put into the system to reach the higher discharge pressure.

Figures 3.25 and 3.26 show the pressure enthalpy diagram for the $CO_2$ system. Both are done at an evaporating temperature of 283*K* and a discharge pressure of 10000kPa. The gas cooler outlet temperature is changed from 288 to 308*K* and the drastic change in the P-h diagram can be seen. The reduction in heating capacity could be clearly seen from the figures as the gas cooler outlet temperature increases. The effect of the added superheat could also be seen from the figures.

**Figure 3.25: P-h diagram: T_ev = 283K; T_gc = 288K and P_dis = 10000kPa.**

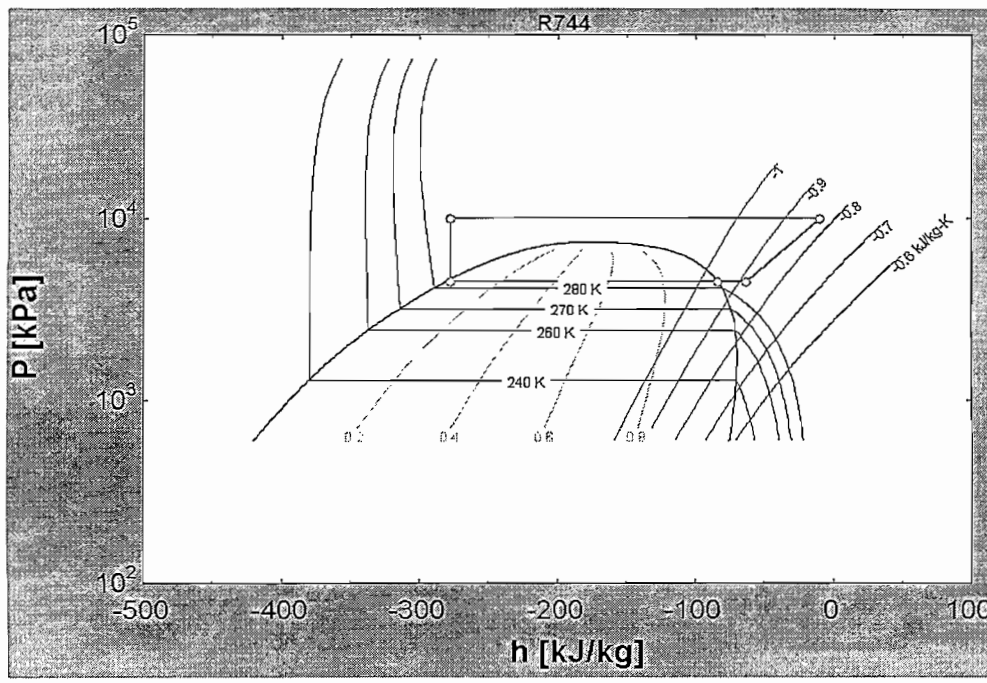

Figure 3.26: P-h diagram: T_ev = 283K; T_gc = 308K and P_dis = 10000kPa.

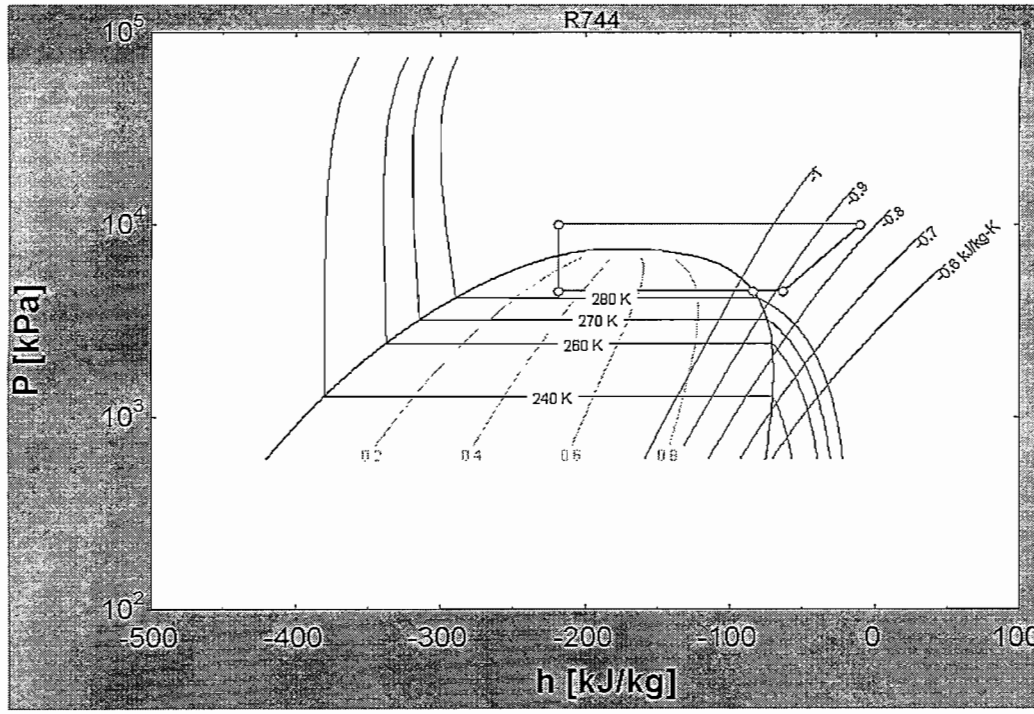

## 3.5 Characterizing of the $CO_2$ System

The final step in the process is to characterize the system into two equations in terms of the system's heating capacity and COP. This will enable us to compare the $CO_2$ system with the R-22 system for which a characterization already exists in terms of heating capacity and COP.

For the $CO_2$ system to be compared with an R-22 system a reasonable condition had to be chosen at which to run the $CO_2$ system. It was chosen to run the compressor at a constant discharge pressure of 10000kPa, this is possible with the expansion valve implemented in the system, correct refrigerant charge and with a variable speed pump determining the mass flow of the water.

A discharge pressure of 10000kPa was chosen because of the following reasons:

- The water heating profile will not cross the gliding gas cooler outlet temperatures profile.
- It is well within the boundaries within which the polynomials were determined and will give an accurate result.
- It is within the running boundaries of the compressor chart and within the capabilities of the compressor chosen.
- It is a feasible discharge pressure for inlet water temperatures of up to 30°C.
- It is an optimum running pressure considering COP and heating capacity.
- It is a high enough pressure to ensure that a high evaporating temperature will not be higher than the gas cooler outlet temperature which is also connected to a pressure.

To characterize the $CO_2$ system, equations for the system in terms of COP and heating capacity had to be determined. The equations also have to be in terms of gas cooler outlet temperatures and evaporating temperatures since these variables will determine at which conditions the system is running and in turn will determine the COP and heating capacity of the system.

Therefore it was assumed that for a certain inlet water temperature, the gas cooler outlet temperature must be $5K$ higher than the inlet water temperature. It is known that the delta temperature between the refrigerant and medium could be lower but $5K$ is a reasonable and easily achievable delta. The delta temperature is implemented

because the simulations that will be done to compare the $CO_2$ system with the R-22 system will be in terms of the water inlet temperature and the gas cooler outlet temperature should react to the inlet water temperature's value. Therefore the delta temperature implemented will ensure that the gas cooler outlet temperature is always higher than the water inlet temperature.

For the evaporating temperature it was decided that the evaporation temperature will be $7K$ lower than the ambient wet bulb temperature. This is an assumption which in practice has shown to be more or less accurate. The delta temperature is implemented because the simulations that will be done to compare the $CO_2$ system with the R-22 system will be in terms of the evaporation temperature. The delta implemented will ensure that the system is run at an evaporating temperature of $7K$ lower than the wet bulb temperature which is known.

The simulations are done within a wider spectrum of running conditions. It is done for evaporating temperatures of -5, 0, 5 and $10K$ respectively with the delta temperature between the evaporating temperature and ambient wet bulb temperature implemented in the EES program (given in Appendix A). The water inlet temperature is varied from 278 to $303K$ as shown in Table 3.8. The delta temperature between the inlet water temperature and gas cooler outlet temperature is implemented in the EES program as shown in Appendix A.

The results are shown in Table 3.8.

**Table 3.8: Results for a discharge pressure of 10000kPa with varying evaporating temperatures and gas cooler outlet temperatures.**

| | | | | P_dis = | 10000 | kPa |
|---|---|---|---|---|---|---|
| | | T_wi | T_gc | Q_h | P | COP |
| T_ev | -5 (268) | 278 | 283 | 50.87 | 14.18 | 3.588 |
| | | 283 | 288 | 48.94 | 14.18 | 3.451 |
| | | 288 | 293 | 46.89 | 14.18 | 3.307 |
| | | 293 | 298 | 44.68 | 14.18 | 3.151 |
| | | 298 | 303 | 42.23 | 14.18 | 2.978 |
| | | 303 | 308 | 39.37 | 14.18 | 2.776 |
| | 0 (273) | 278 | 283 | 60.62 | 15.87 | 3.819 |
| | | 283 | 288 | 58.25 | 15.87 | 3.67 |
| | | 288 | 293 | 55.74 | 15.87 | 3.512 |
| | | 293 | 298 | 53.04 | 15.87 | 3.342 |
| | | 298 | 303 | 50.04 | 15.87 | 3.153 |
| | | 303 | 308 | 46.54 | 15.87 | 2.932 |

| | | | | P_dis = | 10000 | kPa |
|---|---|---|---|---|---|---|
| | | T_wi | T_gc | Q_h | P | COP |
| T_ev | 5 (278) | 278 | 283 | 71.38 | 17.05 | 4.186 |
| | | 283 | 288 | 68.49 | 17.05 | 4.016 |
| | | 288 | 293 | 65.43 | 17.05 | 3.837 |
| | | 293 | 298 | 62.14 | 17.05 | 3.644 |
| | | 298 | 303 | 58.48 | 17.05 | 3.429 |
| | | 303 | 308 | 54.2 | 17.05 | 3.178 |
| | 10 (283) | 278 | 283 | 78.46 | 17.58 | 4.462 |
| | | 283 | 288 | 78.71 | 16.53 | 4.763 |
| | | 288 | 293 | 74.99 | 16.53 | 4.537 |
| | | 293 | 298 | 70.98 | 16.53 | 4.294 |
| | | 298 | 303 | 66.52 | 16.53 | 4.025 |
| | | 303 | 308 | 61.32 | 16.53 | 3.71 |

We now have sufficient data to characterize the system at an operating discharge pressure of 10000kPa. The data attained is read into the EES program shown in Appendix A.

The EES program has all the variables that are shown in Table 3.8 in terms of the wet bulb temperature and water inlet temperature. From the results given to the EES program it can make a profile fit through the equations, determining the coefficients built into the formulas in the EES program. Once the coefficients are determined they can be replaced within the formula leaving only the ambient wet bulb temperature and the water inlet temperature as the unknown. We now have two formulas, one for determining the COP of the system and one for the determining the heating capacity of the system in terms of ambient wet bulb temperatures and water inlet temperatures. Therefore these two equations can give the systems COP and heating capacity for any wet bulb temperature and any water inlet temperature.

The two equations were found to be:

- $$COP = 3.626 + 6.925\times10^{-3}\cdot T_a - 1.331\times10^{-2}\cdot T_w - 1.065\times10^{-3}\cdot T_a\cdot T_w + 4.622\times10^{-3}\cdot T_a^{\,2} - 4.428\times10^{-4}\cdot T_w^{\,2} \quad [3.25]$$
- $$Q = 47.51 + 2.131\cdot T_a - 0.1785\cdot T_w - 0.02479\cdot T_a\cdot T_w + 5.58\times10^{-2}\cdot T_a^{\,2} - 6.202\times10^{-3}\cdot T_w^{\,2} \quad [3.26]$$

The power of the system can also be calculated with equation [3.5]. With the power, heating capacity and COP known, a close comparison between the $CO_2$ system and R-22 system can be done. This is done in Chapter 4.

# CHAPTER 4

# COMPARISON BETWEEN ILH, R-22 AND $CO_2$ SYSTEMS

# *CHAPTER 4*

## *4. COMPARISON BETWEEN ILH, R-22 AND $CO_2$ SYSTEM*

This chapter compares an in-line electrical heating (ILH) system and R-22 heat pump system with the $CO_2$ heat pump system described in the previous chapter. The three heating systems are compared based on performance criteria under the same conditions pertaining to where they are situated and on the demand for hot water.

This chapter will be divided into the following sections:

- System Setup.
  - Scenario.
  - Component Sizing.
- Summer and Winter Day Analysis.
- Year Analysis.

## 4.1 System Setup

In chapter 3 the method for deriving the formulas for a $CO_2$ heat pump system in terms of COP and heating capacity was discussed. The same equations were derived by M-Tech Industrial (Pty) Ltd. for a heat pump system operating with R-22 as refrigerant. These equations are now implemented into the WHSIM Statistical program (Rousseau, 2006) which can be used to compare the two systems, and they are also compared to a system having only an ILH. The ILH system is also implemented in the programme used to determine the performance.

The WHSIM Statistical program describes and predicts the performance and power consumption of a heat pump under any circumstances taking into consideration the location and weather and will be used to compare the three systems under the same given conditions. It is a software application containing weather data for certain areas in South Africa and different setup possibilities like for instance a hotel situation. The scenario surrounding the implementation of the three systems are given in Table 4.1. The program contains historic weather data of South Africa so the heat pump systems can be compared for every half hour over a period of a total year.

### 4.1.1 Scenario

Table 4.1: Scenario for the system set up.

| Scenario | Hotel |
|---|---|
| Profile | Twin peak consumption |
| Occupancy | 190 persons |
| Water consumption per person (summer) | 75 litres |
| Location | Johannesburg |
| Energy tariff | Megaflex |
| Number of vessels | 2 |
| Vessel capacity | 7900 litres |
| Connection of vessel set up | Series |
| Heat pumps capacity | 50kW |
| In-line heater capacity (used with heat pumps) | 48kW |
| In-line heater capacity (on its own) | 72kW |

The installation is set up with a typical hotel situation. It is set that the occupancy of the hotel is 190 persons and it is set that each person will use an average of 75 litres of hot

water per day. The WHSIM Statistical software is programmed to increase the water consumption with a certain factor for the winter time. It is assumed that the hotel is at maximum capacity for the full year.

Figure 4.1 is a schematic representation of a typical layout of the components as mentioned above.

Both the heat pump systems are evaluated with the heat pump installed in parallel with two storage vessels in series. The ILH system is installed in the same way as the heat pumps but with the ILH in parallel with the series-connected vessels. The capacity of one storage vessel is 7900 litres giving a total storage capacity of 15800 litres. For the system there are two thermostats determining the operation of the heat pump system and the in-line heater system. The thermostats are situated near the top of the hot vessel and the bottom of the cold vessel.

It is important that both the systems are compared at the same ambient conditions and at the same demand for hot water by users. When compared under the same conditions a clear comparison could be derived to see how the systems will operate in relation to each other. For comparison purposes the location was selected as Johannesburg and will therefore be operated at the same weather conditions over a period of one year. WHSIM can also show the results for a single day in summer and a single day in winter for more detailed hourly comparisons. The summer day was chosen as the 9$^{th}$ of December and the winter day as the 29$^{th}$ of July.

The winter periods are considered to be from the first of June to the end of August and the summer periods are from the first of September to the end of May. The input files for the above-mentioned are shown in Appendixes B.

Figure 4.1: Layout of the system.

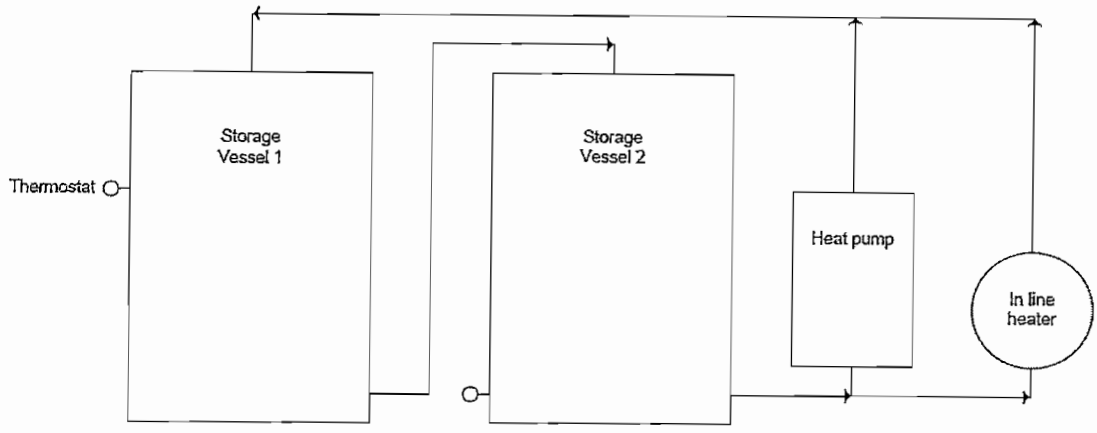


An in-line heater with a heating capacity of 48kW with a discharge temperature of 60°C is installed as a backup for when the heat pump system is not able to operate due to low ambient conditions or when the demand for hot water is more than what can be generated by the heat pump. The ILH is a two stage heater using only its full capacity when necessary. The minimum dry bulb temperature at which the heat pump system can operate is set at 5°C; therefore the heat pump system will not operate below a dry bulb ambient temperature of 5°C and the in-line heater will come in operation should this occur. The storage vessel supplying the heat pump with water is set to turn off the heat pump when the supply temperature of the water reaches 30°C. Therefore the inlet water temperature to the heat pump system will not exceed 30°C.

### *4.1.2 Component Sizing*

The three systems described are an R-22 heat pump, a transcritical $CO_2$ heat pump (both of 50kW nominal heating capacity as described in the previous chapter), and the ILH which is a 72kW step up electrical heating system. The two heat pump systems consist of an ILH (48kW) as well to give some support and therefore, when used on its own, a bigger capacity ILH (72kW) is needed to provide its own backup and to ensure that the ILH system on its own will be enough to keep up with the demand.

An in-line heater can be implemented as a backup system for the heat pump to help in situations where i) the heat pump is not operating at low ambient temperatures, or ii) conditions of extreme water consumption. The storage capacity can be given as input and the demand profile for hot water can be chosen as well.

The three systems can now be compared to one another under the same conditions as if all of the systems were installed in the same place and with the same hot water demand under the same conditions. The three systems are compared with each other operating at one summer and one winter day and are then compared over a running period of one year.

## 4.2 Summer and Winter Day Analysis

The following section is dedicated to the day analysis, one for winter and one for summer, of the three different systems as described in section 4.1 - one system containing the $CO_2$ heat pump, one the R-22 system and the last containing only the 72kW ILH.

Figure 4.2 shows the summer daily normalised water consumption profile for the hotel case study. This is a typical twin peak profile where there is a higher demand for hot water in the mornings between 06:00 and 08:00 and then again at between approximately 18:00 to 21:00 in the evening.

**Figure 4.2: Daily water consumption for all three systems (summer).**

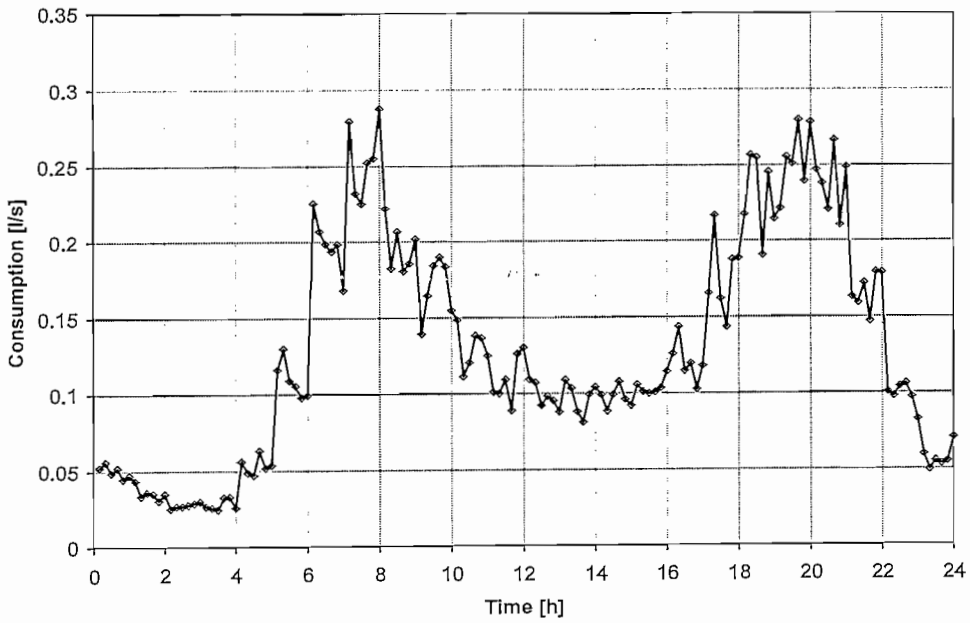

Figure 4.3: Daily water consumption for all three systems (winter).

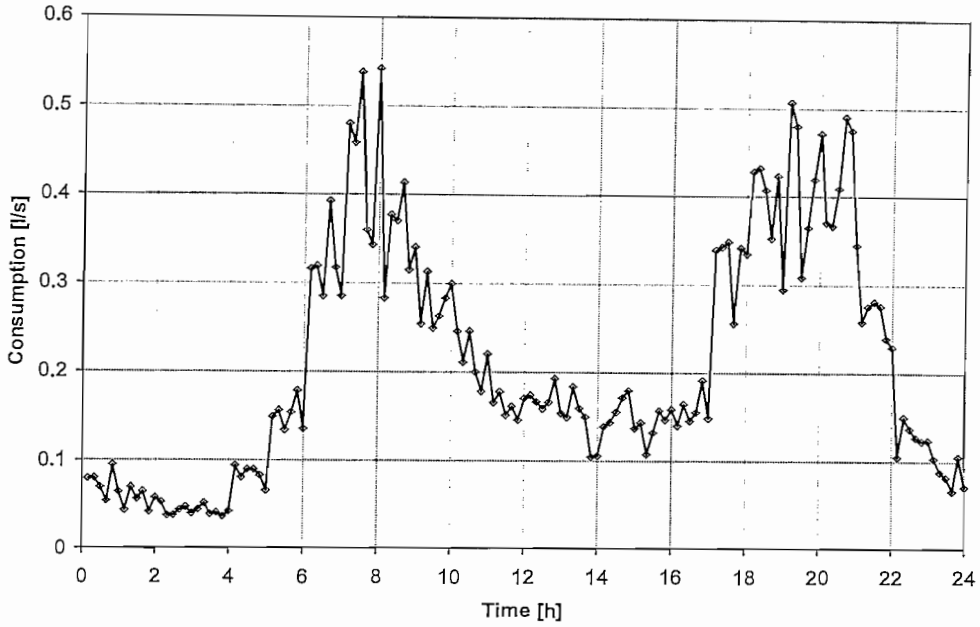


Figure 4.3 shows the winter daily normalised water consumption that is higher than for summer.

The weather conditions for all three the systems are shown in figure 4.4 and 4.5 for the summer and winter condition respectively. The blue line shows the dry bulb ambient temperature and the red line the wet bulb temperature in degrees Celsius.

For the winter condition it can be seen that the dry bulb ambient temperature is below 5°C up until just past 08:00 which confirms why the heat pump systems only came into operation at that time of hour.

Figure 4.4: Weather conditions for all three systems (summer).

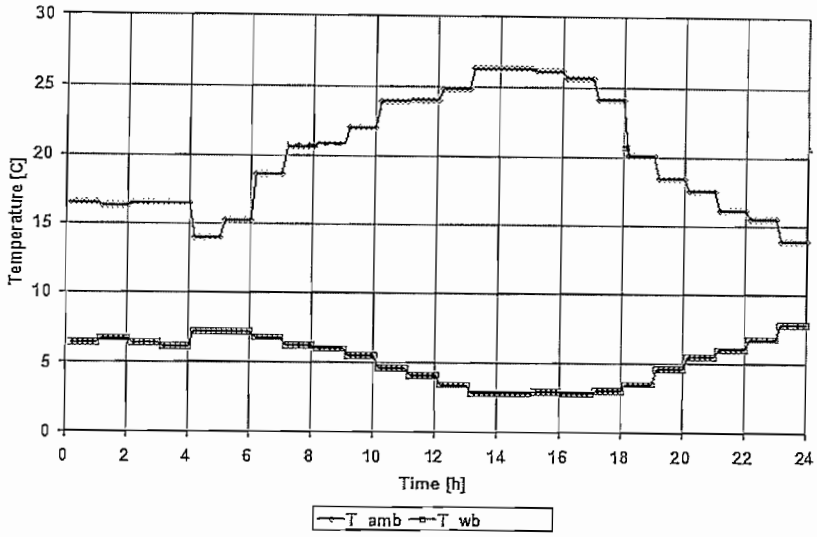


Figure 4.5: Weather conditions for all three systems (winter).

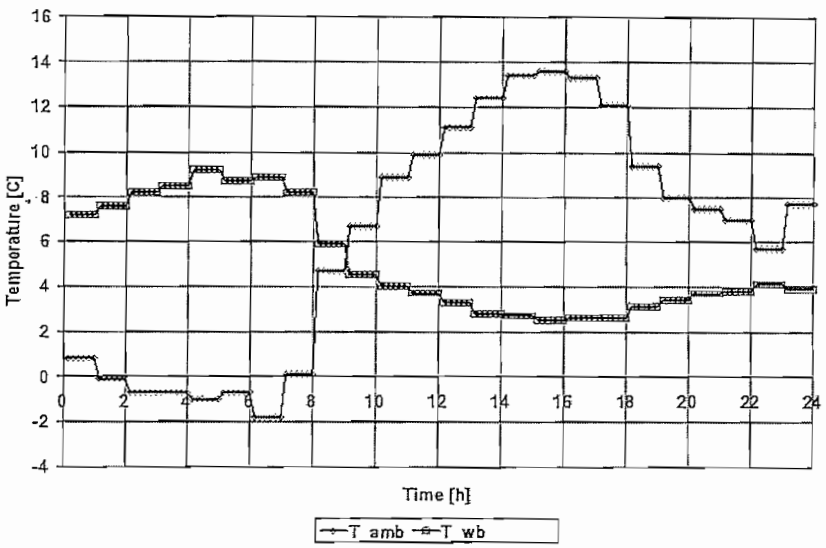


Figure 4.6 shows the supply temperatures inside storage vessel 1 for all three the systems. Figure 4.7 shows the bottom temperatures inside storage vessel 2 for all three the systems. These temperatures are for the summer condition.

It can be seen that the temperature profiles for the three systems do not vary much. This is because the conditions at which the systems are operating are exactly the same and

therefore the demand for hot water is the same and also because the systems are closely matched as far as their capacities are concerned.

It can be seen that the bottom temperatures of storage vessel 2 are at 30°C for all three systems. This is because the thermostat is set at this temperature to ensure that the heat pump does not have an inlet water temperature of above 30°C. Thus when the bottom thermostat senses a temperature of 30°C the system will turn of and has now reached the favourable temperature. Both storage tanks are considered to be at the desired temperature.

Storage vessel 1 has a temperature of up to 60°C and therefore the hotel and its recipients will receive hot water at these temperatures, heat losses in the pipe network neglected. From the top temperatures in storage vessel 1 of all three systems it can be seen that the systems are all capable of keeping up with the hot water demand under the summer conditions.

There is a bigger deviation in the bottom temperatures of storage vessel 2 because when the system is in operation cold municipal water enters at this point.

Figure 4.6: Top temperatures of vessel 1 for all three systems (summer).

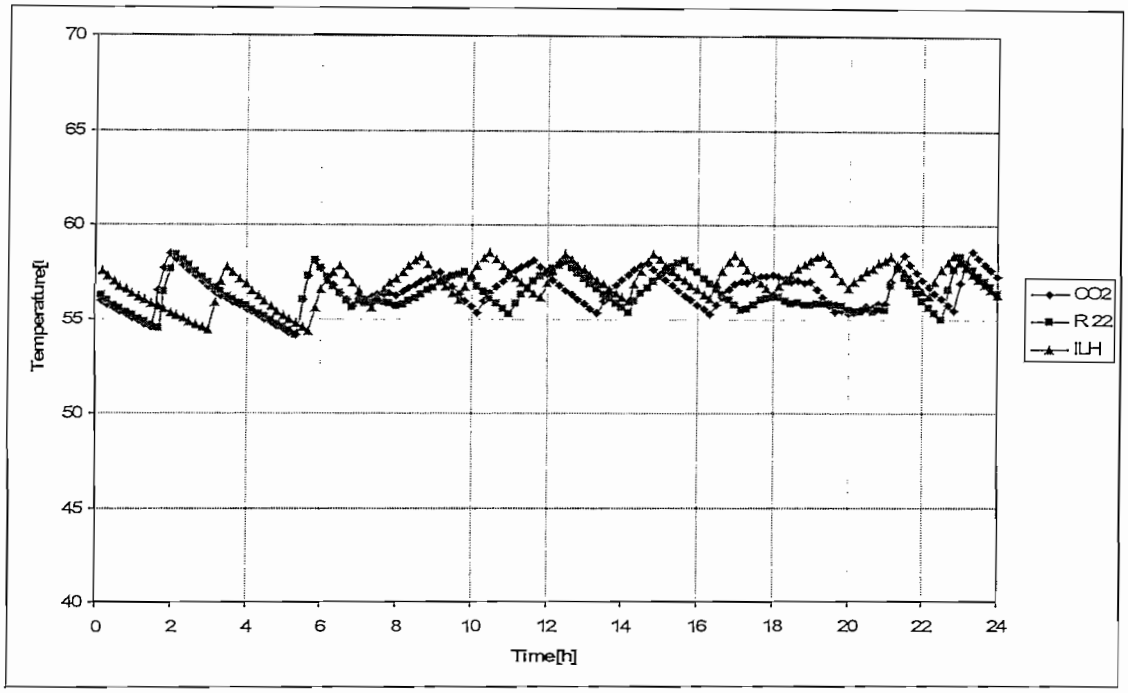


Figure 4.7: Bottom temperatures of vessel 2 of al three units (summer).

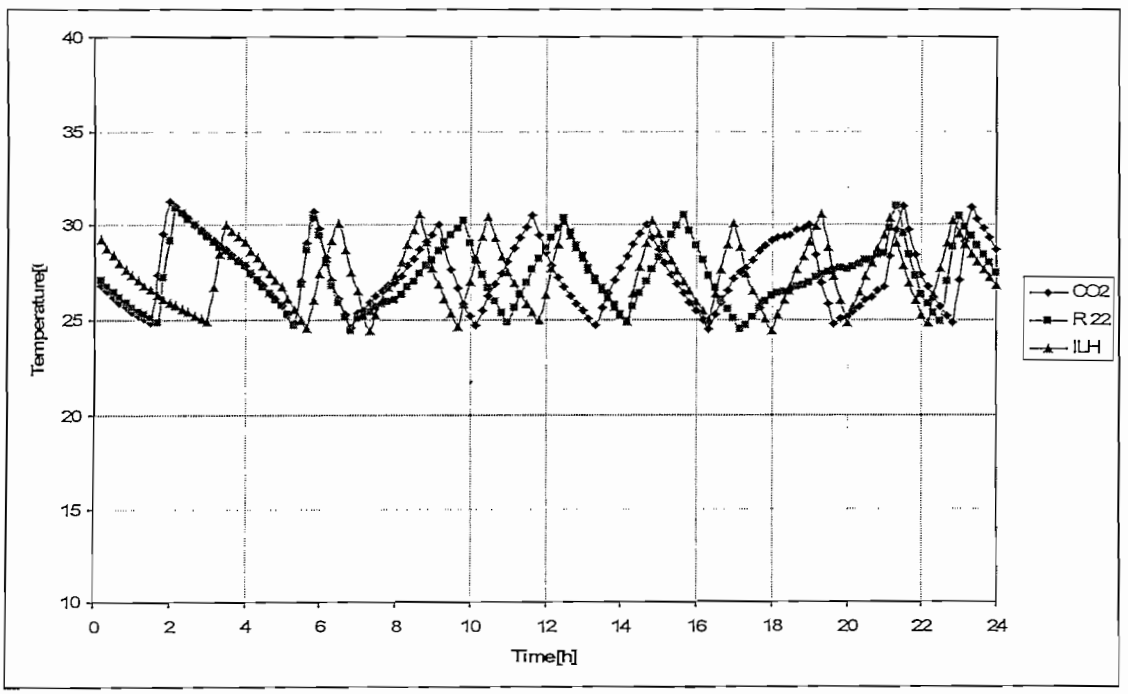

For winter, figure 4.8 shows the top temperatures inside storage vessel 1 for all three the systems, and Figure 4.9 shows the bottom temperatures inside storage vessel 2 for all three the systems.

From the bigger deviation in the temperature of the storage vessels it can be seen that the hot water demand for the winter period is higher than for the summer condition. The larger temperature drop in storage vessel 1 could be because the heat pump is most likely not operating at that period of the morning due to low ambient conditions and are therefore struggling to keep up with the demand for hot water. This could also be seen because the ILH does not have a significant temperature drop since it can operate at low ambient temperatures.

The difference in the water temperatures at the bottom and top thermostats are much bigger in storage vessel 1 for the winter period compared to the summer period. This could be because the demand for hot water is not as easily met as for the summer conditions and the tanks are losing temperature easier because of the colder ambient surroundings.

The in-line heater will most likely also be in operation more often than for the summer period due to the larger water consumption and heat losses in the winter. The ILH system will also have to be in operation more often because it can be seen that at certain periods the ILH system is also struggling to cope with the demand and therefore has a slight decrease in its temperature profile.

Figure 4.8: Top temperatures of vessel 1 of all three units (winter).

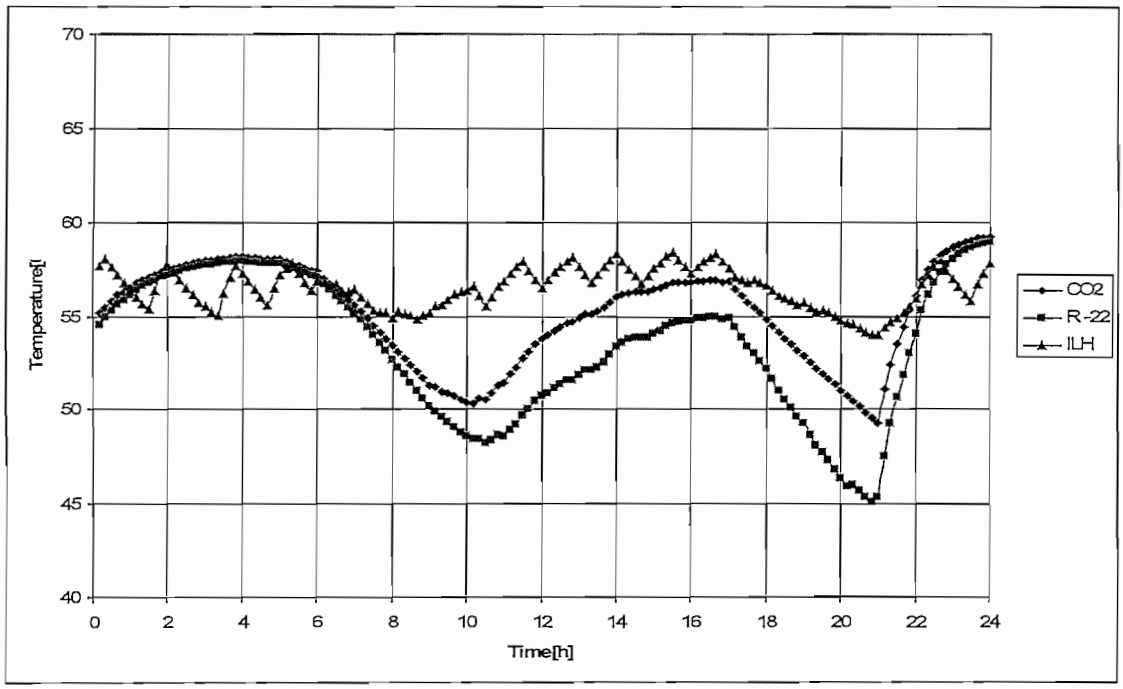


Figure 4.9: Bottom temperatures of vessel 2 of al three units (winter).

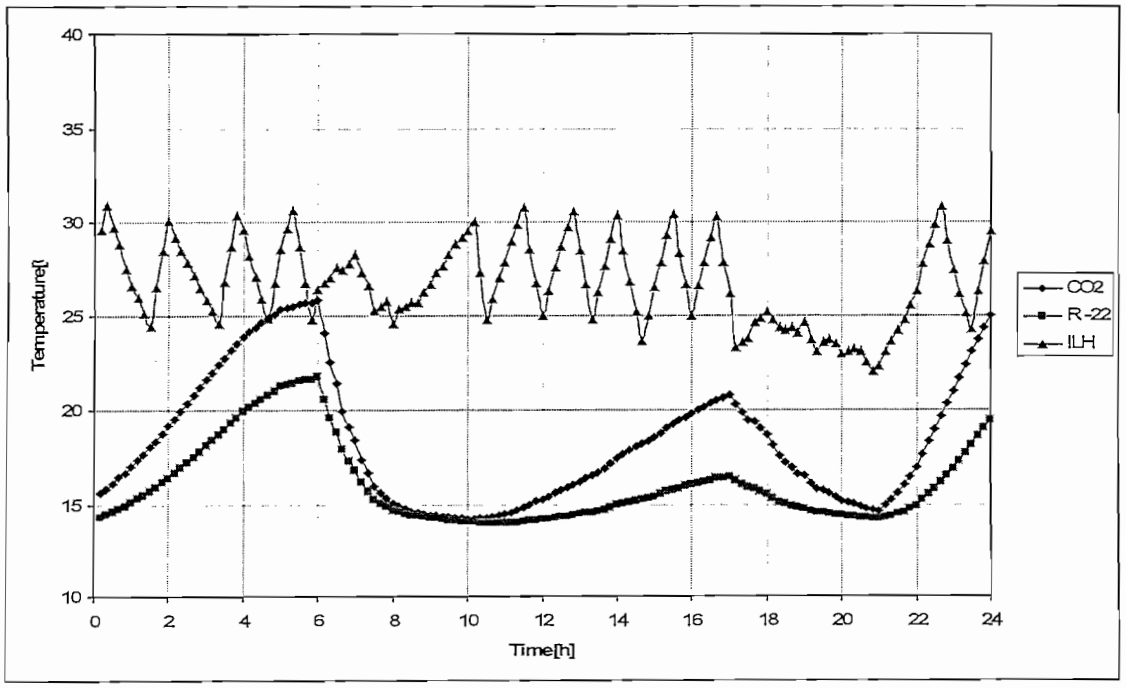

For both heat pump systems the top temperature of storage vessel 1 is kept at a reasonable temperature and the two systems are still able to provide hot water of approximately 50°C to the hotel. Only once does the R-22 system drop to a supply temperature of about 45°C. Therefore it is good to see that at cold ambient conditions the system seems to be keeping up with the hot water demand satisfactory, regardless the fact that the R-22 system drops to 45°C at one point. The ILH system manages to keep the top temperature more constant and is thus keeping up with demand to a higher degree than the two heat pump systems. This is because the ILH is able to be in operation the whole time even for the coldest conditions and it has a bigger heating capacity than the heat pump systems. Therefore if the heat pumps are unable to operate they only have a backup ILH of 48kW, whereas the ILH system has 72kW of heating capacity regardless of the ambient conditions.

The most interesting difference between the two heat pump systems is the variation in the storage vessel temperatures. It can be seen that the overall temperature for the $CO_2$ system is a bit higher than that of the R-22 system, with a maximum deviation of 8% in storage vessel 1. The top temperature of storage vessel 1 of the R-22 system drops well below 50°C for two times during the day. From the water temperature profile curves it can be depicted that the $CO_2$ system is keeping up with the demand easier than the R-22 system and it seems that the increase in water temperature of the $CO_2$ storage tanks is faster than it is for the R-22 storage vessels. The ILH system on average keeps the two storage tanks at its desirable temperature better than the heat pump systems do. This can be seen from figure 4.8 where the storage tank of the ILH system has a more constant water outlet temperature.

The $CO_2$ system will have a shorter operating time than the R-22 system because it seems the $CO_2$ system is reheating the storage vessels faster than the R-22 system. It is also known that the COP of the $CO_2$ system is highly dependable on the inlet water temperature and this could also mean that the performance of the system will still be good at winter conditions because of the colder inlet water temperature at the colder ambient conditions.

In a comparison between the heat pump systems and the ILH system it is seen that the $CO_2$ heat pump system is operating closer to the ILH system having only a 5°C temperature difference in the supply to the hotel than the ILH.

Table 4.2 gives the summarized results for both the heat pump systems and the ILH system for the one winter day and one summer day. The table includes the total daily water consumption that was used by the occupants. The average outlet temperature is the average temperature supplied by the two heat pump systems to the storage vessel 1 and will be the supply temperature to the building. It finally gives the average heat pump COP for a full day.

The daily water consumption by the recipients are more or less the same for all three the systems in the summer and winter condition. The increase of hot water demand in the winter condition can be clearly seen. This corresponds with the water temperature profiles shown for the winter analysis above. Therefore the heat pump systems will clearly be operating more frequently at the winter conditions.

**Table 4.2: Summer and winter summarized results for all three systems.**

| | Total daily water consumption | Ave outlet Temp | Ave COP |
|---|---|---|---|
| **Summer** | | | |
| $CO_2$ | 11173.7 l | 58.0 C | 3.09 |
| R-22 | 11130.3 l | 58.0 C | 2.77 |
| ILH | 11232.1 l | 57.8 C | 1 |
| **Winter** | | | |
| $CO_2$ | 18061.0 l | 59.1 C | 3.33 |
| R-22 | 18300.4 l | 58.8 C | 2.63 |
| ILH | 17714.5 l | 58.9 C | 1 |

The outlet temperatures for all three the systems are more or less the same for both the heat pump systems and ILH system at both the summer and winter conditions. This is expected since both the heat pump systems are manufactured with either a head pressure valve or a variable speed pump determining the water flow that ensures a constant discharge temperature from the heat pumps. The ILH has a water regulating valve ensuring a constant discharge temperature. It can be expected that for the winter conditions the water mass flow will be lower than for the summer conditions.

The average COP for the $CO_2$ heat pump system is 10.4% higher at the summer conditions than for the R-22 system and for the winter conditions the $CO_2$ heat pump system it is 21.1% higher than for the R-22 system. It can therefore be claimed that the $CO_2$ heat pump system is a more effective system than the R-22 heat pump system. This corresponds with the statement made about the water temperature profiles in figures 4.8 and 4.9 that the $CO_2$ heat pump system seems to be coping better with the demand for hot water than the R-22 system.

An interesting occurrence that can be observed from table 4.2 is that the average COP of the $CO_2$ system is higher at the winter condition than it is for the summer condition. This can be due to the fact that the inlet water temperature is lower in the winter condition than for the summer condition and because the $CO_2$ system could be less affected by the ambient conditions than the R-22 system. It is known that the inlet water temperature plays a big role when it comes to the performance of the $CO_2$ heat pump system.

The daily power consumption of the two heat pump systems during summer are shown in figure 4.10 and figure 4.11 respectively, with the daily power consumption of the ILH system shown in figure 4.12. The green line shows the power consumption of the heat pump and will be at a maximum of 18kW. The purple line shows the power consumption of the in-line heater and will either be at 24kW when operating in one step and will be at 48kW when fully operating. For the in line heater the purple line will be at 72kW when operating and will be equal to the total power consumption. The red line is the total power consumption of the heat pumps together with the in-line heater when in operation.

The R-22 heat pump is in operation longer at a time than the $CO_2$ system. The short running time of the ILH system shows that it is able to keep up with the hot water demand sufficiently for the summer condition. The difference between a heat pump system and an ILH system can be clearly seen from the power consumptions. Here it can be seen that the heat pump uses about 55% less power to heat the same amount of water as the ILH does.

Figure 4.10: Daily power consumption for the $CO_2$ heat pump system (summer).

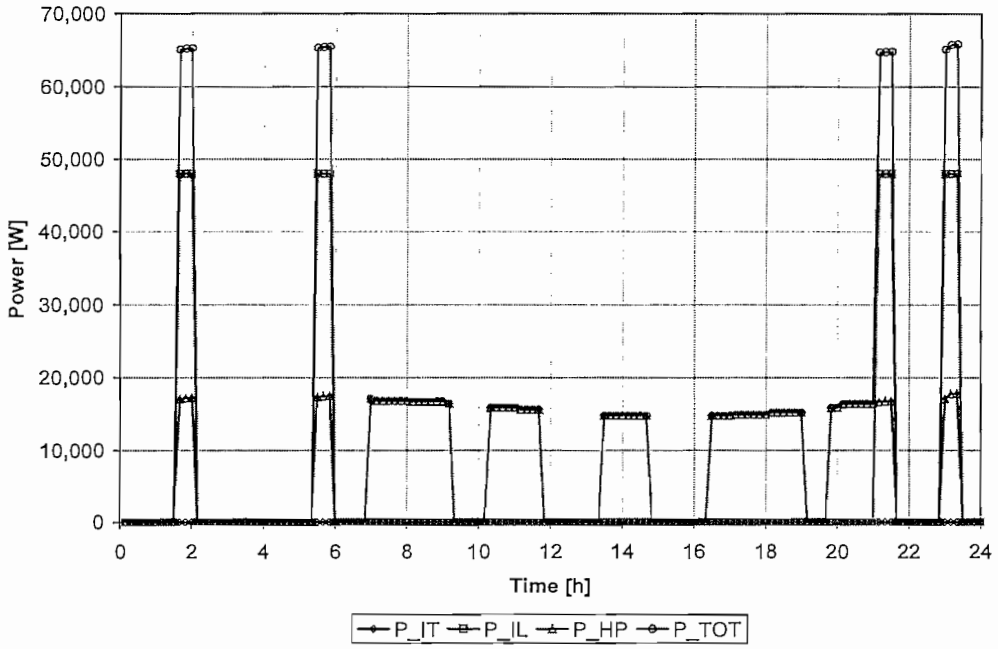


Figure 4.11: Daily power consumption for the R-22 heat pump system (summer).

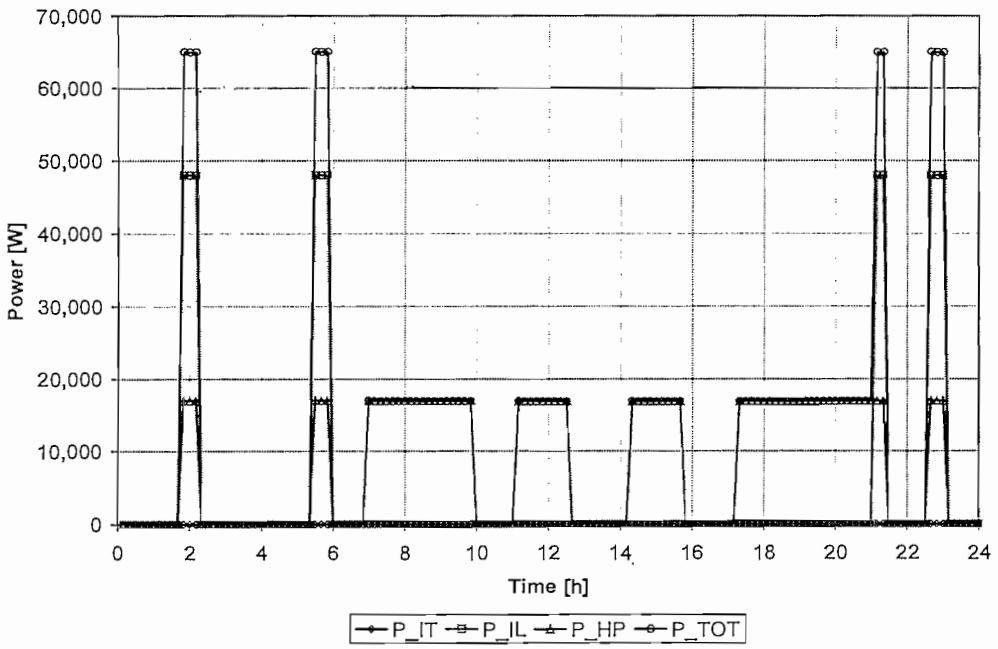

Figure 4.12: Daily power consumption for the ILH heat pump system (summer).

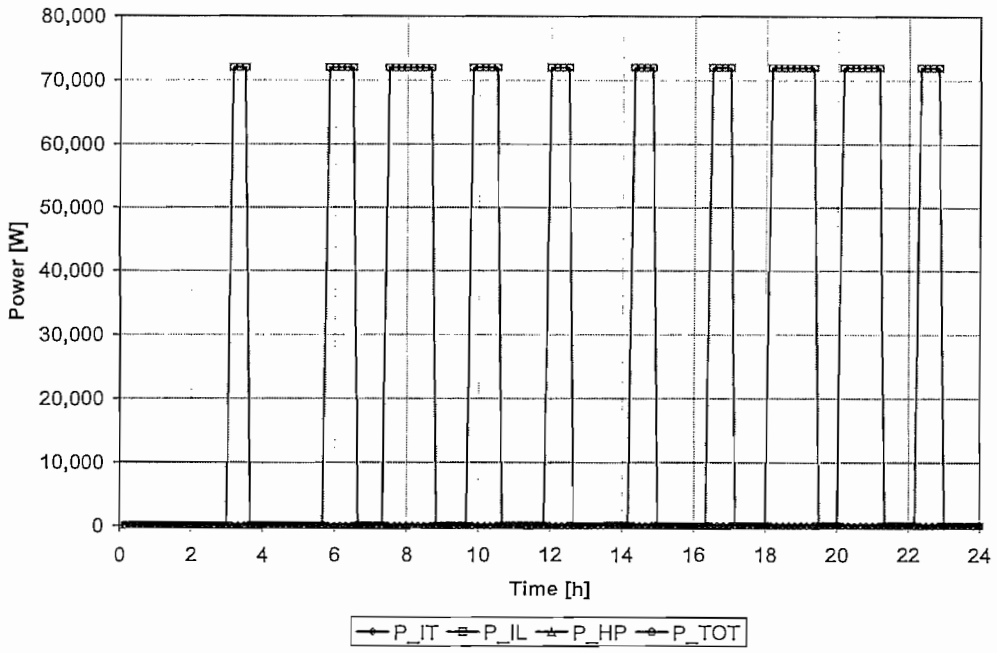


Table 4.3: Total run time for the three systems (summer).

| | Total run time ILH | Total run time HP | Total Power Consumption |
|---|---|---|---|
| $CO_2$ | 120 min | 660 min | 1647563 W |
| R-22 | 110 min | 700 min | 1715385 W |
| ILH | 520 min | 0 min | 3740000 W |

Table 4.3 gives the summer total running time of all three systems and the operating times of the backup in-line heater for the two heat pump systems. The run time for the R-22 heat pump is 40 minutes longer than for the $CO_2$ heat pump and the operating time for the in line heater in the R-22 system is 10 minutes longer than for the $CO_2$ system. Therefore it can be seen that the $CO_2$ system will be more efficient than the R-22 system because of its higher COP. The total running time of the ILH system is much less than for both the heat pump systems, showing that the ILH system is keeping up well with the hot water demand.

The total power consumption for the summer day period is shown in table 4.3. It shows that the R-22 system uses about 4% more power than the $CO_2$ system. The reason for

this is because of the longer operation period of the R-22 system compared to the $CO_2$ system. These results show that the $CO_2$ system is more efficient than the R-22 system under the same situation and conditions. Here the big difference in power consumption between the heat pump systems and ILH system is evident. The ILH system uses a lot more power although it is not in operation as much as the heat pump systems.

The winter daily power consumption of the two heat pump systems are shown in figure 4.13 and figure 4.14 respectively and the ILH system in figure 4.15. From the figures it can be seen that during winter, the two heat pump systems must operate longer because the ambient temperatures are much lower than for the summer condition and the water consumption is higher. The ILH system is in operation more often for the winter conditions and it could also be seen that it has to operate longer from 06:00 to 10:00 in the morning and then again from approximately 17:00 to 23:00 in the evening. This is because of the higher consumption rate at those specific times of day. Although the ILH systems is operational for a substantial part of the day, it is not required to be in operation for the whole day showing that it is still able to keep up with the hot water demand under the winter conditions.

The power savings gained by using a heat pump can be seen from the power consumption profiles of the heat pump systems and the ILH system. From these figures it is clear that there is a big advantage in using a heat pump rather than an ILH system when it comes to peak demand power usage.

Both heat pump systems only come into operation after 08:00 in the morning because the ambient temperature is typically below 5°C. At temperatures lower than 5°C the heat pumps will not come into operation because there is no heat to extract from the surrounding air and the evaporator could begin to freeze if it has any condensate on it. During these times the in-line heater will operate and this can be seen from the figures. The ILH system is not controlled by the ambient conditions and can therefore be operational through the entire day as seen in figure 4.15. The in-line heater consists of two stages of equal capacity so that the heater is only in operation at half of its capacity at certain periods. This is done to limit kVA contribution during peak periods.
From both of the heat pump system figures it can be seen that the in-line heater turns off when the heat pumps come into operation and the in-line heater switches to half

capacity during the peak hours. A system is more efficient if it is not necessary for the in-line heater to operate concurrently with the heat pump.

Figure 4.13: Daily power consumption for the $CO_2$ heat pump system (winter).

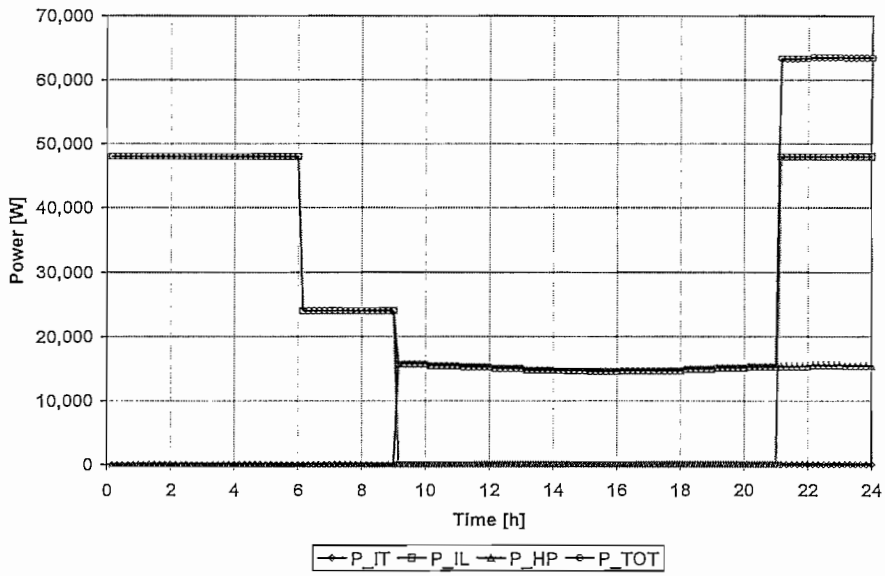


Figure 4.14: Daily power consumption for the R-22 heat pump system (winter).

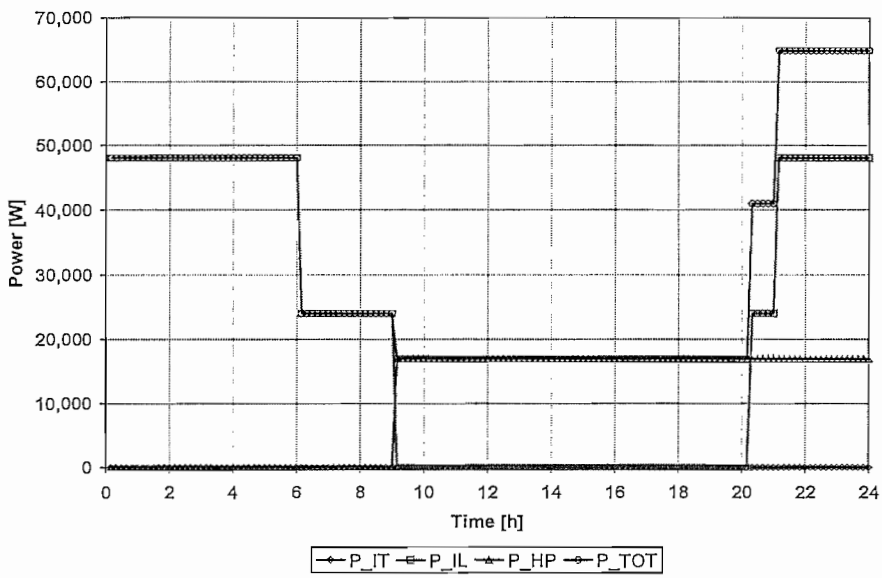

Figure 4.15: Daily power consumption for the ILH heat pump system (winter).

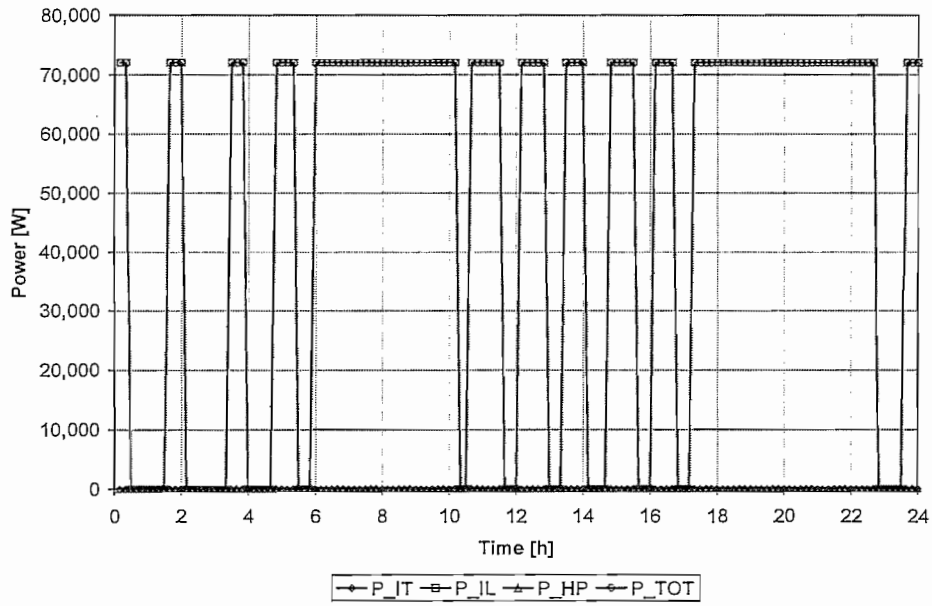


When the heat pumps are in operation it could be seen that they are in operation for the remaining time that the ambient conditions allow. This shows that the low surrounding ambient temperatures and the bigger demand for hot water ensures that the heat pump is required to operate at all times. From about 21:00 in the evening both the heat pump and in-line heater is operational, this however is during the off-peak hours and does not contribute excessively to the electricity bill.

Table 4.4: Total runtime for the in-line heater and heat pump for all three systems (winter).

| | Total run time ILH | Total run time HP | Total Power Consumption |
|---|---|---|---|
| $CO_2$ | 730 min | 900 min | 4384864 W |
| R-22 | 770 min | 900 min | 4668307 W |
| ILH | 980 min | 0 min | 7056000 W |

Table 4.4 gives the total running time of all three systems and the operating time of the in-line heater for the two heat pump systems in winter. The operating time for the in-line heater within the R-22 system is 40 minutes longer than for the $CO_2$ system. This is not too much but still shows that the $CO_2$ system is coping better with the demand for hot water and with the lower ambient conditions than the R-22 system. This is because of the lower inlet water temperature to the $CO_2$ heat pump which results in a better COP for

the $CO_2$ system. The ILH system is in operation a lot more than was necessary for the summer condition although it is still a lot less operational than the heat pump systems including their backup in line heaters.

The total running time for all three the systems are to a certain extent higher during the winter condition than during the summer condition. This is expected due to the lower ambient temperatures and the increase in demand for hot water at the winter conditions. This shows that both the heat pump systems will be more efficient and cost effective in the summer period because of the higher energy available in the surrounding ambient conditions.

The total power consumption is also higher for the R-22 system than for the $CO_2$ system, as it was under the summer conditions. This is again the result of the $CO_2$ system having a higher COP than the R-22 system and a lower total operation time. The total power consumption for the winter condition is much higher than for the summer condition because the in-line heater is in operation more often under the winter conditions and uses a lot more power than the heat pumps use when operating on their own. The ILH system's power consumption is still a lot more than that of the heat pump systems but it can be seen that the difference between the heat pump systems and ILH system are less for the winter conditions than it was for the summer condition. The reason being that in the winter the heat pump systems in-line heaters are more operational and consumes a lot more power than the heat pumps.

## 4.3 Year Analysis

In this section the same heat pump systems and ILH system are compared to each other over a period of a year. All three the systems are simulated with the same demand in hot water, occupancy and conditions as stipulated in section 4.1. The WHSIM Statistical program contains the weather data for the area in which the heat pumps are placed for a period of a year and can therefore give an accurate analysis of the systems over this period.

Figure 4.16 shows the seasonal daily water consumption for the three systems. There is a considerable increase in hot water consumption for the colder months than for the warmer months reaching its peak at round about the middle of winter. Therefore, when designing a hot water system it should be designed to have a sufficient heating capacity for the winter months, because this is when the system will be operating under its most strenuous conditions. There should be a sufficient amount of storage capacity to meet the hot water demand.

**Figure 4.16: Summary of yearly water consumption for all three the systems.**

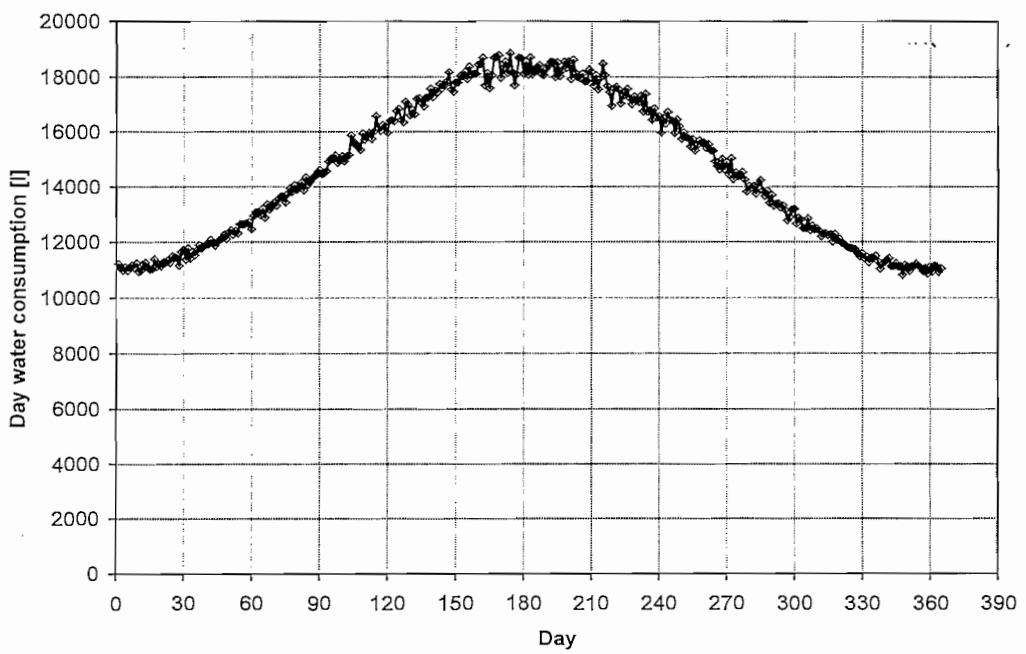

From figure 4.17, figure 4.18 and figure 4.19 the daily minimum water supply temperature to the building for the three systems can be seen. In the winter months there is a slight drop in the supply temperature due to the fact that the demand for hot water is higher than the heating capacity of the heat pump system combined with the storage capacity. The supply temperature is still sufficient for use by the occupants.

The R-22 heat pump system has a larger drop in the water supply temperature than the $CO_2$ system during the winter period. The $CO_2$ heat pump system average supply temperature is above 50°C, where the R-22 system average temperature drops below 50°C a few times. This is due to the fact that the R-22 system has a lower COP, especially during the winter period, and is therefore less efficient than the $CO_2$ system. From figure 4.19 it could be seen that the ILH does not have any problems in keeping up with the hot water demand, this is because it has a higher heating capacity than the heat pump systems.

**Figure 4.17: Summary of yearly minimum water supply temperature for the $CO_2$ system.**

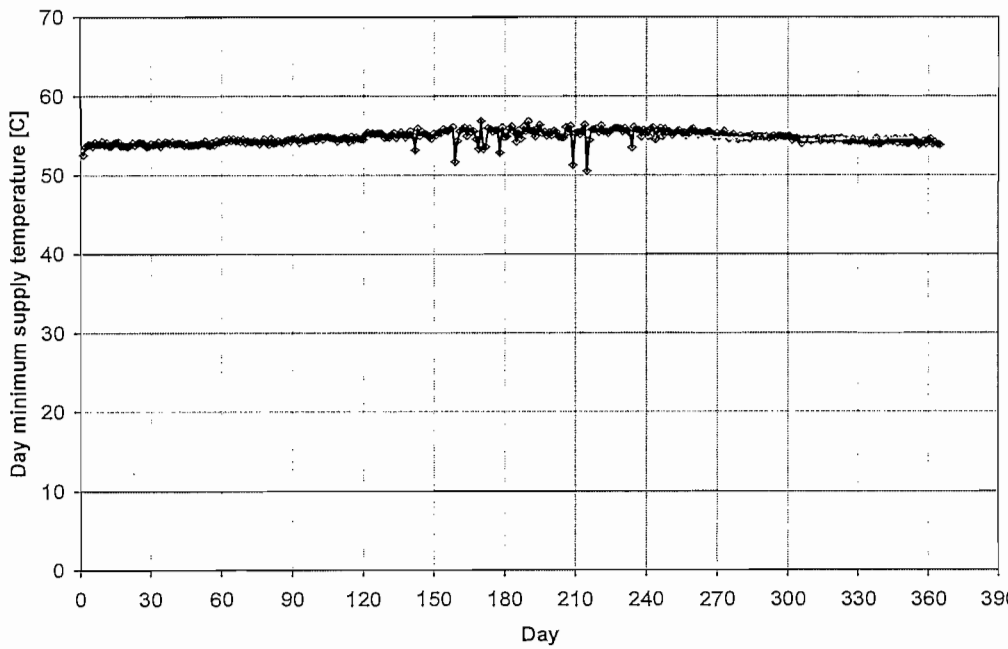

Figure 4.18: Summary of yearly minimum water supply temperature for the R-22 system.

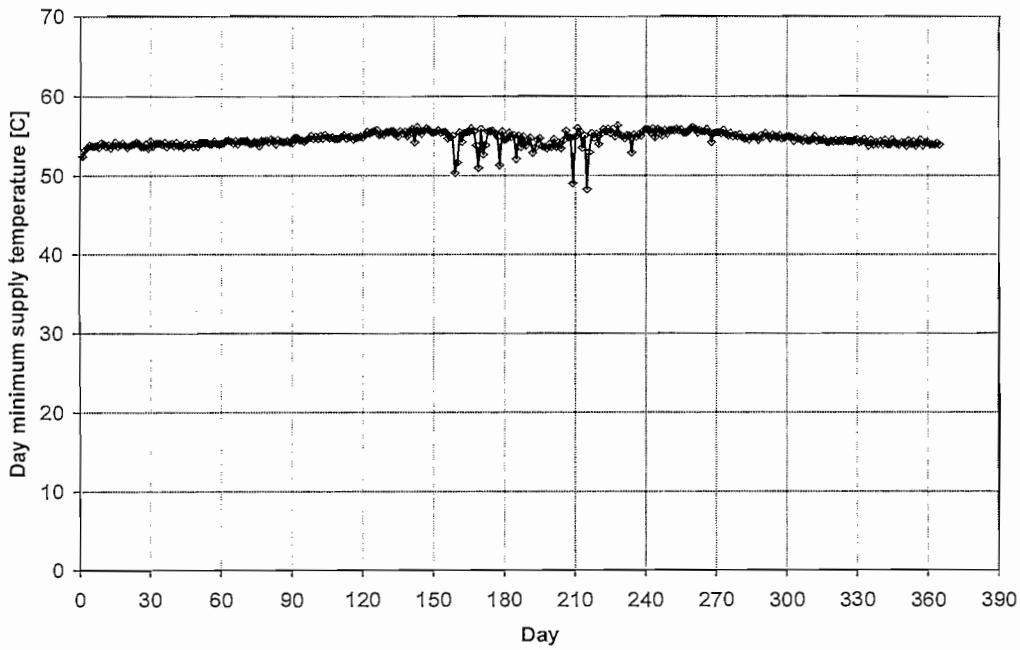


Figure 4.19: Summary of yearly minimum water supply temperature for the ILH system.

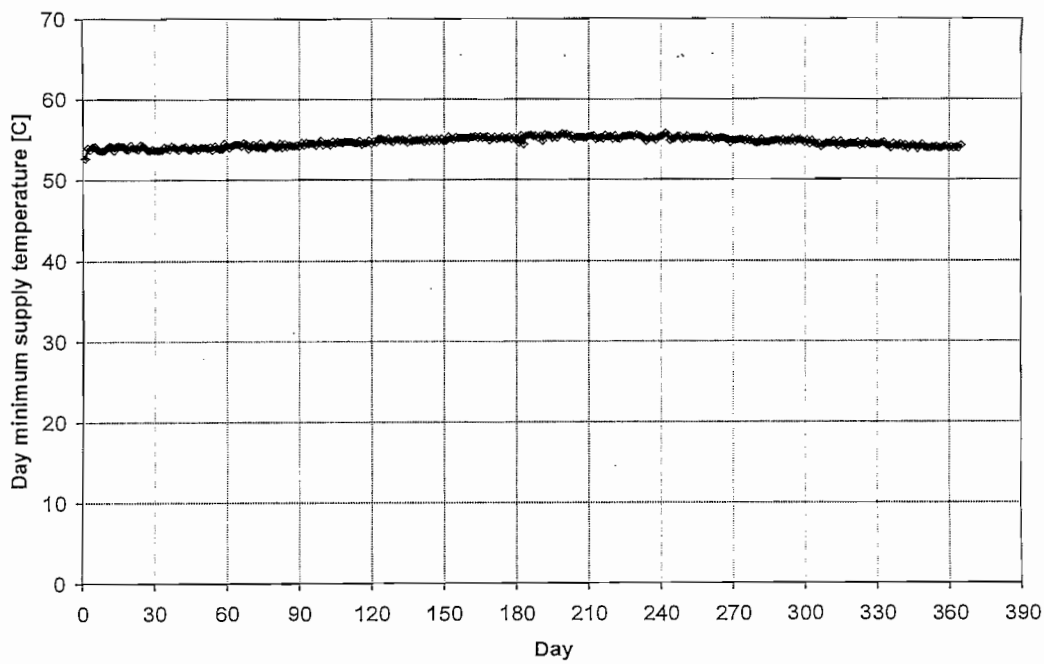

The daily energy consumption over a period of one year is shown for all three the systems in figure 4.20, figure 4.21 and figure 4.22. There is a linear increase in the power consumption as the year draws closer to the winter months. There is a direct influence of the water consumption on the power consumption which can be seen from the water consumption and energy consumption profiles. The deviation in the energy consumption profile for the heat pump systems during the winter months is because the in-line heater will be in operation more often, due to lower ambient conditions affecting the heat pump COP. It can be seen that the power consumption is much higher for the ILH system than it is for the heat pump systems, reaching a maximum of 1200kWh per day compared to the less than 800kWh per day for the heat pump systems.

The power consumption for the R-22 heat pump system is higher, reaching a maximum of almost 800kWh as opposed to the energy usage of the $CO_2$ system which is just above 700kWh in the winter months due to the difference in COP. The power consumption during the summer months is more or less the same for both the heat pump systems since the in-line heater is not in operation as much as during the winter months.

**Figure 4.20: Summary of yearly energy consumption for the $CO_2$ the system.**

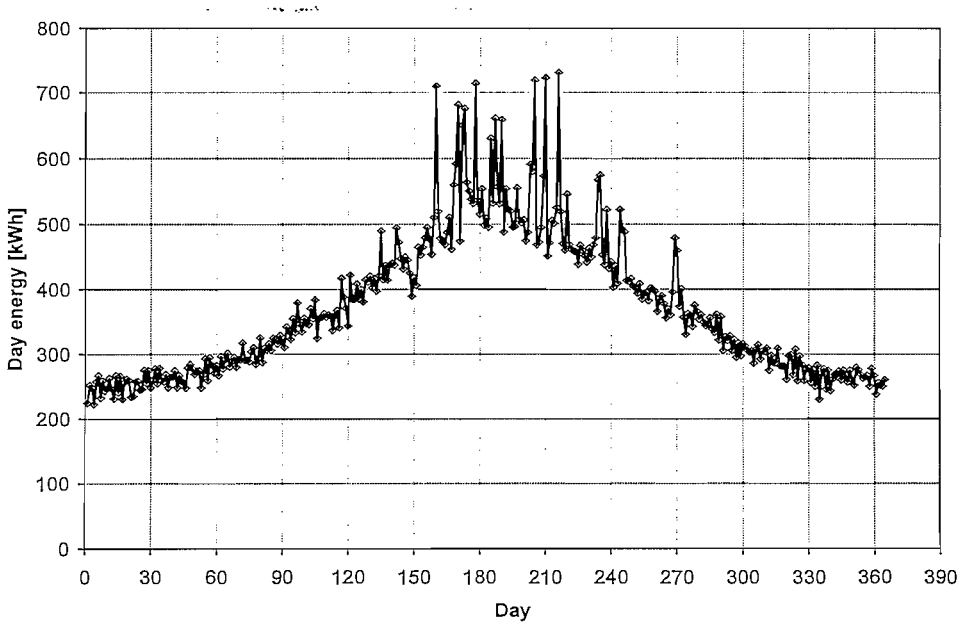

Figure 4.21: Summary of yearly energy consumption for the R-22 the system.

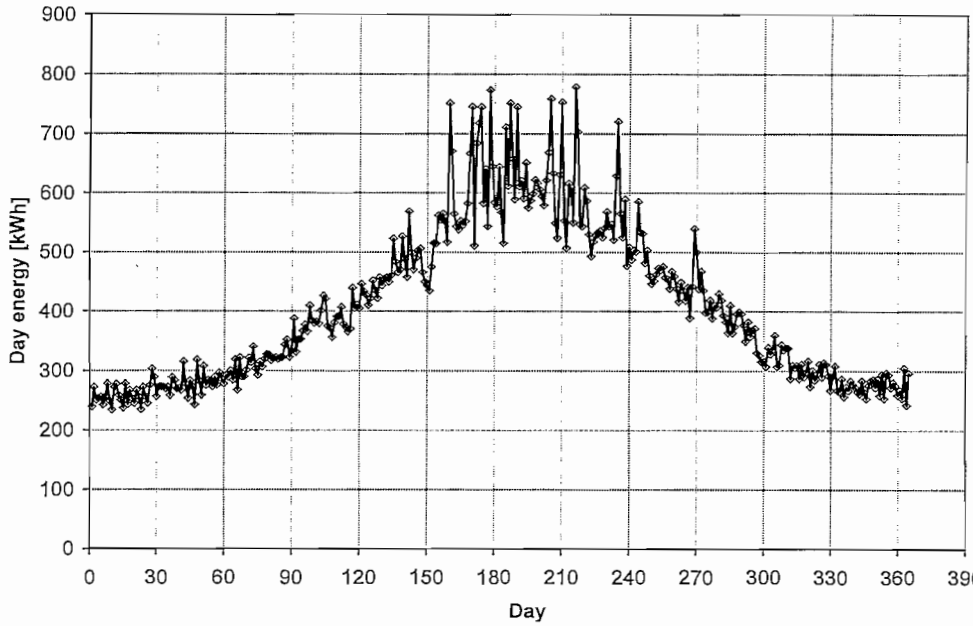


Figure 4.22: Summary of yearly energy consumption for the ILH the system.

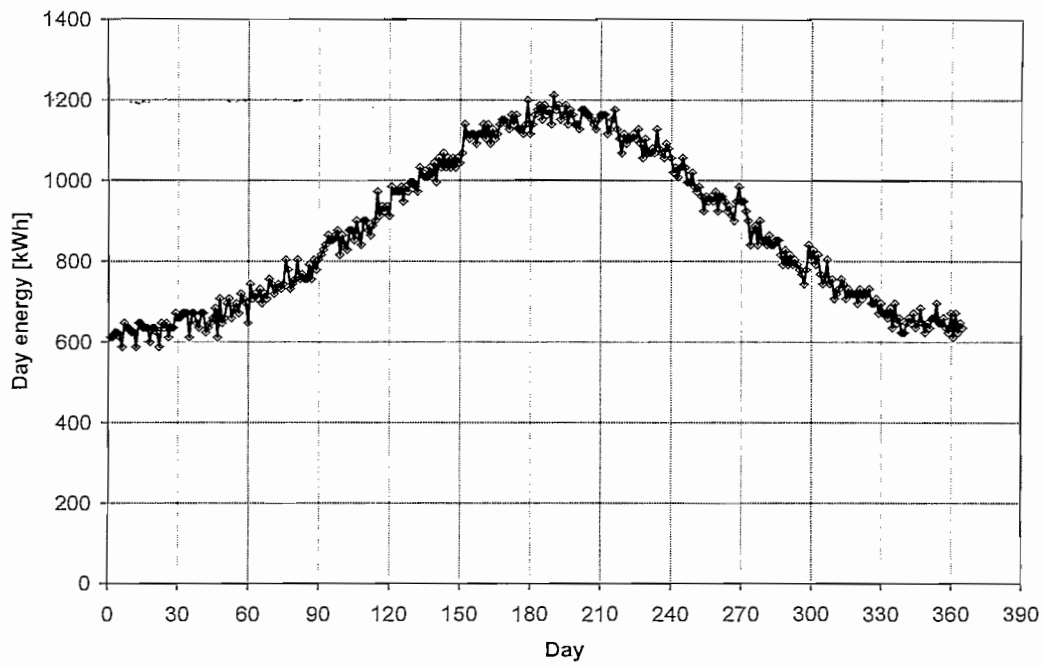

Table 4.5 shows the summary of the annual water consumption and the annual energy consumption on a monthly basis for all three the systems. The increase in energy consumption between January and July for the R-22 system is 58.1%, for the $CO_2$ system it is 53.6% and for the ILH system it is 45.8%. The greater increase in energy consumption for the heat pump systems is because the in-line heaters will be in operation more often in the winter than it will be in the summer.

There is a 4.5% saving in the energy consumption of the $CO_2$ heat pump compared to the R-22 heat pump for the above-mentioned months. This shows that the increase in energy demand from the summer to the winter is 4.5% less for the $CO_2$ heat pump system.

**Table 4.5: Monthly summary of water and energy consumption.**

| System | R-22 | | $CO_2$ | | ILH | |
|---|---|---|---|---|---|---|
| Month | Consump | Energy | Consump | Energy | Consump | Energy |
| - | [l] | [kWh] | [l] | [kWh] | [l] | [kWh] |
| Jan | 347000 | 8051.1 | 348000 | 7755.6 | 349000 | 19524 |
| Feb | 339000 | 7814.2 | 339000 | 7491.9 | 341000 | 18720 |
| Mar | 423000 | 9686.4 | 424000 | 9276.8 | 426000 | 23148 |
| Apr | 463000 | 11541 | 464000 | 10611 | 467000 | 26268 |
| May | 533000 | 14410 | 532000 | 13090 | 532000 | 31416 |
| Jun | 552000 | 17972 | 548000 | 16035 | 542000 | 33888 |
| Jul | 570000 | 19243 | 565000 | 16722 | 559000 | 36060 |
| Aug | 536000 | 17421 | 532000 | 14896 | 528000 | 33792 |
| Sep | 466000 | 13947 | 464000 | 12174 | 465000 | 28860 |
| Oct | 421000 | 11553 | 421000 | 10310 | 423000 | 25488 |
| Nov | 360000 | 9118.5 | 361000 | 8556.6 | 362000 | 21528 |
| Dec | 345000 | 8502.6 | 345000 | 8118.9 | 347000 | 20136 |

The total water consumption and energy consumption for the year is given in table 4.6 for all three the systems. The most important difference to note is the total annual energy consumption of the two heat pump systems. The R-22 system uses 9.4% more energy in total for the year than the $CO_2$ system. This shows the difference in energy demand for a system with a higher COP compared to a system with a lower COP.

The savings that can be realised by using a heat pump system instead of an ILH system is clearly indicated here. There is a 57.8% increase in the total energy usage over the period of one year for the ILH system when compared to the $CO_2$ heat pump system.

**Table 4.6: Yearly summary for water and energy consumption.**

| **R-22 heat pump system** | | | |
|---|---|---|---|
| Year_total_consumption | = | 5350000 | [l] |
| Year_total_energy | = | 149000 | [kWh] |
| **$CO_2$ heat pump system** | | | |
| Year_total_consumption | = | 5340000 | [l] |
| Year_total_energy | = | 135000 | [kWh] |
| **ILH heat pump system** | | | |
| Year_total_consumption | = | 5340000 | [l] |
| Year_total_energy | = | 319000 | [kWh] |

From the results found in chapter 4 it is clear that the $CO_2$ system has a better COP than the R-22 system and will thus be a more energy efficient system than the R-22 system.

# CHAPTER 5

# ECONOMICAL COMPARISON BETWEEN ILH, R-22 AND $CO_2$ SYSTEM

# *CHAPTER 5*

## *5. ECONOMICAL COMPARISON BETWEEN ILH, R-22 AND $CO_2$ SYSTEM*

This chapter focuses on the economical evaluation of the three systems described in the previous chapter. The two main areas that will be discussed are the operational cost and the capital cost. In this chapter a clear view will be given to see which system is the most cost effective and will generate the best savings over a period of time.

This chapter will be divided into the following sections:

- Operational Cost.
- System Cost.

## 5.1 Operational Cost

The tariff and rates used was taken from the latest figures available from Eskom. Eskom is South Africa's distributor and supplier of power from rural to industrial applications. The tariff structure used is Megaflex which is generally used in the commercial and industrial sectors. This is listed in more detail in Appendix C. Electricity charges are based on a c/kWh method. There are certain rates depending on what time of year and what time of day the energy is being used. Table 5.1 gives a summary for the rates used to calculate the operational cost of the three systems.

**Table 5.1: Megaflex electricity tariffs.**

| | Peak [c/kWh] | Standard [c/kWh] | Off-Peak [c/kWh] | Network demand [R/kVA/month] |
|---|---|---|---|---|
| Summer | 29.99 | 18.41 | 12.91 | 9.00 |
| Winter | 107.25 | 27.94 | 14.96 | 9.00 |

The winter months are taken as June to August and the summer months September to May. The peak demands are based on when energy consumption is at its greatest in South Africa and therefore the tariffs charged for energy consumption during these periods of the day are more expensive. Figure 5.1 shows the time table for the peak, off-peak and standard tariff rates.

**Figure 5.1: Peak, off-peak and standard time periods, Eskom (2009/10).**

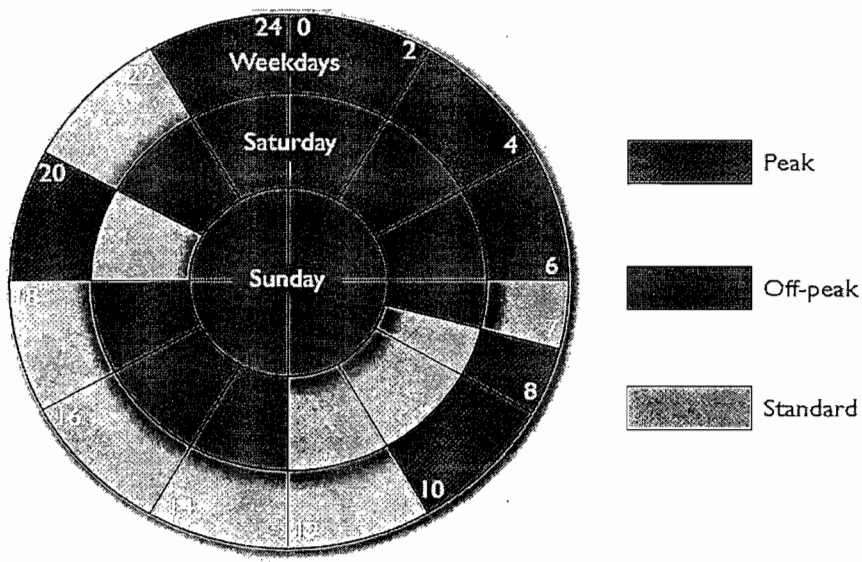

Figure 5.2 shows the monthly energy consumption of all three systems and it is used to explain the difference in operating cost between the three systems. The ILH system uses on average 57.5% more energy per month to deliver the same heating capacity as the $CO_2$ heat pump system and will definitely be the more expensive system when it comes to its operating cost. The R-22 system uses 9.5% more energy per month on average as the $CO_2$ system. The other reason for the R-22 heat pump system having higher energy consumption is because of its lower COP resulting in more power required for the same thermal heating. It is clear that all three the systems use more energy in the winter time when it is colder than in the summer time mainly due to the higher water consumption.

Figure 5.2: Monthly energy use.

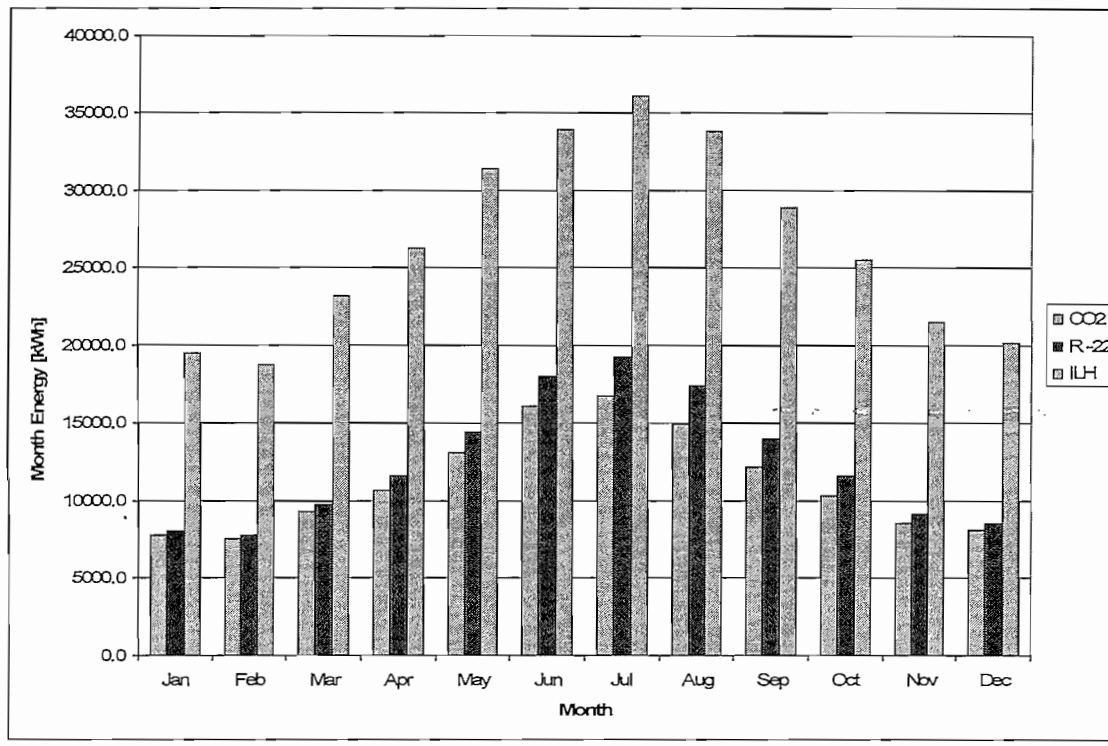


The total monthly energy cost for all three systems are shown in figure 5.3. The operating cost of the ILH system is 65% more for the whole year than for the $CO_2$ heat pump system. The operating cost of the R-22 heat pump system is also 12% more than that of the $CO_2$ heat pump system as a result of the energy consumption shown in figure 5.2.

The in-line heaters are in operation more during the winter time and thus increase the operating cost of the heat pump systems and the ILH system in the winter time.

Figure 5.3: Monthly energy cost.

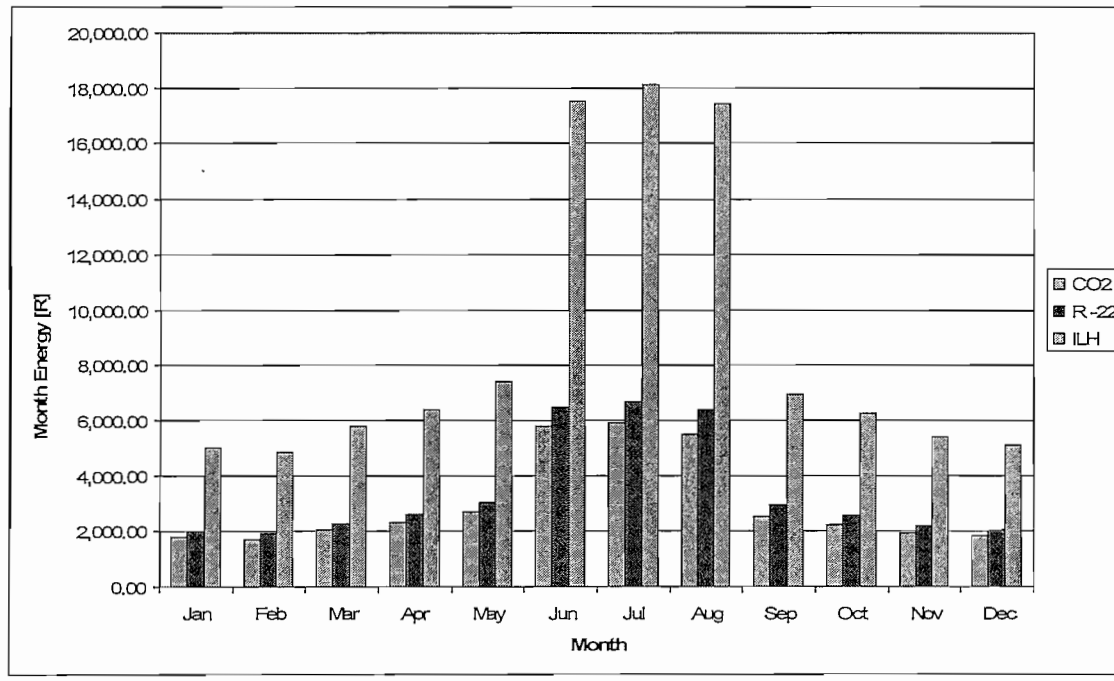


Table 5.2: Monthly energy cost summary.

| | R 22 | $CO_2$ | ILH |
|---|---|---|---|
| Month | Cost | Cost | Cost |
| - | [R] | [R] | [R] |
| Jan | 2,001.70 | 1,782.00 | 5,005.60 |
| Feb | 1,939.50 | 1,727.60 | 4,819.00 |
| Mar | 2,267.70 | 2,071.40 | 5,770.00 |
| Apr | 2,593.50 | 2,293.60 | 6,384.50 |
| May | 3,047.90 | 2,681.30 | 7,423.00 |
| Jun | 6,450.90 | 5,796.50 | 17,530.00 |
| Jul | 6,691.10 | 5,919.10 | 18,137.00 |
| Aug | 6,365.20 | 5,479.70 | 17,439.00 |
| Sep | 2,958.50 | 2,518.30 | 6,917.20 |
| Oct | 2,581.90 | 2,211.10 | 6,237.00 |
| Nov | 2,172.10 | 1,917.10 | 5,390.00 |
| Dec | 2,065.10 | 1,834.00 | 5,097.30 |
| **Total** | **41,135.10** | **36,231.70** | **106,149.60** |

Table 5.2 shows the summary of the monthly energy cost for all three systems. The annual operating cost for the R-22 system is R4, 903.40 more than that of the $CO_2$ heat pump system. The ILH system has an operating cost of R69, 917.90 more than the $CO_2$ heat pump system. Figure 5.4 shows the percentage difference between the operating costs of the three systems.

**Figure 5.4: Cost difference between the three systems (%).**

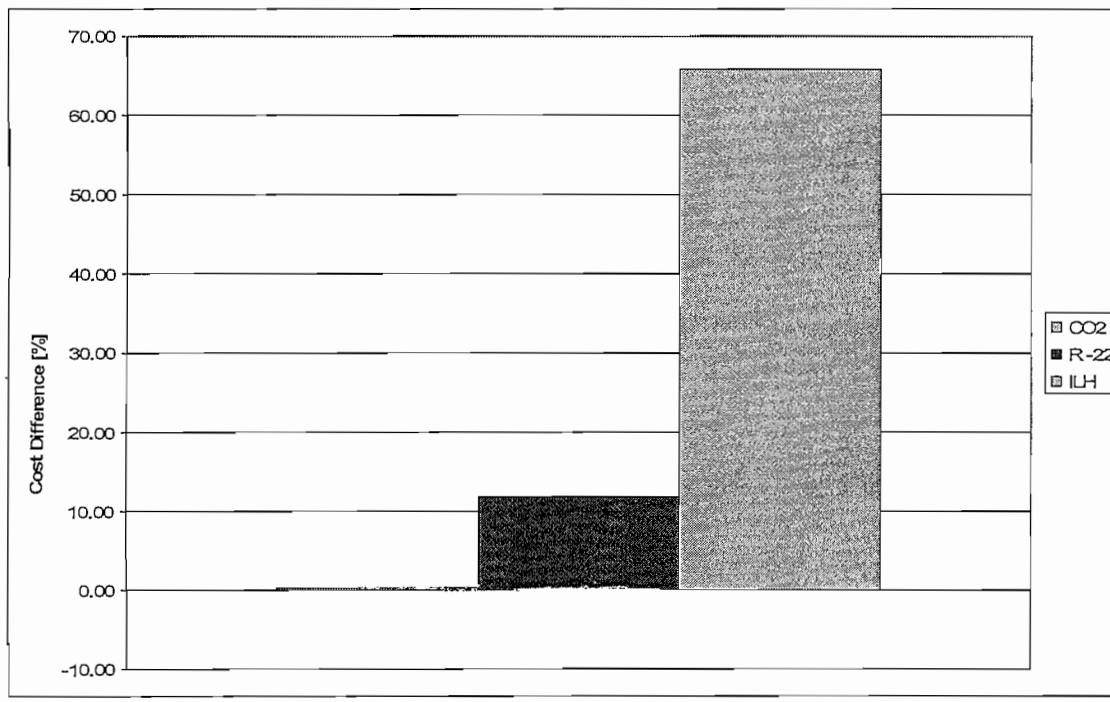


The R-22 system is 11.92% more expensive over a period of one year and the ILH system 65.87% more expensive than the $CO_2$ system. The ILH cannot compete with a heat pump system when it comes to its operating cost seeing that it is more than 50% more expensive than a heat pump system. The 11.92% difference in operating cost between the two heat pump systems are quite substantial and it shows that on operation the $CO_2$ heat pump system will be a lot more cost effective than the R-22 system.

The operating cost pertaining to the three systems are very important since South Africa is in a power crisis where businesses are forced to save power and at the time of publishing the results of this study, the price of electricity is scheduled to go up drastically again in the near future. As the cost of electricity increases the difference in

the operating costs will become more substantial between the two heat pump systems. Therefore the $CO_2$ heat pump system has a substantial advantage because of its lower operating cost and lower energy usage.

Figure 5.5: Operating cost over a period of ten years.

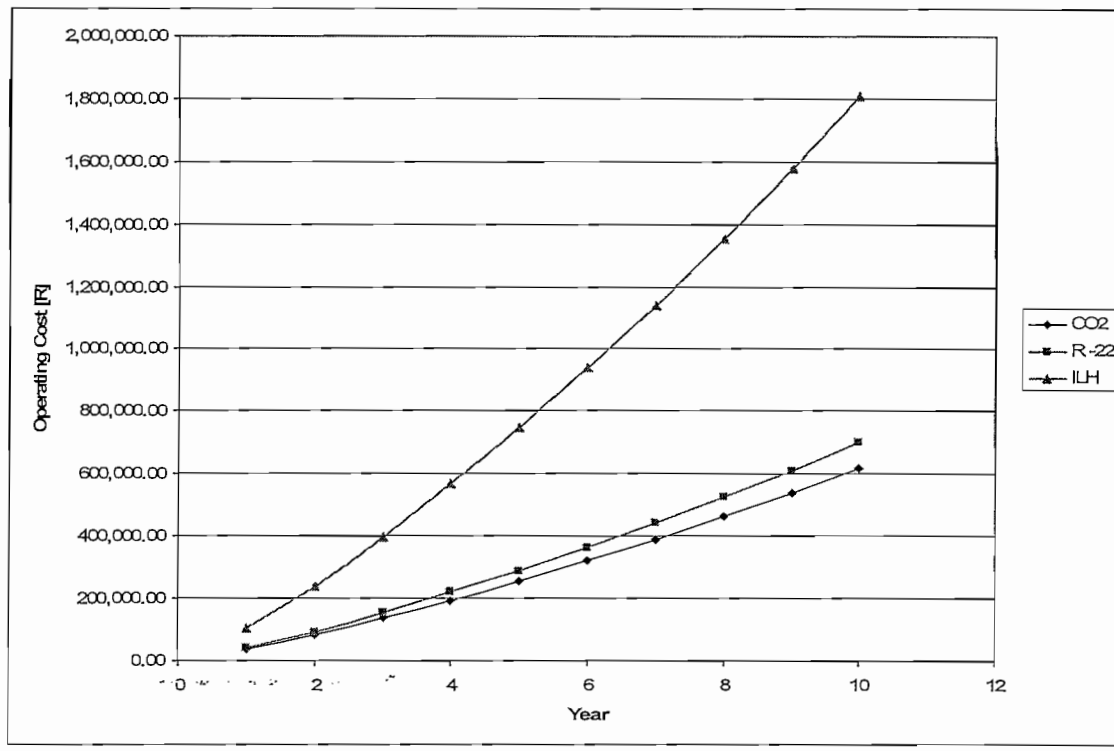


The energy cost tariff is taken as was found from the tariff rates, an increase in the tariff rates is taken to be 25% for the first two years and then 10% thereafter. This is from a prediction made for the increase in tariff rates for South Africa over the following years. Figure 5.5 shows the total operating cost for the first year and the accumulated operating cost for the years to follow including the increase in tariff rates for a period of ten years. Therefore with the increase in tariff rates taken into account the operating cost alone for the $CO_2$ heat pump system will be R3, 030,781.71 for ten years. The operating cost for the R-22 heat pump system and ILH system will be R3, 440,951.12 and R8, 879,414.04 respectively.

## 5.2 System Cost

The capital cost of the three systems plays a significant role when a consumer has to choose a system. For the capital cost calculation the following were taken into account:

- Component costs.
- Manufacturing labour.
- Mark-up.

This was done so that the costing is realistic in terms of what the consumer would have to pay when he orders anyone of the systems. The R-22 heat pump cost was obtained from a local manufacturer, so has the in-line heater cost.

The $CO_2$ system cost was projected according to the same principle applied to the costing of the R-22 system. The price for the compressor was received from the manufacturers of DORIN compressors, while the cost for the control equipment was received from Danfoss (2002). The cost of the gas cooler was determined by KAORI which specified a brazed plate heat exchanger to give the acquired heating capacity.

The costs of the three systems are given in table 5.3.

Table 5.3: Capital cost of all three systems.

| $CO_2$ system | R-22 system | ILH system |
|---|---|---|
| R 240,444.00 | R 212,302.00 | R 72,706.00 |

There is a big difference between the cost of the two heat pump systems and the ILH system. This is because a heat pump is a more expensive and detail-manufactured machine compared to the in-line heater. The cost difference between the R-22 and $CO_2$ system is 11.7% which is a relatively small difference, therefore not crucial. The main reasons for the cost difference between the two heat pump systems are because the $CO_2$ system is a new concept and its components are not mass-produced at this stage (compared to R-22 components).

Therefore the $CO_2$ compressor is potentially a lot more expensive than the R-22 compressor. The systems control components like the expansion valve is more expensive because of the higher pressures at which the $CO_2$ is operating. Because of the higher pressure the pipes would also be more expensive because they should be able to withstand higher pressures than what is necessary for the R-22 system, but the cost difference is not that big because the $CO_2$ is able to operate with smaller diameter pipes than the R-22 system which lowers the cost again.

Figure 5.6: Present value vs. Life expectancy.

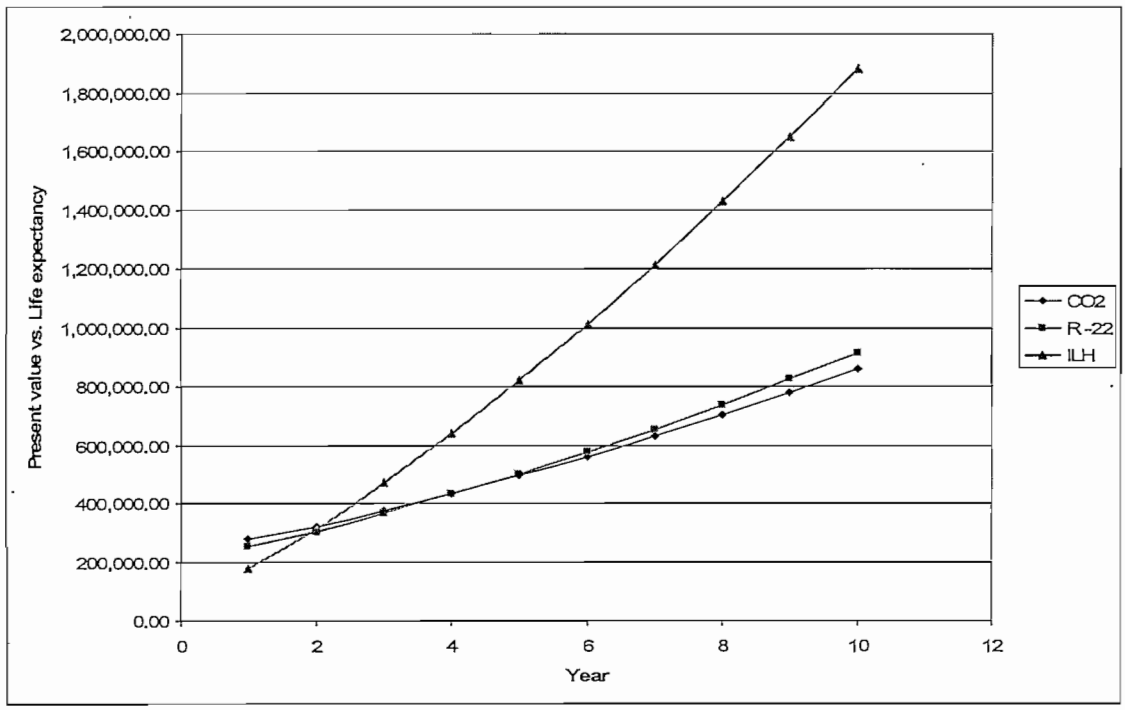


Figure 5.6 shows the present value cost of the systems over a period of ten years and depicts the life expectancy of the three systems. Each system's capital cost was implemented in year one including the operating cost of the first year and thereafter the accumulated operating cost is shown with the increase in tariff rates as previously mentioned. When comparing Figure 5.6 with Figure 5.5 the effect of capital cost on a system's life cycle cost can be seen. The ILH system has a low capital cost and therefore will be the less expensive choice to install when considering the first year of the system's life. However, it can be seen that just before two years the ILH system will

already be costing its owner more than the two heat pump systems would because of its high operating cost.

For the two heat pumps it is clear that the higher capital cost of the $CO_2$ machine makes it a more expensive option when considering the two systems. The $CO_2$ heat pump system will cost the consumer more initially than it would cost to install the R-22 system. However, it can be seen that after a period of four years the $CO_2$ system will be the less expensive option because of its lower operating cost.

# *CHAPTER 6*

# *CLOSURE*

# CHAPTER 6

# 6. CLOSURE

## 6.1 Conclusions

This study aimed to start the research and development of $CO_2$ as a refrigerant in a heat pump system at the North-West University. A thorough discussion of the refrigerant properties was done to acquire a better understanding of the topic.

The main advantages of $CO_2$ are that it is a natural refrigerant with zero ozone depleting potential (ODP), negligible global warming potential (GWP) and is also non-flammable and non-toxic. Worldwide there is a lot of pressure on governments to ensure that global warming is subdued and the phasing out of HFC and HCFC refrigerants are already implemented, stimulating thorough research for the implementation of environmentally friendly gasses.

A critical issue of $CO_2$ is its high operating pressure of up to 130 bar. This results in the development of $CO_2$ components to be more difficult due to the risks that can occur when operating the system at these pressures. $CO_2$ has a low critical point and will operate in a transcritical state when used for heat pump applications. It therefore makes use of a gas cooler on the high pressure side to cool down the refrigerant but will not condensate the refrigerant. The advantage with gas cooling is that water temperatures of up to 90°C is possible to achieve compared to the usual 60°C when working with conventional refrigerants.

A $CO_2$ heat pump system was characterized to determine the performance thereof under any operating condition. It was identified that the $CO_2$ heat pump system efficiency depends on the gas cooler outlet temperature which is determined by inlet temperature of the water. A comparison between a $CO_2$ heat pump system and R-22 heat pump system was done using an ILH system as a reference for energy consumption.

The $CO_2$ heat pump showed on average a 15% better coefficient of performance (COP) than the R-22 heat pump. The effect of the COP difference could clearly be seen in the annual energy consumption of the two systems. The R-22 heat pump system uses 9.4% more energy than the $CO_2$ system. The $CO_2$ heat pump system costs 11.7% more than the R-22 heat pump system. This is mainly due to it being a relatively new technology and the components used with $CO_2$ as a refrigerant is not mass produced yet. The cost of the $CO_2$ components should drop as the technology improves and the demand for the components increases. The R-22 heat pump system has a higher operating cost of about 11.9% when compared to the $CO_2$ system. Even though the $CO_2$ system is currently more expensive than the R-22 system it has a lower operating cost resulting in an additional capital expense payback period of about 4 years.

To conclude, $CO_2$ as refrigerant is definitely a feasible option to be used in a heat pump system. Not only is it an environmentally friendly gas, but it has a better operating cost and is more energy efficient. With the phasing out of HFC and HCFC refrigerants combined with the electricity crisis in South Africa, $CO_2$ definitely has a future as a refrigerant in the refrigeration market.

## *6.2 Recommendations for further work*

Based on the work done in this study and the results found the following has been identified as areas requiring further attention:

- .A study needs to be conducted specifically on the gas cooler to get a better understanding of the thermodynamic process when operating in a transcritical state.
- Component models need to be developed for a detailed system simulation to assist in the design and sizing of system components.
- The development of a prototype $CO_2$ heat pump system will be valuable for the research to generate practical results for simulation model verification.
- Applications surrounding $CO_2$ as a refrigerant needs to be investigated further. The possibility to heat water to 90°C could lead industrial applications for the $CO_2$ technology.

# *REFERENCES*

ANON (a). s.a. All about carbon dioxide. Toromont Process Systems. 42p.

ANON (b). s.a. . Heat pumps can cut global emissions by up to 8%. IEA/OECD Technical research institute of Sweden, Heat Pump Programme. 8p.

ANON (c). s.a. The friendly side of $CO_2$. YARA, Powerpoint.

ANON (d). s.a. The widest CO2 compressor range, carbon dioxide for all your needs. DORIN Innovation, Technical Brochure of the DORIN compressor range.

APREA, C. & MAIORINO, A. 2008. An experimental evaluation of the transcritical $CO_2$ refrigerator performances using an internal heat exchanger. *International journal of refrigeration* (article in press): 1-6.

BENSAFI, A. & THONON, B. 2007. Transcritical R744 ($CO_2$) heat pumps – technicians manual. SHERPA-CETIAT, France. 62p.

BULLARD, C. 2004-5. Transcritical $CO_2$ systems – recent progress and new challenges. Air-conditioning and refrigeration center, University of Illinois. Review article. 8p.

BUTLER, A. 2007. $CO_2$ transcritical cooling with heat reclaim. RAC cooling with carbon dioxide conference. Space Engineering Services, Bristol. 10p.

CALM, J.M. 2008. The next generation of refrigerants – historical review, considerations and outlook. *International journal of refrigeration,* (31):1123-1133.

CECCHINATO, L., CORRADI, M., FORNASIERI, E. & ZAMBONI L. 2005. Carbon dioxide as refrigerant for tap water heat pumps: a comparison with the traditional solution. *International journal of refrigeration* (28):1250-1258.

CHEN, Y., LUNDQVIST, P., JOHANSSON, A. & PLATELL P. 2006. A comparative study of the carbon dioxide transcritical power cycle compared with an organic rankine cycle with R123 as working fluid in waste heat recovery. *Applied thermal engineering* (26):2142-2147.

DANFOSS. 2002a. HFC phase out in Europe. Refrigeration and air conditioning. 16p.

DANFOSS. 2002b. $CO_2$ the refrigerant for commercial refrigeration. Powerpoint.

DORIN Innovation. s.a. The widest $CO_2$ compressor range – carbon dioxide for all your needs. 28p.

ENDOH, K., KUONO, T., GOMMORI, M., TANAAMI, T., MIZUTANI, K. & MIYATA, M. 2006. Instant hot-water supply heat-pump water heater using $CO_2$ refrigerant for home use. 7th IRR Gustav Lorentzen Conference on natural working fluids, Trondheim, Norway. 8p.

ESKOM. 2009/10 Tariffs and charges. 66p.

FARTAJ, A., TING, D.S.K. & YANG, W. 2004. Second law analysis of the transcritical $CO_2$ refrigeration cycle. *Energy conversion and management* (45):2269-2281.

FREUND, P. s.a. Properties of $CO_2$ and carbon based fuels. IPCC special report on carbon dioxide capture and storage, p385-398.

FLEMING, E.A., BROWN, L.M. & COOK, R.I. 1992. Overview of production aspects of operating the Denver unit $CO_2$ flood.

FLEMING, J. s.a. Carbon dioxide as the working fluid in heating and/or cooling systems. Review article. Department of mechanical engineering, University of Strathclyde. 5p.

HASSE, V., EDERBERG, L. & COLBOURNE, D. 2008. Proklima natural refrigerants, sustainable ozone- and climate-friendly alternatives to HCFCs. Deutsche Gesellschaft fur Technische Zusammenarbeit. 402p.

HUFF, H. & SIENEL, T. 2006. Commercial sized $CO_2$ heat pump water heater – North American field trial experience. 7th IIR Gustav Lorentzen Conference on natural working fluids, Trondheim, Norway. 6p.

KASAI, K. & SHIBATA, Y. 2005. Development of a new type heat exchanger for natural refrigerant $CO_2$ heat pump water heaters. DAIKEN air conditioning R&D lab, Japan. 5p.

KERN, R., HARGREAVES, J.B., WANG, J.F., WHITE, S.D. & CLELAND D.J. 2006. Performance of a prototype heat pump water heater using carbon dioxide as the refrigerant in a transcritical cycle. 7th IIR Gustav Lorentzen Conference on Natural Working Fluids, Trondheim, Norway. 8p.

KIM, M., PETERSEN, J. & BULLARD, C. 2003. Fundamental process and system design issues in $CO_2$ vapour compression systems. *Progress in energy and combustion cycles*, (30):119-174.

KUWABARA, O, KOBAYASHI, M., MUKAIYAMA, H., ISHIKAWA, M., MUKUNOKI, K. & HONMA, N. 2006. Performance evaluation of a $CO_2$ heat pump heating system. 7th IIR Gustav Lorentzen Conference on natural working fluids, Trondheim, Norway. 8p.

LUKITOBUDI, A.R. 2008. Utilization of $CO_2$ (R744) as refrigerant. AITMI workshop – Inovation solutions of $CO_2$ nowadays, Yogyakarta. Powerpoint. 19p.

MADSEN, K.B. 2008. Course on carbon dioxide as a refrigerant given by Cool Concerns (presenter Jane Gartshore). www.coolconcerns.co.uk . Danish Technological Institute.

MCQUAY INTERNATIONAL. 2002. Refrigerants application guide.

NEKSA, P., PETTERSEN, J. & SKAUGEN, G. s.a. $CO_2$ refrigeration, air-conditioning and heat pump technology. SINTEF NTNU. 13p.

NEKSA, P., REKSTAD, H., ZAKERI, G.R. & SCHIEFLOE, P.A. 1998. $CO_2$ heat pump water heater: characteristics, system design and experimental results. *International journal of refrigeration* (21):172-179.

NEKSA, P. 2002. $CO_2$ heat pump systems. *International journal of refrigeration* (25):421-427.

NEKSA, P. 2004. CO2 as refrigerant for systems in trans-critical operation principles and technology status. Sept. SINTEF Energy Research, Norway. EcoLibrium. 6p.

NEKSA, P. 2006. $CO_2$ as refrigerant, an option to reduce GHG emissions from refrigeration, air conditioning and heat pump systems. SINTEF energy research, Trondheim, Norway. 3p.

NRTB. 2005. Natural Refrigeration Transition Board, Ltd.

PALANDRE, L. 2004. HCFC's and HFC's emissions from the refrigerating systems for the period 2004-2015.

PARSCH, W. 2002. Status of compressor development for R-744 systems. VDA Alternate Refrigerant Wintermeeting.

PEARSON, A.B. 2005. Carbon dioxide - new uses for an old refrigerant. *International journal of refrigeration*, (28):1140-1148.

PEARSON, A.B. 2006. District heating systems with $CO_2$ as refrigerant. 7th IIR Gustav Lorentzen Conference on natural working fluids, Trondheim, Norway. 8p.

PEARSON S.F. 2006. Highly efficient water heating system. 7th IIR Gustav Lorentzen Conference on natural working fluids, Trondheim, Norway. 8p.

PISANO, G. s.a. The use of carbon dioxide in refrigeration and heat pump systems. Officine Mario DORIN S.p.A., Italia. 8p.

ROUSSEAU, P.G. 2006. WHSIM Statistical. M-Tech Industrial Pty. (Ltd.)

RASMUSSEN, B.D. 2003. Refrigerant cycles – cycle processes with carbon dioxide. Danfoss $CO_2$ Workshop, Powerpoint. 11p.

R744.com (a), 2008-02-22. Industry visits Australia's first $CO_2$-only supermarket system. http://www.r744.com/articles/2008-02-22-industry-visits-australia-first-co2-only-supermarket.php Date of access: 23 Oct. 2008.

R744.com (b), 2008-04-04. $CO_2$ technology more cost-effective by the day. http://www.r744.com/news/news_ida323.php Date of access: 26 Oct 2008.

R744.com (c), 2008-02-01. High efficient Eco-Cute heat pumps launched. http://www.r744.com/news/news_ida286.php Date of access: 26 Oct 2008.

SARKAR, J., BHATTACHARYYA, S. & GOPAL RAM, M. 2004. Optimization of a transcritical $CO_2$ heat pump cycle for simultaneous cooling and heating application. *International journal of refrigeration* (27):830-838.

SARKAR, J., BHATTACHARYYA, S. & GOPAL RAM, M. 2006. Simulation of a transcritical $CO_2$ heat pump cycle for simultaneous cooling and heating applications. 7th IIR Gustav Lorentzen Conference on Natural Working Fluids, Trondheim, Norway. 6p.

SARKAR, J. 2007. Optimization of ejector expansion transcritical $CO_2$ heat pump cycle. *Energy* (33):1399-1406.

SARKAR, J., BHATTACHARYYA, S. & RAMGOPAL, M. 2007. Transcritical $CO_2$ heat pump prototype development for simultaneous water cooling and heating. International congress of refrigeration, Beijing. 8p.

SARKAR, J. 2008. Transcritical $CO_2$ heat pump simulation model and validation for simultaneous cooling and heating. International refrigeration and air conditioning conference, Purdue. 8p.

STENE, J. 2007. Integrated $CO_2$ heat pump systems for space heating and hot water heating in low-energy houses and passive houses. International Energy Agency Heat pump programme (32). 14p.

STENE, J. 2004. Residential $CO_2$ heat pump system for combined space heating and hot water heating. NTNU: Norwegian University of Science and Technology. (Thesis – PhD). 324p.

STENE, J. s.a. High-efficiency $CO_2$ heat pump water heater systems for residential and non-residential buildings. SINTEF energy research, 7465 Trondheim, Norway. 7p.

SIENEL, T. & HUFF, H. 2006. Control bifurcation issues of transcritical $CO_2$ heat pump water heaters.

SUB, J. & KRUSE, H. 1998. Efficiency of the indicated process of $CO_2$-compressors. *International journal of refrigeration*, (21):194-201.

TAIRA, S. 2008. The development of high temperature water heating using $CO_2$ heat pump. (Product development group). DAIKEN. Powerpoint. 17p.

TAIRA, S. 2008. The development of heat pump water heaters using $CO_2$ refrigerant. Daiken Industries limited. 17p.

THONON, B. 2006. The SHERPA project natural refrigerants for heat pumps. 7th IIR Gustav Lorentzen Conference on natural working fluids, Trondheidm, Norway. 8p.

UNEP, 2007. Montreal Protocol on substances that deplete the ozone layer. 2006 Assessment report of the technology and economic assessment panel. 162p.

WANG, R.Z. & LI, Y. 2006. Perspectives for natural working fluids in China. *International journal of refrigeration* (article in press): 1-14.

WOLF, F., HAFNER, A. & CHASSEROT, M. 2006. Latest development & perspectives in R744 technology. Powerpoint. 16p.

WHITE, S.D., YARRALL, M.G., CLELAND D.J. & HEDLEY R.A. 2002. Modeling the performance of a transcritical $CO_2$ heat pump for high temperature heating. *International journal of refrigeration*, (25):479-486.

YANG, J., MA, Y., LIU, S. & ZENG, X. 2006. Comparison investigation on the heat transfer characteristics for supercritical $CO_2$ fluid and conventional refrigerants. 7th IIR Gustav Lorentzen Conference on natural working fluids, Trondheidm, Norway. 6p.

YOKOYAMA, R., SHIMIZU, T., ITO K. & TAKEMURA, K. 2005. Influence of ambient temperatures on performance of a $CO_2$ heat pump water heating system. *Journal of environment and engineering*, Japan. 13p.

YOKOYAMA, R., SHIMIZU, T., TAKEMURA, K. & ITO K. 2006. Performance analysis of a hot water supply with a $CO_2$ heat pump by numerical simulation. *JSME international journal* (49):541-549.

YOKOYAMA, R., OKAGAKI, S., WAKUI, T. & TAKEMURA, K. 2008. Influence of operation temperatures on performance of a $CO_2$ heat pump water heating system. *Journal of environment and engineering* (3):61-73.

ZHA, S., HAFNER, A. & NEKSA, P. 2006. Investigation of a transcritical R-744 VOORHEES heat pump system. 7th IIR Gustav Lorentzen Conference on Natural Working Fluids, Trondheim, Norway. 8.

# APPENDIX A

# EES PROGRAMMING

```
"Wynand Groenewald"
"Information found from DORIN innovation- compressor = TCS362-D"
"Fluid is R744(CO2)"
"Simple cycle simulation with equations implemented"

"5. Inlet to Evaporator"
{P_[5] = 4500 [kPa]}                          "P_suc"
{T_[5] = 283 [K]}                             "T_evaporation"
{Q_e = 36.5 [kW]}                             "Cooling capacity"
h_[5] = h_[4]                                 "Constant enthalpy over expansion device"
x_[5] =Quality(R744,h=h_[5],P=P_[5])          "2-phase"
{cp_[5]=Cp(R744,T=T_[5],P=P_[5])}
s_[5]=Entropy(R744,x=x_[5],P=P_[5])

"6. Outlet evaporator"
P_[6] = P_[5]                                 "Evaporation takes place at constant pressure"
P_[7] = P_[5]                                 "in consideration for adding superheat"
T_[6] = T_[5]
T_[7] = T_[6] +10                             "Superheat added"
x_[6] = 1                                     "Gas"
h_[6]=Enthalpy(R744,x=x_[6],P=P_[6])
h_[7]=Enthalpy(R744,T=T_[7],P=P_[7])
Q_e = m_dot_g * (h_[7]-h_[5])
s_[6]=Entropy(R744,x=x_[6],P=P_[6])
s_[7]=Entropy(R744,T=T_[7],P=P_[7])

"8. Outlet Internal heat exchanger suction side"
P_[8]=P_[7]
(h_[8]-h_[7]) = (h_[3]-h_[4])
T_[8]=Temperature(R744,h=h_[8],P=P_[8])
s_[8]=Entropy(R744,T=T_[8],P=P_[8])
T_[4] = T_[3]-0
P_[4] = P_[3]
h_[4]=Enthalpy(R744,T=T_[4],P=P_[4])
s_[4]=Entropy(R744,T=T_[4],P=P_[4])

"1. Inlet compressor"
P_[1] = P_[8]
h_[1] = h_[8]
T_[1] = T_[8]
s_[1] = s_[8]

"2. Outlet compressor and inlet gas cooler"
{P_[2] = 12000 [kPa]}                         "Dischargepressure"
{Q_p = 17.9 [kW]}                             "Compressor work"
{eta_c = 0.9}
Q_h = Q_e + (Q_p*eta_c)
COP = Q_h/Q_p
Q_p = m_dot_g * (h_[2]-h_[1])
T_[2] = Temperature(R744,P=P_[2],h=h_[2])
{h_[2] = Enthalpy(R744,T=T_[2],P=P_[2])}
s_[2]= Entropy(R744,T=T_[2],P=P_[2])
h_s[2]=ENTHALPY(R744,p=p_[2],s=s_[1])
eta_c=(h_s[2]-h_[1])/(h_[2]-h_[1])

"3. Outlet gas cooler"
{T_[3] = 308 [K]}                             "outlet Temp gas
cooler"
P_[3] = P_[2]
h_[3]=Enthalpy(R744,T=T_[3],P=P_[3])
s_[3]=Entropy(R744,T=T_[3],P=P_[3])
```

```
"Coefficients"
{P_[3]=4501}                          "gas cooler outlet"
P_[5]=PRESSURE(R744,T=T_[5],x=1)      "evaporating temperature"

m_dot_g = (-0.0000000021646*P_[3]^2 + 0.000042438*P_[3] -0.20742) +
(0.0000000000023263*P_[3]^2 -0.000000047418*P_[3] + 0.00026913)*P_[5] + (-5.6907E-16*P_[3]^2 +
0.000000000010683*P_[3] -0.00000004147)*P_[5]^2

eta_c = (-0.00000083963*P_[3]^2 + 0.0080456*P_[3] + 8.0327) + (0.0000000014441*P_[3]^2 -
0.000014157*P_[3] -0.010314)*P_[5] + (-0.00000000000096578*P_[3]^2 + 0.0000000096283*P_[3] +
0.000005673)*P_[5]^2 + (3.1092E-16*P_[3]^2-0.00000000000031142*P_[3] -0.0000000017696)*P_[5]^3
+ (-4.8268E-20*P_[3]^2 + 4.8032E-16*P_[3] + 0.00000000000031525)*P_[5]^4 + (2.899E-24*P_[3]^2 -
2.8348E-20*P_[3] -2.4274E-17)*P_[5]^5

"Water-side"
T_wi = 283 [K]
T_wo = 328 [K]
P_w = 300 [kPa]
C_pw=Cp(Water,T=T_wi,P=P_w)
Q_h = m_dot_w * C_pw * (T_wo - T_wi)
```

```
"Wynand Groenewald"
"A Techno-Economical Analysis of a CO2 Heat Pump"
"Final program"
"This program contains the coefficients that were attained and is used to compare our results to the results from the compressor charts"
"Compressor chart used was attained from DORIN innovation- compressor = TCS362-D"
"Fluid is R744(CO2)"

"5. Inlet to Evaporator"

{P_[5] = 4500 [kPa]}                          "P_suc"
{T_[5] = 283 [K]}                             "T_evaporation"
{Q_e = 36.5 [kW]}                             "Cooling capacity"
h_[5] = h_[4]                                 "Constant enthalpy over expansion device"
x_[5] =Quality(R744,h=h_[5],P=P_[5])          "2-phase"

{cp_[5]=Cp(R744,T=T_[5],P=P_[5])}
s_[5]=Entropy(R744,x=x_[5],P=P_[5])

"6. Outlet evaporator"

P_[6] = P_[5]                                 "Evaporation takes place at constant pressure"
P_[7] = P_[5]                                 "in consideration for adding superheat"
T_[6] = T_[5]
T_[7] = T_[6] +10                             "Superheat added"
x_[6] = 1                                     "Gas"
h_[6]=Enthalpy(R744,x=x_[6],P=P_[6])

h_[7]=Enthalpy(R744,T=T_[7],P=P_[7])

Q_e = m_dot_g * (h_[7]-h_[5])

s_[6]=Entropy(R744,x=x_[6],P=P_[6])
s_[7]=Entropy(R744,T=T_[7],P=P_[7])

"8. Outlet Internal heat exchanger suction side"

P_[8]=P_[7]
(h_[8]-h_[7]) = (h_[3]-h_[4])
T_[8]=Temperature(R744,h=h_[8],P=P_[8])
s_[8]=Entropy(R744,T=T_[8],P=P_[8])

T_[4] = T_[3]-0                  "no heat exchange is added through the internal heat exchanger"
P_[4] = P_[3]
h_[4]=Enthalpy(R744,T=T_[4],P=P_[4])
s_[4]=Entropy(R744,T=T_[4],P=P_[4])

"1. Inlet compressor"

P_[1] = P_[8]
h_[1] = h_[8]
T_[1] = T_[8]
s_[1] = s_[8]

"2. Outlet compressor and inlet gas cooler"

{P_[2] = 12000 [kPa]}                         "Discharge pressure"
{Q_p = 17.9 [kW]}                             "Compressor work"
{eta_c = 0.9}
Q_h = Q_e + Q_p

COP = Q_h/P_p

Q_p = m_dot_g * (h_[2]-h_[1])
P_p = Q_p*1.05
```

```
T_[2] = Temperature(R744,P=P_[2],h=h_[2])
{h_[2] = Enthalpy(R744,T=T_[2],P=P_[2])}
s_[2]= Entropy(R744,T=T_[2],P=P_[2])

h_s[2]=ENTHALPY(R744,p=p_[2],s=s_[1])

eta_c=(h_s[2]-h_[1])/(h_[2]-h_[1])

"3. Outlet gas cooler"

{T_[3] = 308 [K]}                              "outlet Temp gas cooler"
P_[3] = P_[2]

h_[3]=Enthalpy(R744,T=T_[3],P=P_[3])
s_[3]=Entropy(R744,T=T_[3],P=P_[3])

"Curve"
T_[2] = T_[20]
T_[3] = T_[30]
DELTAT = (T_[20]-T_[30])/10
P_[2] = P_[20]
P_[3] = P_[30]
DELTAP = (P_[20]-P_[30])/10
h_[2] = h_[20]
h_[3] = h_[30]
s_[2] = s_[20]
s_[3] = s_[30]

duplicate i = 1,9
T_[20 + i] = T_[20 + i -1] - DeltaT
P_[20 + i] = P_[20 + i -1] - DeltaP

h_[20 + i]=Enthalpy(R744,T=T_[20 + i],P=P_[20 + i])
s_[20 + i]=Entropy(R744,T=T_[20 + i],P=P_[20 + i])
  Q_[20 + i] = m_dot_g * (h_[20 + i - 1] - h_[20 + i])
end
Q_[30] = m_dot_g * (h_[29] - h_[30])
Q_tot = sum(Q_[21..30])

"Coefficients"

{P_[3]=4501}                                   "gas cooler outlet"
P_[5]=PRESSURE(R744,T=T_[5],x=1)               "evaporating temperature"

m_dot_g = (-0.0000000021646*P_[3]^2 + 0.000042438*P_[3] -0.20742) +
(0.0000000000023263*P_[3]^2 -0.000000047418*P_[3] + 0.00026913)*P_[5] + (-5.6907E-16*P_[3]^2 +
0.000000000010683*P_[3] -0.00000004147)*P_[5]^2

eta_c = (-0.00000083963*P_[3]^2 + 0.0080456*P_[3] + 8.0327) + (0.0000000014441*P_[3]^2 -
0.000014157*P_[3] -0.010314)*P_[5] + (-0.00000000000096578*P_[3]^2 + 0.0000000096283*P_[3] +
0.000005673)*P_[5]^2 + (3.1092E-16*P_[3]^2 -0.00000000000031142*P_[3] -0.0000000017696)*P_[5]^3
+ (-4.8268E-20*P_[3]^2 + 4.8032E-16*P_[3] + 0.00000000000031525)*P_[5]^4 + (2.899E-24*P_[3]^2 -
2.8348E-20*P_[3] -2.4274E-17)*P_[5]^5

"Water-side"

T_w[1] = 303 [K]
T_w[2] = 332 [K]
P_wi = 300 [kPa]
P_wo = 290 [kPa]

C_pw=Cp(Water,T=T_w[1],P=P_wi)
Q_h = m_dot_w * C_pw * (T_w[2] - T_w[1])

{T_w[1] = T_w[30] }
T_w[2] = T_w[20]
```

```
duplicate i = 1,10
Q_[20 + i] = m_dot_w * C_pw * (T_w[20+i-1] - T_w[20+i])
end

s_w[1]= s_[3]                                   "entropy water"
s_w[2]= s_[2]
```

```
"Determine Coefficients a[0] to a[5] and b[0] tp b[1] to fit equations through Ta and Tw data to give Q and COP"

duplicate i=1, 23
T_a[i] = lookup('lookup 1', i, 1)
T_w[i] = lookup('lookup 1', i, 2)
Q[i] = lookup('lookup 1', i, 3)
COP[i] = lookup('lookup 1', i, 4)

COP_fit[i] = b[0] + b[1]*T_a[i] + b[2]*T_w[i] + b[3]*T_a[i]*T_w[i] +b[4]*T_a[i]*T_a[i] + b[5]*T_w[i]*T_w[i]
err_1[i] = (abs(COP[i] - COP_fit[i]))^2

Q_fit[i] = a[0] + a[1]*T_a[i] + a[2]*T_w[i] + a[3]*T_a[i]*T_w[i] +a[4]*T_a[i]*T_a[i] + a[5]*T_w[i]*T_w[i]
err_2[i] = (abs(Q[i] - Q_fit[i]))^2

end
sumerr_1 = sum(err_1[1..23])
sumerr_2 = sum(err_2[1..23])
sumerr_tot = sumerr_1 + sumerr_2
```

# *APPENDIX B*

# *WHSIM STATISTICAL INPUTS*

Input file for $CO_2$ heat pump system.

```
// Heatpump.cpp
#include "StdAfx.h"
#include "Heatpump.h"
#include "Genutil.h"
Heatpump::Heatpump()
{       initflag = 0;
        Q_hpnom = 0;
        Q_hp = 0;
        COP = 0;
        power = 0;}
Heatpump::~Heatpump(){}void  Heatpump::setparameters(char  *systemname_input,
double Q_hpnom_input, double HP_max_temp, double HP_min_temp){
        initflag = 1;
        strcpy(systemname,systemname_input);
        Q_hpnom = Q_hpnom_input;
        Q_hp = 0;
        COP = 0;
        power = 0;
        initflag = 1;}
bool Heatpump::setheatpumppower(int status, double T_wetbulb, double T_supply){
        bool errorflag = 0;
        double Twb_o, T_hi;
        if (initflag == 0){
                error("Heat pump not initialised, cannot set heat pump capacity");
                errorflag = 1;   }
        Twb_o = T_wetbulb;
        T_hi = T_supply;
        if (status == 1){
                Q_hp = 1000*(47.51
                                        + 2.33*Twb_o
                                        - 0.1785*T_hi
                                        - 0.02579*Twb_o*T_hi
                                        + 0.0558*Twb_o*Twb_o
                                        - 0.006202*T_hi*T_hi);
```

```
            COP = 3.626
                                    + 0.006925*Twb_o
                                    - 0.01331*T_hi
                                    - 0.001065*Twb_o*T_hi
                                    + 0.004622*Twb_o*Twb_o
                                    - 0.0004428*T_hi*T_hi;
            power = Q_hp/COP;  }
        else    {
            power = 0;
            COP = 0;
            Q_hp = 0;       }
        if (errorflag == 0)
            return 1;
        else
            return 0;}
```

Input file for R-22 heat pump system.

```
// Heatpump.cpp
#include "StdAfx.h"
#include "Heatpump.h"
#include "Genutil.h"
Heatpump::Heatpump(){
        initflag = 0;
        Q_hpnom = 0;
        Q_hp = 0;
        COP = 0;
        power = 0;}
Heatpump::~Heatpump(){}void  Heatpump::setparameters(char  *systemname_input,
double Q_hpnom_input, double HP_max_temp, double HP_min_temp){
        initflag = 1;
        strcpy(systemname,systemname_input);
        Q_hpnom = Q_hpnom_input;
        Q_hp = 0;
        COP = 0;
        power = 0;
```

```
        initflag = 1;}
bool Heatpump::setheatpumppower(int status, double T_wetbulb, double T_supply){
        bool errorflag = 0;
        double Twb_o, T_ho;
        if (initflag == 0)          {
                error("Heat pump not initialised, cannot set heat pump capacity");
                errorflag = 1;   }
        Twb_o = T_wetbulb;
        T_ho = T_supply;
        if (status == 1){
                Q_hp = Q_hpnom*(0.994564
                                        + 0.0370009*Twb_o
                                        + 0.000345315*Twb_o*Twb_o
                                        - 0.0031483*T_ho
                                        -0.00015912*Twb_o*T_ho
                                        -4.6942e-5*T_ho*T_ho);
                COP = 5.21333
                                        + 0.103693*Twb_o
                                        + 0.0002237*Twb_o*Twb_o
                                        - 0.068073*T_ho
                                        +0.0003102*T_ho*T_ho;
                power = Q_hp/COP;   }
        else    {
                power = 0;
                COP = 0;
                Q_hp = 0;}
        if (errorflag == 0)
                return 1;
        else
                return 0;}
```

WHProject input file

| | |
|---|---|
| Timestep[s]: | 600 |
| System_input_filename: | ILHPSeriesSystem |
| Placename: | Johannesburg |
| Consumption_dataset: | 1 |
| Number_of_occupants: | 190 |
| Liters_per_person_per_day: | 75 |
| DSM_Intervals_dataset: | 2 |
| Peak_Intervals_dataset: | 1 |
| Month_Classification_dataset: | 1 |
| Energy_Cost_dataset: | 3 |
| Base_temperature: | 60 |
| Initial_temperature: | 55 |
| Initial_days: | 7 |
| Weather_month: | 1 |
| weather_day: | 1 |
| n_years: | 1 |
| print_monthSum: | 12 |
| print_daySum: | 15 |
| print_monthWin: | 8 |
| print_dayWin: | 4 |
| takeoffrate: | 0.1 |
| sum_std_dev: | 0.1 |
| win_std_dev: | 0.15 |
| win_frac_sum: | 1.7 |

| Jan | Feb | Mar | Apr | May | Jun | Jul | Aug | Sep | Oct | Nov | Dec |
|---|---|---|---|---|---|---|---|---|---|---|---|
| 1 | 1 | 1 | 1 | 1 | 1 | 1 | 1 | 1 | 1 | 1 | 1 |

Weather_directory: D:\M-Projek-FIN\EES Programme\WEERDATA\

Inline heat pump series system

| | |
|---|---|
| Fluid_density[kg/m^3]: | 990.0 |
| Fluid_heat_capacity[J/kgK]: | 4182.0 |
| Fluid_thermal_conductivity[W/mK]: | 0.632 |
| Fluid_viscosity[kg/ms]: | 0.000675 |
| Type(P/S): | S |
| Number_of_reservoirs: | 2 |
| Number_of_thermostats: | 2 |
| Number_of_inlineheaters(0/1): | 1 |
| In-line_heater_temperature_set-point[C]: | 60.0 |
| Number_of_heater_stages: | 2 |
| Number_of_heatpumps(0/1): | 1 |
| Heat_pump_min_drybulb_temp[C]: | 5 |
| Heat_pump_max_inlet_temp[C]: | 30 |
| Controller_type(CIT/SIT/ILH/ILHP): | ILHP |
| --- | --- |
| Reservoir_number: | 1 |
| Reservoir_type(V/H): | V |
| Number_of_layers: | 11 |
| Diameter[m]: | 2.2 |
| Length[m]: | 2.0 |
| Thickness_of_lagging[m]: | 0.025 |
| kvalue_of_lagging[W/mK]: | 0.15 |
| Non-dimensional_height_of_intank_heater_position: | 0.05 |
| Intank_heater_capacity[W]: | 0.0 |
| Non-dimensional_height_of_bottom_thermostat_position: | 0.05 |
| Non-dimensional_height_of_middle_thermostat_position: | 0.5 |
| Non-dimensional_height_of_top_thermostat_position: | 0.9 |
| Non-dimensional_height_of_ringmain_return_pipe: | 0.8 |
| Initial_temperatures[C]: | 55.0 |
| --- | --- |
| Reservoir_number: | 2 |
| Reservoir_type(V/H): | V |
| Number_of_layers: | 11 |
| Diameter[m]: | 2.2 |
| Length[m]: | 2.0 |
| Thickness_of_lagging[m]: | 0.025 |
| kvalue_of_lagging[W/mK]: | 0.15 |
| Non-dimensional_height_of_intank_heater_position: | 0.05 |
| Intank_heater_capacity[W]: | 0.0 |
| Non-dimensional_height_of_bottom_thermostat_position: | 0.05 |
| Non-dimensional_height_of_middle_thermostat_position: | 0.5 |
| Non-dimensional_height_of_top_thermostat_position: | 0.9 |
| Non-dimensional_height_of_ringmain_return_pipe: | 0.8 |
| Initial_temperatures[C]: | 55.0 |
| --- | --- |
| Thermostat_number: | 1 |
| Set-point[C]: | 30.0 |
| Dead-band[C]: | 5.0 |

| | |
|---|---|
| Installed_on_reservoir_no: | 1 |
| Installed_in_position(B/M/T): | B |
| --- | |
| Thermostat_number: | 2 |
| Set-point[C]: | 50.0 |
| Dead-band[C]: | 5.0 |
| Installed_on_reservoir_no: | 2 |
| Installed_in_position(B/M/T): | T |
| --- | |
| Inlineheater_number: | 1 |
| In-line_heater_capacity[W]: | 36000 |
| --- | |
| Heatpump_number: | 1 |
| Heatpump_nom_capacity[W]: | 60000 |
| --- | |

# *APPENDIX C*

# *MEGAFLEX*

# Megaflex *[non local authorities]*

| Transmission zone | Voltage | Active energy charge [c/kWh] | | | | | | | | | | | | Transmission network charges [R/kVA/mth] | |
|---|---|---|---|---|---|---|---|---|---|---|---|---|---|---|---|
| | | High demand season [Jun - Aug] | | | | | | Low demand season [Sep - May] | | | | | | Charged on utilised capacity | |
| | | Peak | | Standard | | Off Peak | | Peak | | Standard | | Off Peak | | | |
| | | VAT excl | VAT incl | VAT excl | VAT incl | VAT excl | VAT incl | VAT excl | VAT incl | VAT excl | VAT incl | VAT excl | VAT incl | VAT excl | VAT incl |
| ≤300km | < 500V | 119.09 | 135.76 | 30.93 | 35.26 | 16.50 | 18.81 | 33.22 | 37.87 | 20.34 | 23.19 | 14.21 | 16.20 | R 2.97 | R 3.39 |
| | ≥ 500V & < 66kV | 115.29 | 131.43 | 29.97 | 34.17 | 16.01 | 18.25 | 32.19 | 36.70 | 19.72 | 22.48 | 13.79 | 15.72 | R 2.71 | R 3.09 |
| | ≥ 66kV & ≤ 132kV | 111.11 | 126.67 | 28.91 | 32.95 | 15.47 | 17.64 | 31.05 | 35.40 | 19.04 | 21.71 | 13.34 | 15.21 | R 2.64 | R 3.01 |
| | > 132kV | 107.25 | 122.27 | 27.94 | 31.85 | 14.96 | 17.05 | 29.99 | 34.19 | 18.41 | 20.99 | 12.91 | 14.72 | R 3.34 | R 3.81 |
| > 300km and ≤ 600km | < 500V | 120.27 | 137.11 | 31.22 | 35.59 | 16.67 | 19.00 | 33.55 | 38.25 | 20.52 | 23.39 | 14.35 | 16.36 | R 2.99 | R 3.41 |
| | ≥ 500V & < 66kV | 116.41 | 132.71 | 30.25 | 34.49 | 16.16 | 18.42 | 32.49 | 37.04 | 19.90 | 22.69 | 13.92 | 15.87 | R 2.74 | R 3.12 |
| | ≥ 66kV & ≤ 132kV | 112.21 | 127.92 | 29.19 | 33.28 | 15.62 | 17.81 | 31.36 | 35.75 | 19.22 | 21.91 | 13.45 | 15.33 | R 2.66 | R 3.03 |
| | > 132kV | 108.30 | 123.46 | 28.20 | 32.15 | 15.10 | 17.21 | 30.30 | 34.54 | 18.59 | 21.19 | 13.01 | 14.83 | R 3.38 | R 3.85 |
| > 600km and ≤ 900km | < 500V | 121.46 | 138.46 | 31.53 | 35.94 | 16.82 | 19.17 | 33.87 | 38.61 | 20.72 | 23.62 | 14.47 | 16.50 | R 3.03 | R 3.45 |
| | ≥ 500V & < 66kV | 117.57 | 134.03 | 30.55 | 34.83 | 16.30 | 18.58 | 32.81 | 37.40 | 20.09 | 22.90 | 14.03 | 15.99 | R 2.76 | R 3.15 |
| | ≥ 66kV & ≤ 132kV | 113.32 | 129.18 | 29.46 | 33.58 | 15.75 | 17.95 | 31.65 | 36.08 | 19.39 | 22.10 | 13.56 | 15.46 | R 2.69 | R 3.07 |
| | > 132kV | 109.37 | 124.68 | 28.47 | 32.46 | 15.24 | 17.37 | 30.59 | 34.87 | 18.75 | 21.38 | 13.14 | 14.98 | R 3.42 | R 3.90 |
| > 900km | < 500V | 122.66 | 139.83 | 31.82 | 36.27 | 16.97 | 19.35 | 34.18 | 38.97 | 20.91 | 23.84 | 14.61 | 16.66 | R 3.04 | R 3.47 |
| | ≥ 500V & < 66kV | 118.74 | 135.36 | 30.84 | 35.16 | 16.45 | 18.75 | 33.12 | 37.76 | 20.26 | 23.10 | 14.17 | 16.15 | R 2.79 | R 3.18 |
| | ≥ 66kV & ≤ 132kV | 114.45 | 130.47 | 29.74 | 33.90 | 15.90 | 18.13 | 31.95 | 36.42 | 19.58 | 22.32 | 13.69 | 15.61 | R 2.70 | R 3.08 |
| | > 132kV | 110.46 | 125.92 | 28.73 | 32.75 | 15.38 | 17.53 | 30.86 | 35.18 | 18.93 | 21.58 | 13.25 | 15.11 | R 3.44 | R 3.92 |

| Distribution network charges | | | | | |
|---|---|---|---|---|---|
| Voltage | NAC [R/kVA/mth] | Charged on utilised capacity | | NDC [R/kVA/mth] | Charged on chargable demand |
| | | VAT excl | VAT incl | | VAT excl | VAT incl |
| < 500V | | R 5.93 | R 6.76 | | R 11.24 | R 12.81 |
| ≥ 500V & < 66kV | | R 5.44 | R 6.20 | | R 10.31 | R 11.75 |
| ≥ 66kV & ≤ 132kV | | R 5.26 | R 6.00 | | R 9.99 | R 11.39 |
| > 132kV | | R 0.00 | R 0.00 | | R 9.00 | R 10.26 |

| Reactive energy charge [c/kvarh] | | | | Electrification and rural subsidy [c/kWh] | | Environmental levy [c/kWh] | |
|---|---|---|---|---|---|---|---|
| High Season | | Low Season | | All Seasons | | All Seasons | |
| VAT excl | VAT incl | VAT excl | VAT incl | VAT excl | VAT incl | VAT excl | VAT incl |
| 4.77 | 5.44 | 0.00 | 0.00 | 2.50 | 2.85 | 1.97 | 2.25 |

| Service charge [R/Account/day] | | |
|---|---|---|
| | VAT excl | VAT incl |
| > 1 MVA | R 67.71 | R 77.19 |
| Key customers | R 1 326.91 | R 1 512.68 |

| Administration charge [R/POD/day] | | |
|---|---|---|
| | VAT excl | VAT incl |
| > 1 MVA | R 30.52 | R 34.79 |
| Key customers | R 42.37 | R 48.30 |